Genesis of calcrete and related carbonate rocks in the southern Kenya Rift

A thesis submitted to the
College of Graduate Studies and Research
in partial fulfilment of the requirements
for the Degree of Master of Science
in the Department of Geological Sciences
University of Saskatchewan
Saskatoon

By
GINETTE NICOLE FELSKE

PERMISSION TO USE

In presenting this thesis in partial fulfilment of the requirements for a Postgraduate degree from the University of Saskatchewan, I agree that the Libraries of this University may make it freely available for inspection. I further agree that permission for copying of this thesis in any manner, in whole or in part, for scholarly purposes may be granted by the professor or professors who supervised my thesis work or, in their absence, by the Head of the Department or the Dean of the College in which my thesis work was done. It is understood that any copying or publication or use of this thesis or parts thereof for financial gain shall not be allowed without my written permission. It is also understood that due recognition shall be given to me and to the University of Saskatchewan in any scholarly use which may be made of any material in my thesis.

Requests for permission to copy or to make other use of material in this thesis in whole or part should be addressed to:

Head of the Department of Geological Sciences
University of Saskatchewan
114 Science Place
Saskatoon, Saskatchewan S7N 5E2

OR

Dean
College of Graduate Studies and Research
University of Saskatchewan
107 Administration Place
Saskatoon, Saskatchewan S7N 5A2 Canada

ABSTRACT

Pleistocene to Recent calcretes, which are common in the semi-arid parts of the Kenya Rift Valley, provide clues to interpret regional paleoclimate and paleohydrology. A summary of the calcrete occurrences in or near the southern Kenya Rift Valley is provided to give regional context.

At Lake Magadi and Olorgesailie, calcretes mantle the land surface, inhibiting erosion of the Pleistocene lake and lake-marginal sediments. The calcretes represent a period of no net sedimentation and form an important land surface throughout the basin.

The several calcretes in the area have not been studied in detail to determine their relationship to other sediments in the basin though attempts have been made at calcrete differentiation based on underlying sediments. Several whole-rock samples were taken around the basin predominantly at the south of Lake Magadi to compare the calcretes with each other and their surrounding sediments. At Lake Magadi an extensive calcrete up to 50 cm thick lies at the interface between the Oloronga Beds (780 to 300 ka) and the overlying High Magadi Beds (~23000 to 9000 y BP). The relationship of this calcrete, called the Oloronga-capping calcrete, with the Green Beds (100 to 23 ka) is not obvious in the field but the calcretes are assumed to be older. Based on its chemistry and field relationships, the commonly pisolitic calcrete was formed within the Oloronga Beds though is likely much younger. Chondrite-normalized REE patterns for the calcrete and underlying sediments are consistent with sediment derivation from the Magadi Trachytes, indicating drainage patterns similar to those at present. Based on calcrete microfabrics and stable isotope data the dominant process of formation was through periodic calcite precipitation at or near the groundwater table under dry conditions following a wetter period. Pisoids formed through cycles of circumgranular cracking around reworked calcrete, and around calcite-rimmed lithic or monocrystalline clasts, induced partly due to pressure of calcite crystallization and root growth. Evidence for biotic activity during formation is scarce; rare fungal hyphae and spores were detected under SEM and root-related microfabrics are rare. The data indicate dominantly groundwater calcrete that was overprinted by and possible overprinted upon pedogenic calcrete. The groundwater table during calcrete formation was higher than at present; however, the lake was constricted and low and the calcrete developed marginal to the lake. Laminar calcrete that developed on local trachytic horsts is difficult to date, but is predominantly abiogenic and may have taken many thousands of years to form. Samples from

elsewhere in the basin as well as an in-depth study of the Oloronga Beds would help clarify these possible interpretations.

Olorgesailie is a fossil rich area and an important site for the study of human origins. Understanding the paleoenvironmental context of the hominin fossils and archeology is important for evolutionary studies. The Olorgesailie Formation (1.2-0.5 Ma) has yielded several archaeological finds and is composed of lacustrine, lake marginal and fluvial sediments, and paleosols. It is overlain by the post-Olorgesailie Formation sediments, which are the focus of this study. At the time of this study the stratigraphy of the post-Olorgesailie Formation sediments had not been presented. Part of this thesis provides some details for the calcretes within the sequence and presents a model for their formation. Three calcretes in a stratigraphic section were sampled as well as the intervening sediments. Using several types of analytical data, a model is presented to explain their origin. The three calcretes are distinct, predominantly pedogenic, and reflect fluctuating hydrological conditions, as implied by silica cementation in the middle calcrete. The upper capping calcrete may reflect a very shallow water table.

The last study site targets calcite and silica-cemented conglomerate along the southeast shoreline of Nasikie Engida, a small lake to the north of Lake Magadi. Initially thought to be a calcrete, the deposit at Nasikie Engida, which overlies the High Magadi Beds, is inferred to be a beachrock, which is unusual since Nasikie Engida is not prone to high-energy conditions implied by the conglomerate. This study was undertaken to determine how the deposit formed. Bulk rock samples were taken parallel to shoreline and analysed using geochemistry and microscopy. The conglomerate is likely an alluvial fan deposited reworked locally along the shoreline. The conglomerate lies west of a col at the lowest point between Nasikie Engida and Lake Magadi, suggesting that connection of the lakes and associated hydrological and hydrochemical changes might have been important in forming the deposit. Much of the conglomerate is composed of authigenic components like silica clasts and laminar carbonate clasts. These laminar carbonate clasts are potentially stromatolitic. The silica clasts, which have an internal spherulitic fabric, and silica cement warrant further study.

ACKNOWLEDGEMENTS

Thank you to my advisor, Robin Renaut, for giving me this opportunity and for taking me to Kenya. Thanks also to his colleagues, Bernie Owens and Tim Lowenstein, for their advice in the field, as well as Tom Bonli, Dinka Besic, and Blain Novakovski for their help with sample preparation and analysis.

I couldn't have done this without the support of my parents, Gord and Clara Felske, and my husband, Robert Morrison.

TABLE OF CONTENTS

LIST OF TABLES

LIST OF FIGURES

1. INTRODUCTION

1.1. Overview

Calcrete, also termed caliche or kunkar, is a terrestrial accumulation of calcium carbonate (limestone) that forms either at or below the contemporary land surface, where $CaCO_3$ is precipitated from surface runoff and pore fluids, or from groundwater near the vadose-phreatic fluid contact. Calcrete forms either biogenically, associated with CO_2 loss resulting from plant root transpiration or microbial processes, or abiotically from evaporation or degassing of CO_2 from groundwater within sediments or soils, or from surface flow across exposed bedrock (Goudie, 1973, 1983; Reeves, 1975; Esteban and Klappa, 1983; Wright and Tucker, 1991; Watson and Nash, 1997; Alonso-Zarza, 2003; Wright, 2007; Alonso-Zarza and Wright, 2010; Brasier, 2011). Calcrete formation has often been thought an indicator of contemporary semi-arid conditions, but can also form in other climatic settings (Alonso-Zarza and Wright, 2010).

Calcretes are common in East Africa, in both present and formerly drier regions, particularly in the semi-arid regions of Kenya, Tanzania and Ethiopia. They are also common in the Neogene continental sediments and, in many places, mantle the land surface as resistant erosional remnants. Although widespread, calcretes have rarely been a focus of study in East Africa so little is known about their origins and paleoenvironmental significance. Hay and Reeder (1978) studied their origin in Pleistocene sediments of Olduvai Gorge in Tanzania. Renaut (1993) examined late Pleistocene calcretes on the northern margin of Lake Bogoria. In most examples, however, calcretes are interpreted as representing a relatively 'dry interval' during periods of little net sedimentation, preserved in stratigraphic successions of fluviatile and lacustrine sediments.

Calcrete, locally up to at least 50 cm thick, is exposed in many locations in the southern Kenya Rift, including the greater Magadi basin, which contains modern saline, alkaline Lake Magadi, and the Olorgesailie basin, which contains a thick succession of mid- to late Pleistocene fluvial and lacustrine deposits, and paleosols. These carbonates have been largely ignored. Baker (1958, 1963) gave brief descriptions when geologically mapping the region. Eugster (1980) interpreted the calcrete layers as having formed at the interface between dilute runoff and brine. Using geochemical criteria, he argued that mixing dilute runoff and saline, alkaline waters would lead to supersaturation of calcium carbonate allowing calcite to precipitate, with $CaCO_3$

nucleation occurring on detrital chert fragments, and with further carbonate coatings producing pisoliths. Eugster's (1980) work, however, did not consider the various laterally-equivalent expressions of the calcretes found at Magadi, which can be pisolitic, massive, or laminar. He also considered there to be only one main calcrete horizon, which capped mid-Pleistocene fluvio-lacustrine sedimentary rocks (the 'Oloronga Beds'). Several calcrete horizons are also present in the Pleistocene sediments of the neighbouring Olorgesailie basin to the northeast. The latter have never been studied in detail, but some may be of similar age to those of the neighbouring Magadi basin.

1.2. Objectives

The main aim of this research is to interpret the origins and paleoenvironmental significance of the several types of calcrete in the Magadi and Olorgesailie basins, based on fieldwork (mainly stratigraphic), and petrographic and geochemical analyses of samples collected. A secondary aim is to provide more general criteria that can be used to interpret the many other modern and ancient calcretes in East Africa, including those in Neogene sequences.

Previous research on the sediments of the Magadi basin has focused on understanding:

(1) the origin of the Lake Magadi basin waters and their associated sodium-carbonate evaporites -- mainly trona [$Na_3(CO_3)(HCO_3)\bullet 2H_2O$] and nahcolite ($NaHCO_3$) (Baker, 1958, 1963; Eugster, 1970; 1980, 1986; Jones et al., 1977);

(2) the origin of the abundant cherts, some of which recrystallized from magadiite and sodium-aluminium silicate gel precursors (Eugster, 1967; Eugster and Jones, 1968; Hay, 1968). Many of these cherts contain biological structures (microbialites) now composed of quartz, some of which might have precipitated from a non-crystalline (opal-A) precursor (Behr and Röhricht, 2000; Behr, 2002); and

(3) the many diagenetic minerals (especially zeolites, fluorite and villiaumite) that precipitated in lake- and groundwaters of variable compositions. Some of these minerals precipitated directly from lake or pore fluids to form cements; others formed by reactions between the lake- and pore-fluids with other minerals -- especially detrital volcanic glass (Surdam and Eugster, 1976).

Calcretes and thin carbonate rock coatings cover extensive areas of the land surface in the Magadi-Olorgesailie region, and calcretes are common stratigraphic units in the Quaternary fluvio-lacustrine strata. The calcretes of the southern Kenya Rift have never been studied in detail. This research is the first attempt to examine their stratigraphic context, petrology and geochemistry, and to determine whether they are pedogenic calcretes, influenced mainly by soil and plant processes, or groundwater calcretes, precipitated mainly by abiotic processes at or near the water table. This study also aims to provide new information to help to interpret the long timespan represented by only a thin (~50 cm thick) calcrete at Lake Magadi, and to explain the origin of the calcretes in the sediments that overlie much of the Pleistocene Olorgesailie Formation.

In summary, the aims of this research are to:

1. Determine how the calcretes formed at Magadi and Olorgesailie;

2. Develop a general model for calcrete development in the southern Kenya Rift Valley that can be used to understand the paleoenvironments of their formation, both there and elsewhere in the East African Rift;

3. Determine the origin of unusual carbonate-silica cemented conglomerates along the southern shoreline of Nasikie Engida; and

4. Consider the paleoclimatic conditions during formation of the calcretes.

1.3. Geological and environmental setting

Lake Magadi (Fig. 1-1; 1°53’19.10”S, 36°17’44.85” E: elevation: ~ 600 m) and Olorgesailie (Fig. 1-2; 1°34’40.13”S, 36°26’41.52” E: elevation: ~ 970 m) lie in the southern Kenya Rift, 60 km (Olorgesailie) to 100 km (Magadi) southwest of Nairobi. The Kenya Rift is part of the eastern branch of the East African Rift system (EAR), which extends southwards from the Afar triple junction in Ethiopia through Kenya into Tanzania and further south (Fig. 1-1.).

Rifting began in the Paleogene, ~ 30 million years ago, after a mantle plume rose from below the continental crust and led to domal uplift in central Kenya and Ethiopia (Baker and Wohlenberg, 1971; Chorowicz, 2005; Nyblade, 2011; Halldórsson et al., 2014). Rifting was influenced by old tectonic lineaments inherited from Precambrian basement rocks (McConnell,

1972; Ebinger et al., 1997; Le Turdu et al., 1995), though this interpretation has been questioned because geophysical data imply that the boundary between the Tanzanian Craton and the Mozambique (mobile) Belt lies farther to the east than originally proposed and that a thin layer of Mozambique Belt rocks overlies the Tanzanian Craton (Dawson, 2008). The rift propagated southwards from the Afar triple-junction into Tanzania, which has experienced active rifting only since 1.2 Ma (Dawson, 1992). Southward extension of the eastern arm of the rift was limited by the Tanzanian Craton (Ebinger et al., 1997), as shown by the differences in crustal structure at ~ 2°S (Albaric et al., 2009; Dawson, 1992). At the land surface this is resolved as a diffusion of the relatively narrow rift zone (50 km wide) into a broad plain in northern Tanzania (200 km wide), where the rift zone divides. This is termed the North Tanzanian Divergence (LeGall et al., 2008). The development of the northern Tanzania basins, which include the Natron basin, occurred from ~ 5 to 3.5 Ma (Tiercelin and Lezzar, 2002).

The Kenya Rift is seismically active (Mulwa et al., 2014), experiencing lithospheric thinning due to a rising body of hot mantle (Prodehl et al., 1997). Most recent seismic activity in the Kenya Rift has been recorded just north of Lake Magadi. The recent earthquakes, however, are minor (scale: $M < 4$; Ibs-von Seht et al., 2001). At Lake Magadi, the rift is a structurally complex graben–half-graben depression, trending NNE-SSW parallel to the main border fault, the Nguruman Escarpment, which lies 15–25 km west of the lake (Fig. 1-1). A secondary tectonic direction (NNW-SEE) inherited from the underlying Mozambique Belt basement rocks, termed the Asua-Nandi-Loita shear zone, intersects the main N-S Tertiary rift fault-zone. Faults following this pattern have produced the western arm of Lake Magadi (Dawson, 2008). At the junction between these fracture zones, located near the southern end of the lake, an increase in microcrack porosity may explain the paucity of earthquake events south of the lake, while the north of the lake experiences much more seismicity (Ibs-von Seht et al., 2008). Earthquake swarms recorded to the north, along with anomalies related to a rise of the brittle-ductile transition zone and a gravity anomaly implying mafic material within the crust, indicate the presence of a mid-crustal mafic magma body (Ibs-von Seht et al., 2008). A possible trigger for these swarms is a change in pore pressure from fluid flow or magma degassing (Naujoks et al., 2007).

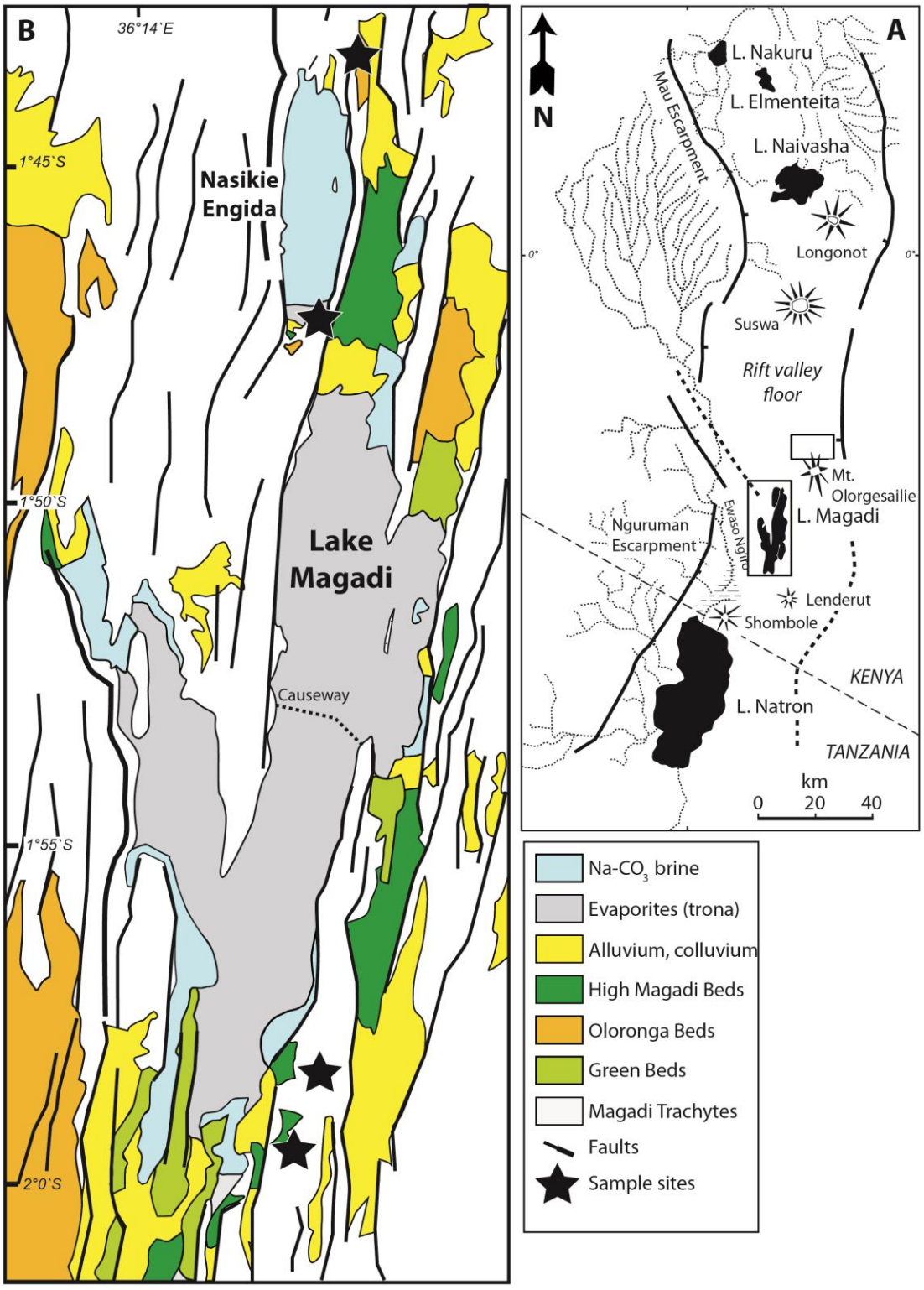

Figure 1-1. Map of Lake Magadi Area. A) Regional location, square boxes indicate map areas shown in 1-1.B and 1-2. B) Geological map of Lake Magadi showing sample locations. Modified from Scott (2010) and Guth and Wood (2013).

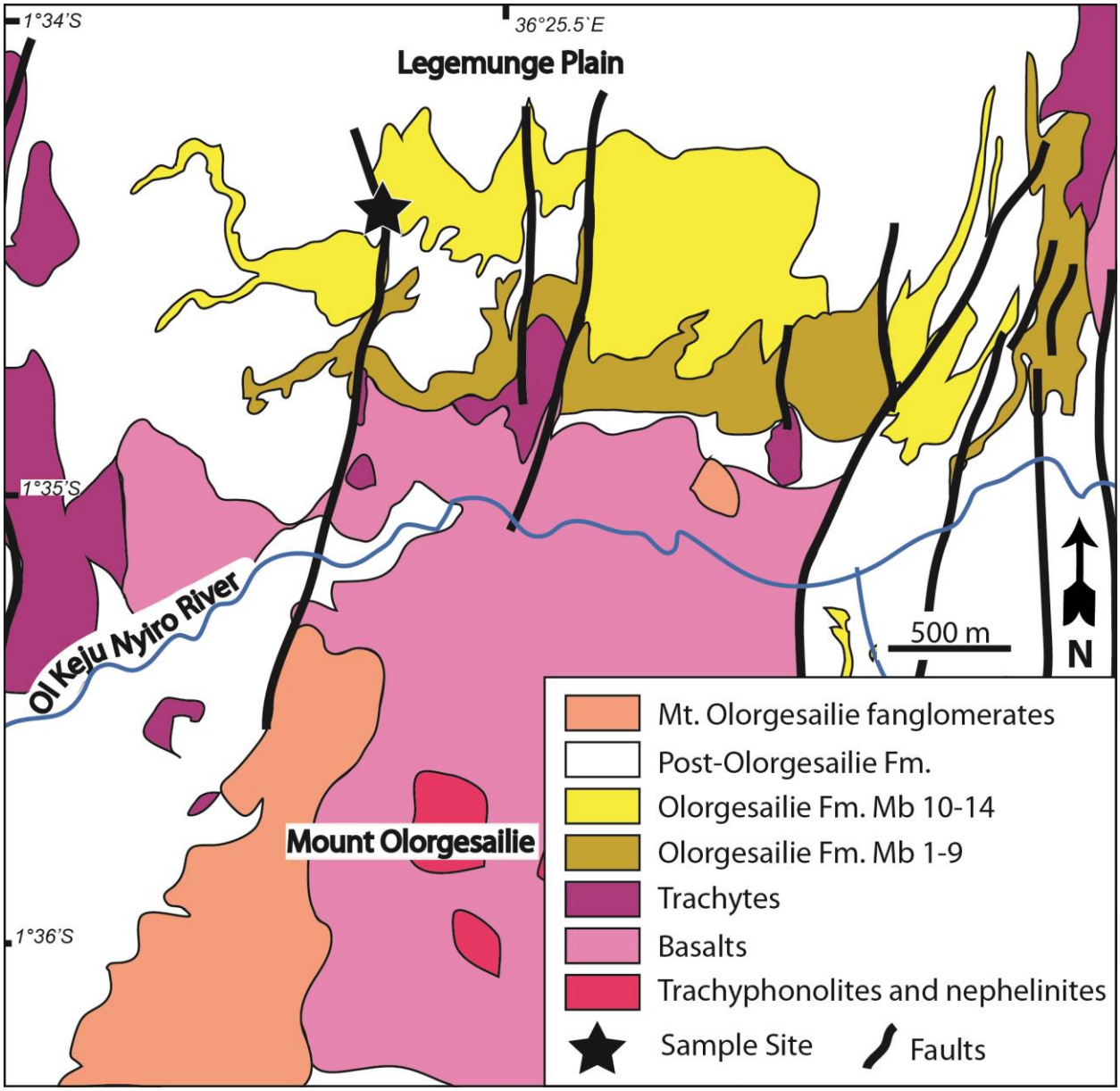

Figure 1-2. Map of Olorgesailie geology. Modified from Owen et al., (2009)

The tectonic record, preserved in the Oloronga Beds of Magadi, the Olorgesailie Formation and the Middle Pleistocene volcanics of Ol Doinyo Nyokie to the NE of Magadi shows that major grid faulting occurred from 0.8 to 0.4 Ma in the Magadi-Natron basin (Fairhead et al. 1972), with episodic faulting continuing until the mid-Pleistocene at Olorgesailie (Isaac 1978) and from 2.25 to 0.36 Ma at Magadi (Dunningham, 2005, cited in Dawson, 2008). Behr (2002) also reported phases of faulting in the Magadi basin during the last 800,000 years,

recorded in the lake sediments. The extensive faulting in the area hinders stratigraphic correlation of the sediments, which are preserved only in discontinuous outcrops.

Many types of volcanic rocks are present in the Kenya Rift, including flood basalt, trachyte and phonolite, and central volcanoes that erupted basalt, trachyte, carbonatite and natrocarbonatite lavas and tephra. Widespread extrusive volcanism in the southern Kenya Rift ceased in the mid-Pleistocene with the Magadi Trachytes, also called 'Plateau Trachytes', which formed from ~ 1 Ma until 0.78 Ma (Fairhead et al., 1972). Flood volcanism in the Kenya Rift ended some time between ~ 0.8 and 0.3 Ma (Baker, 1988), but caldera volcanoes continued to develop in the axial rift. Suswa caldera, ~ 45 km north of Olorgesailie, was active from ~ 240 to < 100 ka (White et al., 2012). Ol Doinyo Lengai, a natrocarbonatite volcano about 100 km to the south of Magadi in northern Tanzania, has been active since ~ 22 ka (Dawson, 2008).

A variety of lakes fill the half-graben depressions of the Kenya Rift. Most of the rift lakes are saline and alkaline with high pH (> 9), reflecting the mineralogy of the rift volcanics, the lack of outlets, and the high evaporation rates that characterize the semi-arid climate. Lake Bogoria, for example, is a shallow (< 10 m), saline, alkaline lake that is fed by ~ 200 hot springs, with TDS (Total Dissolved Salts) values up to 50 g/L for the surface waters and 100 g/L for bottom waters (Renaut et al., 1986; Renaut and Tiercelin, 1994; De Cort et al., 2013). Lake Turkana in northern Kenya, the largest of the Kenya rift lakes, is fed by the Omo River, and has an average of 2500 ppm TDS and pH of 9.2 (Yuretich and Cerling, 1983; Cerling, 1994; Yan et al. 2002). However, freshwater lakes are also present: Lake Baringo, only 22 km from hot-spring-fed saline, alkaline Lake Bogoria, remains fresh (0.9 ±0.3 g/L TDS) despite high rates of evaporation, probably because of subsurface seepage through the underlying faulted volcanic rocks (Tarits et al., 2006). Such differences in salinity between neighbouring lakes within the same geographical area highlight the highly variable nature of the Kenya Rift Valley in terms of climate, hydrology, and tectonics.

1.4. Methods

In total, 37 large samples of calcrete and the associated (host) sediments were collected from the Lake Magadi area and at Olorgesailie during the July-August 2011 field season. R. Renaut had previously collected calcrete samples from the same sites at Magadi in November 1991 and July 1996, several of which were included in this study.

Although widely distributed, calcrete samples were chosen from four areas at Magadi-Olorgesailie, where they are well exposed and their stratigraphic context is clear.

1: Samples were taken and sections measured at the 'Dry Lagoon' of Eugster (1980, 1986, his Fig. 2), where a well-developed calcrete separates greenish silts of the mid-Pleistocene Oloronga Beds from the overlying pale-brown tuffaceous silts of the late Pleistocene High Magadi Beds. This calcrete was also sampled upslope along a 250 m traverse ending at ~ 639 m elevation.

2: Thin carbonates (interpreted as laminar calcrete) that coat Magadi Trachyte ~ 150 m above the fan-delta at Graham's Lagoon were sampled. This limestone coats trachyte ~ 34 m above modern lake level.

3. A calcite-cemented lake-marginal conglomerate was sampled along a ~125 m transect parallel to the southeast shoreline of Nasikie Engida, the small saline lake north of Lake Magadi. The conglomerate overlies High Magadi Beds. When collected, the conglomerate was considered a possible type of calcrete, but this interpretation has been revised based on the results of this study.

4. At Olorgesailie, ~3.3 km NEE from the main Olorgesailie Prehistoric site, a 3.5 m stratigraphic section of downcut post-Olorgesailie deposits was recorded and the three calcrete intervals it contained were sampled as well as the sediments between and below the calcretes.

Large thin sections were prepared of 47 samples and their microfabrics determined using a petrographic microscope. The classification of microfabrics proposed by Wright (1991) was used to make preliminary interpretations.

Scanning electron microscopy (SEM) of 4 samples was undertaken using a JEOL JSM-840A at 20.0 kV on gold-coated, freshly fractured surfaces at the University of Saskatchewan.

Samples were analysed for chemistry by ACTLABS, Ancaster, Ontario, using the following methods: FUS-ICP for major oxides, Be, Sr, V, Zr, and Y; INAA for Au, Ag, As, Ba, Br, Co, Cs, Hf, Hg, Ir, Rb, Sb, Sc, Se, Ta, Th, U, W, and the lanthanides; TD-ICP for Bi, Cd, Cu, Mo, Ni, Pb, S, and Zn.

For stable isotope analysis, calcrete and other sediment samples were heated under vacuum at 200°C for 1 hour to remove volatiles and organic components. Stable isotope values were obtained using a Finnigan Kiel-IV carbonate preparation device directly coupled to the dual inlet of a Finnigan MAT 253 isotope ratio mass spectrometer. Approximately 20–50 micrograms

of sample was reacted at 70°C with 3 drops of anhydrous phosphoric acid for 420 seconds. The CO_2 evolved was then cryogenically purified before being passed to the mass spectrometer for analysis. Isotope ratios were corrected for acid fractionation and ^{17}O contribution using the Craig correction (Craig, 1957), and reported in per mil notation relative to the VPDB scale. Data was calibrated against the international standard NBS-19 ($\delta^{13}C$ = 1.95‰ and $\delta^{18}O$ = -2.2‰ VPDB) with a precision of 0.05‰ and 0.11‰ for $\delta^{13}C$ and $\delta^{18}O$, respectively (n = 25).

Backscattered electron imagery and EDS (energy-dispersive X-ray spectroscopy) analyses were obtained using a JEOL JXA-8600 Superprobe electron microprobe analyser with a setting of 15kV at the University of Saskatchewan using appropriate standards.

X-ray diffraction was accomplished using CuKα radiation with a range of 5 to 81° at the University of Saskatchewan using acetone smears on a Rigaku RU 200 X-ray diffractometer.

1.5. Thesis structure

This thesis contains six chapters including this introductory chapter. Chapter Two reviews the calcrete literature and summarizes calcretes in the East African Rift. The remaining chapters are denoted by study area. Chapter Three describes the calcrete capping the Oloronga Beds at Magadi and an example of the widespread laminar calcrete that coats trachyte bedrock in the Magadi basin. Chapter Four focuses on the post-Olorgesailie Formation calcretes at western Olorgesailie. Chapter Five discusses the unusual Holocene carbonate-cemented conglomerates at Nasikie Engida. The final chapter considers the results of this work and their broader implications, and gives a summary and the main conclusions.

2. CALCRETES IN EAST AFRICA

2.1. Overview of calcretes

2.1.1. Definition and occurrence

Calcretes are terrestrial accumulations of carbonate produced biogenically by root transpiration (e.g. Wright et al., 1995) or microbial processes (e.g. Wright, 1986), or abiotically by the evaporation of shallow groundwater or surface flow within sediments, soils, or on rock surfaces (e.g. Nash and Smith, 2003), both calcareous and non-calcareous, producing at its most evolved state a layer of pervasively calcite-replaced reworked, then re-cemented, material (Stage VI of Machette, 1985). Many terms have been used to describe calcretes, such as "caliche", "kunkar", "cornstone", "croûte calcaire" and others (Goudie, 1983). Calcrete is the preferred term.

Calcretes are found worldwide. An estimated 13% of the current land surface hosts calcrete (Yaalon, 1988). They are present mainly in sediments younger than Silurian, supporting the importance of vascular plants in their formation; however, they may be under-represented in older deposits due to the obfuscation of alteration (Brasier, 2011).

2.1.2. Classification

Calcretes have many morphologies and commonly show vertical variation within a single profile. The carbonate is typically low-Mg calcite although dolomite may also occur (e.g. Hay and Reeder 1978; Colson and Cojan, 1996; Khalaf, 2007). The carbonate is present as diffuse powder, nodules, laminations, cements and grain coatings, pisoids and as massive cemented horizons. The boundaries of the calcrete may cross bedding planes of the host deposits. Where the calcrete is denuded or exhumed and resistant to erosion, it can form an important discontinuity surface of local or regional extent.

Classification of calcretes is difficult because of their wide variety in morphology and occurrence. The most common classification, which is genetic, separates calcretes into 'pedogenic' and groundwater-related ('non-pedogenic') varieties, but these are frequently difficult to distinguish, and individual profiles may have multiple origins. Several methods to

characterize the two have been proposed. Groundwater calcretes, for example, are thought to have a sharp top and a sharp base, whereas pedogenic calcretes may have a gradational base. Another method to determine the realm of genesis is to inspect clast coatings in thin section for pendant cements: typically water in the vadose (aerated, soil) zone above the water table will concentrate at the bases of clasts under gravity, forming a thicker cement. Conversely, groundwater (phreatic) cements are commonly isopachous because they form where water fills all accessible pore spaces.

Calcretes are also classified based on micromorphology viewed in thin section. Textures visible at light-microscopy scale were classified by Wright (1990) as either *alpha* (abiogenic) or *beta* (biogenic) microfabrics (Fig. 2-1).

Beta microfabrics include alveolar septal structures, produced by fungi frequently associated with plant roots; needle-fibre calcite, which is also associated, though not exclusively, with fungal and bacterial activity; and a specific fabric termed *Microcodium*. The origin of *Microcodium* is debatable. It is commonly thought to be the product of root calcification (Košir 2004); however, Singh et al. (2007) and Kabanov et al. (2008), among others, attribute *Microcodium* to the activity of fungi (possibly mycorrhizal) and bacteria in the rhizosphere. The fabric is usually considered biogenic even if the producer(s) is uncertain. Alpha microfabrics include carbonate nodules, in which biotic indicators are not observed; circumgranular cracks; complex crack networks; and grains floating in a matrix.

Alpha microfabrics, which imply diminished biotic processes or their absence, typify groundwater calcretes, whereas beta microfabrics typify pedogenic calcretes. However, these microfabrics are end-members of a spectrum. All factors must be considered before assigning a genetic classification.

Calcretes are part of a terrestrial carbonate continuum and as such they may grade into or be found alongside palustrine carbonates or spring carbonates depending on environmental setting (Alonso-Zarza, 2003; Brasier, 2011). There are some major differences: palustrine carbonates are typically more fenestral and frequently bear charophyte-related fabrics, while spring carbonates have dendritic calcite and encrustations.

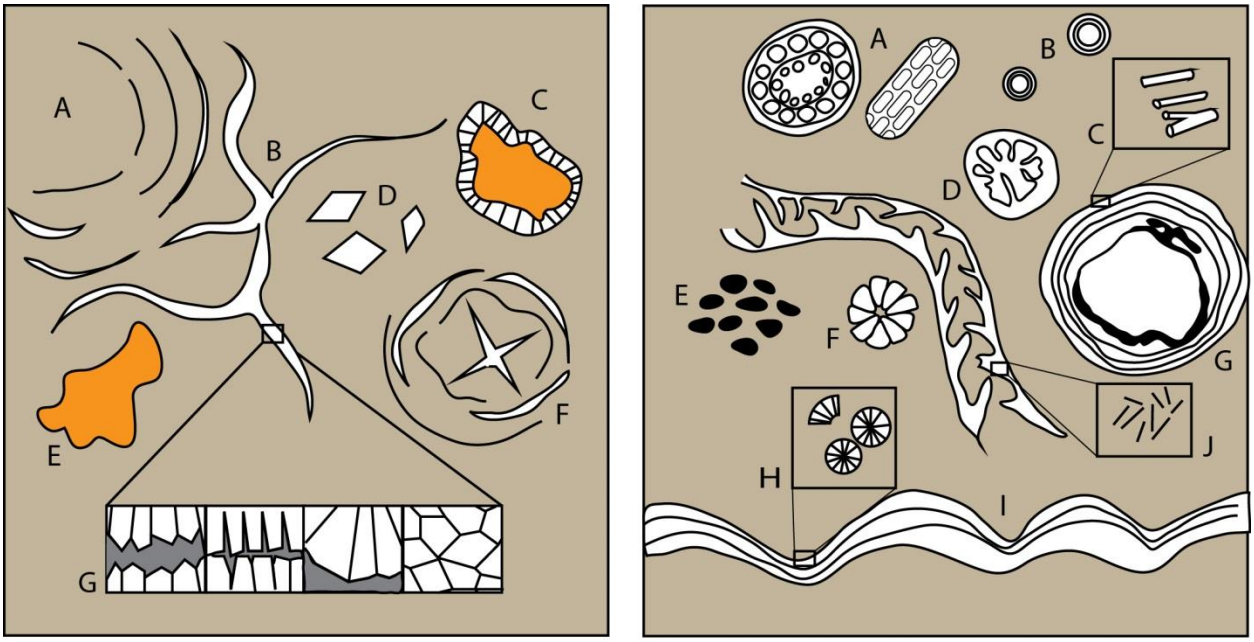

Figure 2-1. *Alpha* and *beta* Microfabrics. ***Alpha***: A) Nodule formation. B) Complex cracks. C) Corona rims around grains. D) Floating euhedral calcite crystals. E) Floating grains. F) Intra-nodular cracks. G) Pore-filling calcite cements; bladed, palisade, botryoidal and mosaic types. ***Beta***: A) Calcified root cells. B) Ooids. C) Calcified filaments. D) Alveolar-septal fabrics. E) Peloids. F) *Microcodium*. G) Microbial coatings. H) Spheroids. I) Wavy-laminar stromatolitic fabric. J) Needle fibre calcite, inferred to be related to microbes. Modified after Wright et al. (1991) and Zhou and Chafetz (2009).

2.1.3. Mechanisms and models of formation

The mechanisms by which calcium carbonate is precipitated include supersaturation induced by evaporation or water removal by plants (evapotranspiration); CO_2 degassing to equilibrate with atmospheric CO_2; the common ion effect, through the addition of chemically different meteoric water and (or) groundwater; root transpiration that decreases soil pCO_2; conversion by fungi of oxalic acid to calcium oxalate, which is then transformed into calcium carbonate through bacterial bio-oxidation (Verrecchia and Dumont, 1996); and direct precipitation by microbial mediation (Monger et al., 1991).

Calcium availability is commonly the limiting factor in carbonate mineral formation. Ca may be sourced from the soil or sediment by chemical alteration, from biotic material (skeletal), from calcium-enriched groundwater or percolating runoff, or from rain and windblown dust. In the East African Rift, calcium may also be supplied from carbonatite ash, although globally this

is a rare source (Hay and Reeder, 1978; Alonso-Zarza and Wright, 2010). The carbonate is supplied by meteoric water, percolating from above ('*per descensum*' model of Goudie, 1973). For calcretes formed at or near the water table, however, bicarbonate can be supplied by groundwater, with carbonate species (HCO_3^- and CO_3^{2-}) sourced from below, travelling as ions in the capillary zone above the groundwater table ('*per ascensum*' model of Goudie, 1973, and Wright and Tucker, 1991).

2.1.3.1. Pedogenic calcretes

Pedogenic models of calcrete formation are better developed than those for non-pedogenic calcretes. These include, for example, the well-known model of Machette (1985), building on earlier work by Bachman and Machette (1977) and Gile et al. (1966), who established stages of calcrete formation on non-calcareous deposits (Fig. 2-2 A). They proposed six stages of calcrete formation, which take into account the grain size of the host material. For deposits with high gravel content (> 50%), stage I is the least developed, consisting of thin, discontinuous coatings on the bases of grains. Stage II has continuous coatings which range from thin to thick on the tops and bottoms of grains. At stage III, a calcrete with coarse clasts becomes progressively more indurated, with much precipitated carbonate amassed between clasts proceeding towards full cementation. For deposits that initially had less gravel (< 20%), stage I consists of carbonate-encrusted filaments in the soil or paleosol, and thin coatings on ped surfaces. Small (0.5–4 cm), soft carbonate nodules have developed by stage II, and by stage III, those nodules have grown together and the matrix has been cemented.

For the first three stages (I to III), the soil is still morphologically a soil; from stages IV to VI, however, the soil is firmly indurated and the morphology of the calcrete no longer differs between coarse and fine-grained host material. Laminae up to 1 cm thick develop in stage IV, covering the earlier cemented horizon (s) and coating fracture surfaces, forming a calcrete from 0.5–1 m thick. Stage V includes thicker calcite laminae (> 1 cm) which coat vertical surfaces as well as fractures, and pisolites (pisoids). Stage V calcretes are typically 1–2 m thick. Calcretes at stage VI consist of an indurated horizon that has undergone brecciation and re-cementation several times, leading to multiple generations of pisolites and laminae that often build from older generations of lithified carbonate. Such calcretes are commonly more than 2 m thick.

Though the stages of this model are successive, the time it takes for each stage to develop is highly variable. Two calcareous soils that formed during the same time interval can have different profile characteristics that, in turn, represent different stages of calcrete formation.

Another common model for pedogenic calcretes (Esteban and Klappa, 1983), describes a profile of calcrete ranging from host material to hardpan at the top and is essentially equivalent to a stacked VI stage model (Fig. 2-2 B). Calcretes have also been categorized based on morphology for geotechnical use (Netterberg and Caiger, 1983).

The American soil classification uses soil-profile terms to indicate a calcrete, which in their parlance is a 'K horizon', as well as 'calcic horizon' (for less developed forms), and a 'petrocalcic horizon' (for indurated horizons). K horizons denote discrete accumulations of calcium carbonate within a soil profile with a 'K-fabric'—the coating of grains with carbonate. K horizons are usually found within B horizons, which are zones of illuviation, and are also termed Bk horizons, though $CaCO_3$ accumulations are also found in C horizons. Soils in which calcretes form are typically aridisols, vertisols, mollisols and alfisols (Soil Survey Staff, 1999; Wright and Tucker, 1991), and calcisols, and durisols (IUSS Working Group WRB, 2015). In the Canadian soil classification system, zones of secondary carbonate accumulation are referred to as 'Cca', for mineral zones of calcium carbonate accumulation, and 'Cc' or 'Ccc' for cemented horizons (Soil Classification Working Group, 1998).

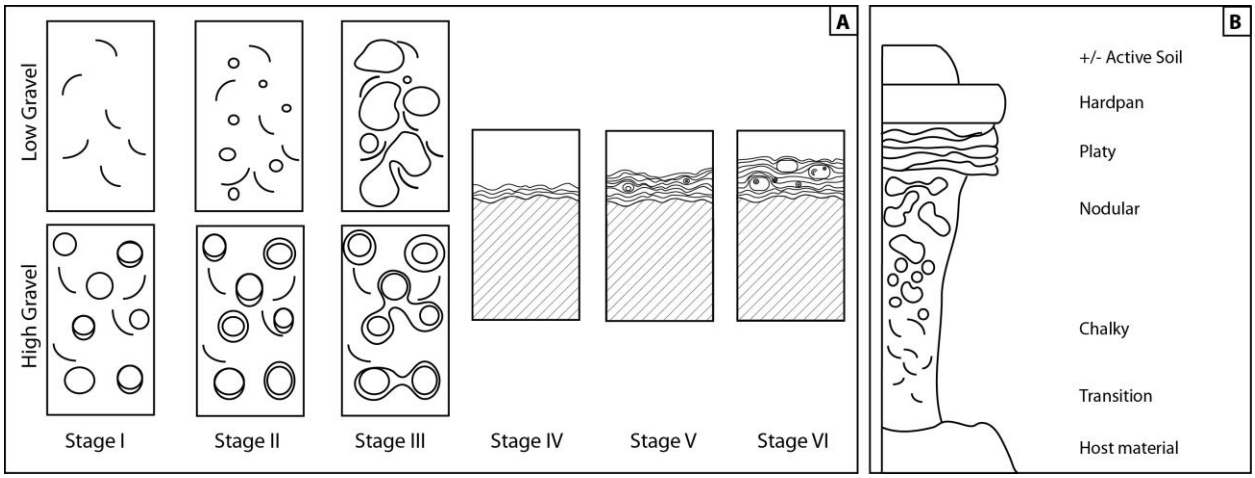

Figure 2-2. Previous page. Models of pedogenic calcrete formation. A) The VI-Stage model of Machette (1985) built upon work by Gile et al. (1966). See text for explanation.. B) Idealized pedogenic calcrete profile of Esteban and Klappa (1983).

2.1.3.2. Non-pedogenic calcretes

Carbonate cementation in non-pedogenic calcretes occurs at, or slightly above, the contemporary groundwater table and results from CO_2 degassing, precipitation from saturated groundwater, or from the 'common-ion effect' (Goudie, 1983). If the groundwater table is shallow (i.e. less than ~ 1 m), calcite precipitation can also be accomplished by evaporation, evapotranspiration, or other biotic processes.

Carlisle (1983) classified non-pedogenic calcretes into four genetic types: superficial calcretes, gravitational-zone calcretes, groundwater calcretes, and detrital and reconstituted calcretes.

Superficial calcretes, also termed laminar calcrete and gully-bed cementation, involve the surficial transport of carbonate in runoff. Laminar calcretes can also form from cyanobacterial activity (Verrecchia et al., 1995), from root activity (Alonso-Zarza, 1999, Alonso-Zarza and Jones, 2007), or from physicochemical processes (Carlisle, 1983).

Groundwater calcretes are further subdivided using geomorphic constraints: lake marginal calcretes (Renaut, 1993; Sakai et al., 2010), deltaic calcretes (Carlisle, 1983), channel calcretes (Nash and Smith 1998; Nash and McLaren, 2003; Nash and Smith, 2003; McLaren, 2004), valley calcretes (Pimentel et al., 1996; Jutras et al., 2007), and alluvial fan calcretes (Stokes et al., 2007). Groundwater calcretes are typically composed of mostly alpha microfabrics that often preserve the original sediment texture, and can be up to several meters thick (Carlisle, 1983). Carbonate cementation happens at or a few cm above the capillary fringe, at, or just below the water table. Instead of a predominantly vertical transport of calcium and carbonate, these ions are transported laterally which can lead to extensive deposits.

Lake marginal calcretes and deltaic calcretes can be produced when and where waters of different salinities mix, or the water table becomes sufficiently high for evaporation to proceed. Change in water table depth is accomplished by a change in topographic gradient, as with a delta, or by lacustrine clays forming a semi-impermeable barrier which aids in keeping the water table high. Lake margin calcretes may grade into palustrine carbonates, which are the lacustrine

equivalent of peritidal deposits. Differences in water table level, plus mixing waters, are mechanisms by which the other types of groundwater calcrete are formed (Jutras et al., 2007).

Channel calcretes are lensoid carbonate-cemented channel sediments containing mostly alpha microfabrics, commonly with a gradation in cement crystal size —from coarse spar in the bottom of the channel where water remains longest, to micrite at the periphery (McLaren, 2004). Valley calcretes are similar in morphology but are more laterally extensive.

Alluvial-fan calcretes occur when the rate of sedimentation producing the fan decreases, and the groundwater table is sufficiently high for evaporation to take effect (Stokes et al., 2007). As sedimentation ceases, fan-surface sediment stabilization occurs, usually by plant colonization, so pedogenic calcretes can sometimes develop. Stokes et al. (2007) noticed that the distal end of the fan showed more pedogenic features, whereas the proximal fan had groundwater features, mirroring the lesser soil development in the proximal fan compared to the distal portion.

Calcretes commonly show composite fabrics in which inferred vadose and phreatic indicators overlap (Renaut, 1993; Bustillo and Alonso-Zarza, 2007; Khalaf, 2007). This is expected: in lake marginal sediments, calcretes may form during prolonged periods of low-water levels but remain within the influence of shallow fluctuating groundwater; if that area then undergoes a rise in lake level, older calcretes may be partly overprinted by the rising groundwater.

2.1.4. Climatic and other paleoenvironmental inferences

Calcretes form predominantly in semi-arid climates. If the rainfall is too high, the carbonate is leached from the profile; if too low, it becomes immobile. Optimal conditions are generally thought to occur where there is distinct seasonality – a wet season to move the carbonate, and a drier season where some carbonate can precipitate in the profile (Goudie, 1973; Wang et al., 1994; Passey et al., 2010). There are, however, exceptions. Strong et al. (1992), for example, studied a Holocene calcrete from northern Yorkshire, UK, and inferred that it represented accumulation in a cool temperate climate. Though many hot semi-arid regions have calcrete occurrences, cold semi-arid regions also yield calcretes, because precipitation (i.e. rain, snow) is the main factor: a calcrete in the Chinese Loess Plateau was found to form during colder, drier periods that post-dated pedogenesis (Rowe and Maher, 2000). Calcretes have been

found on all continents including Antarctica (McPherson, 1979; Retallack et al., 2007) and are indicative of mean annual precipitation of about ~ 100-–500 mm, though estimates range from 50 to > 1,000 mm/year (Goudie, 1973; Alonso-Zarza, 2003).

Calcretes may provide paleoenvironmental clues to the water source, temperature, amount of rainfall, and types of vegetation present during their formation. Pedogenic carbonates have been widely researched in terms of their C and O isotopes (Talma and Netterberg, 1983; Cerling, 1984; Quade et al., 1989; Cerling, 1992; Quade and Cerling 1995; Nordt et al., 1998; Robinson et al., 2002; Levin et al., 2004; Wynn, 2007). C isotopes are influenced predominantly by CO_2 from plant respiration as well as soil pCO_2, which is correlated with atmospheric pCO_2, and some have used calcretes to determine ancient pCO_2 levels (Robinson et al., 2002). C isotopes of soil carbonate are in equilibrium with the soil environment (Cerling, 1984; Quade et al., 1989). Soil carbonate $\delta^{18}O$ is related to the meteoric water from which the carbonate precipitates and is also a function of temperature (Cerling, 1984; Dworkin et al., 2005). Plant respiration has no effect on isotope fractionation of oxygen. For example, stable isotopes from stage II calcretes indicated drought conditions in New Mexico at ~ 9 ka (Deutz et al., 2001). Budd et al. (2002) used stable isotopes to determine the overprinting of a pedogenic calcrete by groundwater diagenesis. Using a clumped isotope thermometer, Passey et al. (2010) found a seasonal bias in carbonate formation in Neogene deposits near Lake Turkana using paleosol carbonates from the Nachukui and Shungura Formations. Because of the surficial nature of calcretes, care must be taken to interpret the paleoenvironmental conditions throughout the formation of the calcrete and its diagenetic history to have an accurate stable isotope interpretation (Kraus, 1999; Budd et al., 2002). Little research has been done on the stable isotopes of groundwater calcretes, though some studies suggest that $\delta^{18}O$ may be used to determine the sources of groundwater (Raidla et al., 2012). One study of Mississipian groundwater and pedogenic calcretes showed a positive correlation between $\delta^{13}C$ and $\delta^{18}O$ in the groundwater calcretes while the pedogenic calcretes did not show such a pattern (Jutras et al., 2007).

By determining the $\delta^{13}C$ value from calcretes, it is possible to state whether C3, C4, or CAM vegetation was dominant during calcrete formation (Cerling, 1984; Quade and Cerling, 1995; Alam et al., 1997; Levin et al., 2004; Behrensmeyer et al., 2007). The vegetation that uses the C_4 metabolic pathway is more enriched in the heavier isotope (^{13}C) than the vegetation using

the C_3 pathway, which preferentially uses the lighter ^{12}C atom. These values are reflected in both the soil organic matter stable isotopes and the soil carbonate stable isotopes. C isotopes for C_4 in carbonate are -11 to -13‰, whereas for C_3 they are -24 to -30‰ (Tanner, 2010). Plants which use the Crassulacean acid metabolism (CAM) pathway, such as succulents, have values that overlap both C_3 and C_4 vegetation, and are adapted to arid environments. The true values may vary from region to region but, in general, C3 vegetation has much lower $\delta^{13}C$ values than C4 vegetation.

Other paleoclimate information from calcretes is gleaned by measuring depth to carbonate (DTC) in a vertical profile; DTC is shallower in arid regions than more humid regions (Retallack, 2004). In studies of vertisols, Nordt et al. (2006) inferred that if the carbonates had not undergone diagenesis, DTC could be used to estimate paleoprecipitation. This method, however, cannot always be used: erosion of sediments overlying the calcrete, for example, can produce erroneous interpretations.

Ichnofossils can also help when interpreting the settings of calcrete formation. Fossil bee nests and other insect traces linked to the *Celliforma* ichnofacies have been found in calcretes in Spain (Alonso-Zarza and Silva, 2002), Uruguay (Alonso-Zarza et al., 2011), and the Canary Islands (Genise et al., 2013). In the Ogallala Formation (Miocene-Pliocene) in Kansas, for example, ant nests were found to be a major structural element in calcrete, perhaps even promoting calcrete development (Smith et al., 2011). Ants and termites typically live in well-drained soils in semi-arid environments and may be expected in certain calcrete deposits.

2.1.5. Timing of formation

Calcretes can form in timespans from 1000s to 100,000s of years (Machette, 1985; Wright and Tucker, 1991; Alonso-Zarza and Wright, 2010). Hay and Reeder (1978) found that due to the high calcium content and easy weatherability of natrocarbonatite ash, calcretes near Oldoinyo Lengai volcano in Tanzania, 90 km south of Magadi, formed in only about 1000 years. Additionally, Wynn and Retallack (2001), who studied paleosols that had developed on carbonatite host material of the Nyakach Formation in SW Kenya, stated that calcareous hardpans on carbonatite may form in less than 600 years. They also gave an age estimate for Bk horizons forming in similar conditions as 2–30 ka.

Groundwater calcretes generally form more quickly than pedogenic calcretes; for example, channel calcretes of Wadi Dana in southern Jordan, which are up to 5 m thick, were estimated to have formed in 2000 to 3000 years (McLaren, 2004).

However, because multiple phases of calcrete development might be represented in a single complex profile, caution is needed when using calcretes for dating unless the stratigraphy is clear (Candy et al., 2003). For young calcretes, absolute age dating may be attempted using ^{14}C, ESR, and U-series disequilibrium methods (Candy et al., 2003; Rowe and Maher, 2000).

2.2. Calcretes in East Africa

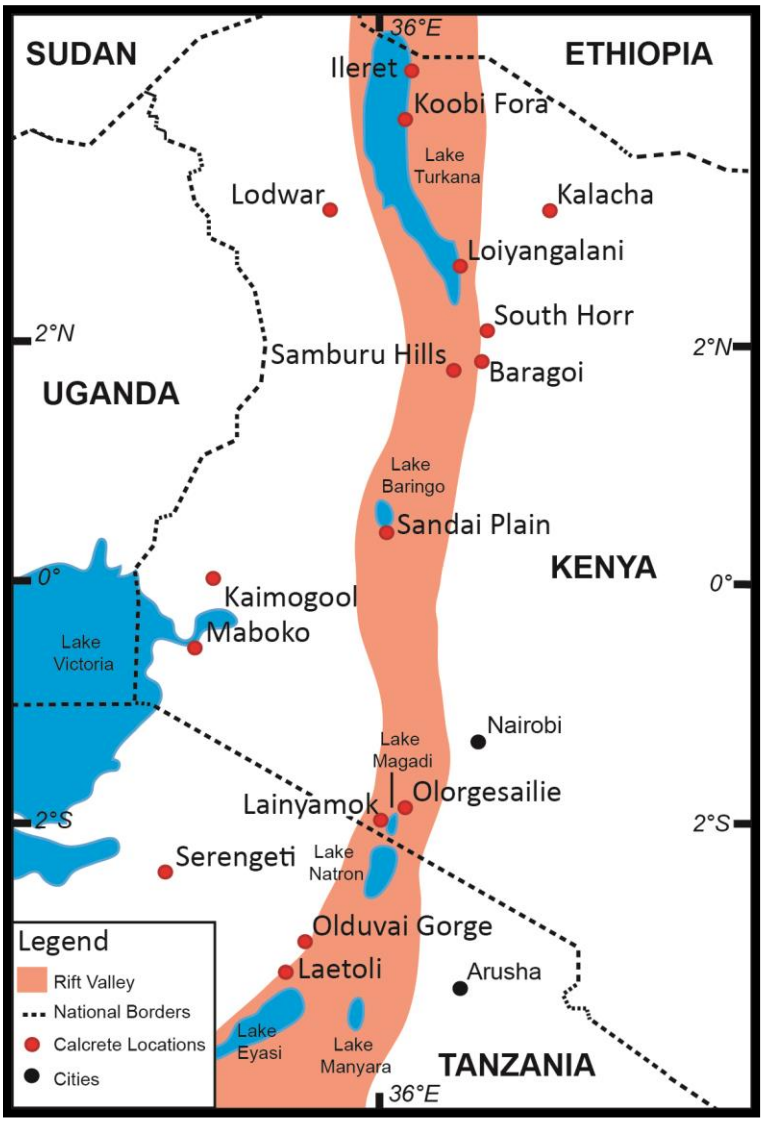

Figure 2-3 Locations of calcretes reported in the Kenya Rift Valley and northern Tanzania.

2.2.1. Association with archeological sites

Most archeological sites in East Africa are associated with present or former land-surfaces so some sediment sequences with artefacts and terrestrial faunal remains contain calcretes. Calcretes form a hard surface resistant to erosion that may protect underlying, less lithified sediments and any fossils or artefacts that they contain. Calcification is also effective in

preserving fossil bones (Bishop, 1966; Pickford, 1986). Pedogenic calcretes form near land surfaces that are used by animals and can sometimes incorporate a wide range of terrestrial faunal and floral debris. If all necessary parameters are met, calcretes may be radiometrically dated creating a temporal framework for sites of archeological importance.

That artifacts and vertebrate fossils are associated with, or lithified within, calcretes and other deposits that imply dry climates is not surprising. In relatively humid times, lakes might have filled the relatively narrow rift valley with its steep margins, leaving little room for habitation. During wetter periods, fresh water was available: animals and hominins would not have had to live near lakes, and ephemeral streams would often have been perennial, so vertebrates roamed farther from shorelines. In contrast, sites near more reliable sources of fresh water, including dilute springs, would have been more frequently occupied during drier times.

2.2.1.1. Olorgesailie, Kenya

The Pleistocene Olorgesailie Formation is a series of lacustrine, fluviatile and volcaniclastic sediments, and paleosols in the Kenya Rift Valley, ~ 35 km northeast of Magadi (Fig. 2-3). Many calcrete intervals are found within the formation, which contains abundant stones tools and vertebrate fossils including *Homo erectus*. Olorgesailie has long been a site of archeological exploration (Isaac, 1977, 1978), and determining how adaptation to the paleoenvironment affected early hominin behaviour and evolution has been part of this ongoing effort. A detailed record of changing environmental conditions during sedimentation has been developed for the 14 members of the formation (Owen et al., 2011, 2012, 2014). Calcretes in the post-Olorgesailie Formation sediments are discussed in Chapter 4.

Paleosols punctuate the Olorgesailie Formation, with the best developed paleosols occurring in Members 1, 7, and 11. These paleosols indicate relatively lower lake levels and the dominance of terrestrial environments during those times (Owen et al., 2008b). Calcretes are found mainly in Member 2, though carbonate nodules of uncertain origin are present at other stratigraphic intervals. Paleosols that contain abundant stone tools and vertebrate fossil bones and tracks, named UM1p and UM7p (for Upper Member 1 or 7 paleosol), commonly contain local pedogenic carbonate nodules (Deocampo et al., 2010). In Member 2, a marker horizon (‘EC’) contains crack-filling carbonate cement and casts of salt crystals, indicating a period of

increased aridity, possibly during a phase of seismic activity (Owen et al., 2012). Generally, the calcretes are considered horizons linked to periods of lake desiccation (Owen et al., 2008b) because they are associated with lake sediments containing fossil diatoms that imply increasing salinity and pH. Potts et al. (1999), however, described a nodular carbonate layer in upper Member 1 that resulted from a rise in the water table, and suggested that hominins would have found the contemporary climate and environment habitable. These carbonate nodules, however, might have formed by precipitation from groundwater, possibly linked to mixing of concentrated alkaline groundwater (because the preceding period was inferred to have been drier) with later dilute Ca-bearing meteoric water, leading to supersaturation of $CaCO_3$. Carbonate nodules in the UM7p paleosol, in contrast, are associated with pedogenic features.

Once fresh water resources had dried up or had become too saline or alkaline to drink, animals, including hominins, would have been be forced to move on, as might have been the case for example at UM7p at Olorgesailie. The latter may represent up to 190,000 years as a land surface, but has few fossils and artifacts (Deocampo et al., 2010). There remains a potential 'sweet spot' where conditions are just right, not only for preservation of artifacts and fossils, but also for formation of calcrete and carbonate-rich soils.

2.2.1.2. Lainyamok, Kenya

Lainyamok is a fossil-bearing locality about 8 km west of Lake Magadi that was studied by Potts et al. (1988) and Shipman et al. (1983). The mid-Pleistocene sediments there consist of mainly mudflow and lacustrine silts with three "khaki layers" as well as three carbonate horizons. Two of these limestones have 'boxwork' and 'honeycomb' structures—the carbonate forms around silt clasts as well as through cracks—and are interpreted to have formed at a lake margin from evaporative processes (Fig. 2-4). The third limestone, probably of lacustrine origin, caps the sediments, which are similar to the mid-Pleistocene Oloronga Beds of the main Magadi basin (Baker 1958), implying that the Lainyamok sediments are an outlying extension of the Oloronga Beds (Shipman et al., 1983). Age estimates of the fossil-bearing horizons in the sediments at Lainyamok are 0.70–0.56 Ma, which overlaps with the Oloronga Beds.

Fossils and artifacts found within the khaki-coloured sediments consist of a hominin maxilla fragment, a hominin femur and teeth, bones of several types of bovids and other large

animals, and a scattering of stone tools. However, due to lack of evidence for a butchery site, Potts et al. (1988) concluded that the accumulation of bones was due to hyena activity. Fossils were also found in the calcrete: the capping limestone contains fossil Suidae (Shipman et al., 1983).

Figure 2-4. - Calcrete profile from Lainyamok. First photo shows outcrops in the graben; calcrete is the resistant unit. Second photo shows the honeycomb calcrete. Photos from R. Renaut.

2.2.1.3. Olduvai, Laetoli, and Peninj, northern Tanzania

Calcretes and lacustrine carbonates, including stromatolites (Hillaire-Marcel and Casanova, 1987), are present in the northern Tanzania rift. Ol Doinyo Lengai, an active carbonatite volcano, and other older carbonatite centers in the area provided a source of abundant easily-dissolved calcium.

At Olduvai Gorge, Tanzania, carbonatite tuffs provided the material for calcretes, which formed at several levels within the Olduvai Beds, and range from 2000 y BP to 2.0 Ma (Hay and Reeder, 1978). Most of the calcretes are in sediments less than 600,000 years old. The host sediments are nephelinitic eolian tuffs from Kerimasi (older) and Ol Doinyo Lengai (younger) volcanic centers to the NEE. Calcretes are typically structured as a massive calcrete, possibly oolitic or pisolitic, overlain by a discontinuous laminar calcrete up to 4 cm thick (Fig. 2-5). Typically the calcretes are at and possibly controlled by disconformities in the underlying sediments. Hay and Reeder (1978) interpreted the Olduvai calcretes to be pedogenic but for one in the lower Masek Beds (calcrete dated at 0.5–0.6 Ma) interpreted to have resulted from

groundwater processes because of very thick coatings on the large pisoliths. These calcretes formed in a shorter time frame than most, which seems incongruent with their stage of formation (IV of Gile et al., 1966)—only a few thousand years as opposed to the general 100,000 years for that stage—because carbonatite ash is abundant in the area, providing abundant Ca and CO_3 for the carbonates to form (Hay and Reeder, 1978).

Figure 2-5. - Calcrete profile from Olduvai showing ~2 cm thick laminar carbonate coating massive calcrete. Photo from R. Renaut.

Calcretes and calcrete features are common at the Laetoli site, about 50 km SE of Olduvai Gorge, with many localities showing one or more calcrete horizons in section. The calcretes are concentrated in the Upper Laetolil Beds (3.63–3.85 Ma) and Upper Ndolanya Beds (2.66 Ma) (Harrison, 2011), with calcretes also occurring in the most recent sediments, the Ngaloba Beds (Late Pleistocene, Silal Artum site). A capping calcrete is present above the Lower Laetolil Beds in the Lobileita site (Harrison and Kweka, 2011). These calcretes appear to be largely pedogenic, as they are associated with predominantly pedogenically-modified sediments,

though some are described as “calcretised tuffs” and “diagenetic calcretes” (Ditchfield and Harrison, 2011) indicating that physicochemical processes were involved in forming them. The chemical composition of the carbonatite tuffs is such that modification through meteoric weathering would lead to carbonate cement (Hay and Reeder, 1978). Pedogenic calcretes appear to be correlated with topographic position; such calcretes are typically not found at the valley floor at Laetoli.

At Localities 9 and 10W at the Laetoli site, calcretes preserve termite hives probably made by *Macrotermes* (Darlington, 2011). These local calcretes occur as stacked horizontal layers 3–5 cm thick separated by narrow horizontal cracks and take on the form of termite galleries. Additionally, poorly preserved termite hives have a distinct “vermiform calcrete” structure occurring in soft matrix.

Calcretes in the Upper Ndolanya Beds are pedogenic and may have blocked drainage of a plain similar to the modern situation of the Serengeti, where local calcretes just below the land surface hinder drainage (Anderson and Talbot, 1965).

West of Lake Natron is the Peninj area (Fig. 2-3). Like Olduvai, Peninj has produced many archeological discoveries since the 1960s, including a mandible from *Paranthropus boisei* (e.g. Isaac, 1965; Torre et al., 2008; Diez Martín et al., 2009). The archeological sites were found within the Pleistocene Peninj Group and are interpreted as butchery sites located near where animals were killed (Dominiguez-Rodrigo et al., 2002). Dominiguez-Rodrigo et al. (2002) found that fossils and artifacts above a paleosol developed on carbonatite tuff had become cemented to the tuff by a bio-precipitated laminar carbonate within a river channel, preserving the original positions of the bones and tools. These occur within the dominantly deltaic Humbu Formation of the Peninj Group (Isaac, 1967).

2.2.1.4. Koobi Fora, Kenya

On the northeastern shoreline of Lake Turkana is the archeological site of Koobi Fora. Found in the 1960s, it has since yielded important Pliocene and Pleistocene fossils and artifacts of several species of hominins, in particular the genera *Homo* and *Australopithecus* (Spoor et al., 2007). The Koobi Fora Formation, part of the Omo Group, is located around the northeast of the lake and includes eight members. Pedogenic carbonates are common in all members (Gathogo and Brown, 2006). Pedogenic carbonates and calcretes are less well developed in the Turkana

region than those farther south. Cerling et al. (1988) surmised that the relative lack of calcretes compared to those of southern Kenya and northern Tanzania results from differing parent material and from basin dynamics—higher subsidence rates have meant less time for soils and calcretes to mature.

Carbonate nodules and other forms of pedogenic carbonate are found in many locations throughout the Koobi Fora Formation in the Ileret area. For example, the first interval of the fluvio-lacustrine Lonyumun Member has clay-rich mudstones at its top with rhizoliths and carbonate concretions, indicating a pedogenic calcrete (Gathogo and Brown, 2006). Another calcrete forms part of an important discontinuity surface between the Lonyomun Member and the overlying Lokochot/Tulu Bor Member representing a time interval of 0.46 Ma (Kidney, 2012). Within the Chari Member, a pedogenic calcrete overlies lacustrine fossiliferous sandstones and mudstones. This calcrete is associated with rhizoliths as well as sparse fossil termite nests of *Termitichnus* (Gathogo and Brown, 2006). These calcretes are associated with fluvial floodplain deposits. The Nachukui and Shungura Formations, which lie west and north (in Ethiopia) of the lake respectively, are correlatable with the Koobi Fora Formation (Tiercelin et al., 2010), and also contain pedogenic carbonates that record an increase in C_4 vegetation since 4 Ma (Levin et al., 2011). Using a clumped isotope thermometer, Passey et al. (2010) showed a seasonal bias in carbonate formation taking place in these soils that formed at temperatures greater than 30°C.

At Ileret, located near the northeastern shoreline of Lake Turkana in northern Kenya, a calcrete layer (Main Ileret Caliche) overlying the KBS member of the Koobi Fora Formation was estimated to have formed at 1.54 Ma based on supra- and subjacent tuffs, providing a minimum age for a fossil *Homo erectus* skull found in the sediments beneath it (Spoor et al., 2007).

Calcretes are used to help determine paleoenvironmental conditions in early hominin times. Cerling et al. (1988) used the stable isotope record of paleosol carbonates (calcretes) in the Koobi Fora Formation to determine a shift from predominantly C_3 vegetation to C_4 vegetation (grasses) at about 1.8 Ma, noting that the present conditions are the most arid since then. The expansion of grasslands has been widely discussed in the context of hominin evolution. Quinn et al. (2013) analysed stable isotopes of pedogenic carbonates near lithic archeological sites in the Nachukui and Koobi Fora Formations and found that those sites had a higher proportion of C_3 vegetation, indicating a preference of hominins for wooded areas.

2.2.1.5. Nyanza Rift Valley, southwest Kenya

The Miocene Nyakach Formation consists of fluvial deposits, lahars and paleosols (Saggerson, 1952), and is located in the Nyanza Rift Valley at Kaimogool. The paleosols have yielded many vertebrate fossils, including *Kenyapithecus* (Pickford, 1985). Calcretes there consist of Bk horizons, with carbonate nodules of varying sizes, carbonate rhizoliths, and diffuse carbonate (Wynn and Retallack, 2001), which would be classified a Stage II pedogenic calcrete, or possibly stage III (Gile et al., 1966). These horizons are thought to have developed fairly rapidly (<600 years for the best developed) as they formed within carbonatite sediments. The Bk horizons and depth to carbonate were used to interpret the past climate as arid to very arid.

Also part of the Nyanza Rift Valley, several paleosols in the Miocene Maboko Formation at Maboko Island in Lake Victoria in SW Kenya contain carbonate nodules (Retallack et al., 2002). A hardpan calcrete occurs within a carbonatite ash paleosol which formed within 600 years. The carbonate horizons, or Bk horizons in soil terminology, are mostly shallow and precipitation amounts were calculated to be 300–500 mm mean annual precipitation, using a modified depth to carbonate equation of Retallack (1994), indicating a dry climate when they were forming (Retallack et al., 2002).

2.2.2. Southern Lake Turkana, Kenya

At Baragoi in the rift valley about 50 km south of Turkana, superficial deposits show incipient calcrete features. Small carbonate nodules were found in soil near ephemeral streams (Baker, 1963). These soils, composed of fine sand and clay, were contrasted with more eroded soils that had the finer grained element winnowed away. Two modes of formation seem possible. The first is by seasonal drying of the stream, which would cause the dissolved carbonate to precipitate by evaporative concentration. The second is by mixing of comparatively dilute meteoric water from the stream with more concentrated shallow groundwater.

Several calcrete horizons are found throughout a 160 m-thick sequence of the Kajong Formation in the south Turkana region at Loiyangalani. Within the calcite-cemented mudstones, silts, sands, and conglomerates of the Kajong Formation the calcretes are pedogenic and up to

1.5 m thick (Williamson and Savage, 1986). The calcrete-bearing units are playa deposits that also include stromatolites. The Kajong Formation is overlain by olivine basalts and pyroclastics of the Loiyangalani Basalts that were dated to roughly 18–19 Ma (Williamson and Savage, 1986).

At Loperot and Kajong at the southwestern and southeastern margins of Lake Turkana, a heavily calcretised basement surface up to 5 m thick outcrops underlies the Kajong Formation. This substrate is likely the mid-Cenozoic erosion surface widely recognized throughout East Africa (Williamson and Savage, 1986).

2.2.3. Other calcrete occurrences in the East African Rift

Calcretes also occur elsewhere in the rift valley related to a variety of deposits. In western Tanzania calcrete nodules are present in alluvial fan deposits of the Permian Ndeke Group, part of the Karoo Supergroup (Dypvik et al., 2001; Dypvik and Nilsen, 2002). These calcrete nodules are associated with hematite, are early diagenetic, and show stages of recrystallization from original micrite to poikilotopic calcite (Dypvik and Nilsen, 2002).

Towards the south of Tanzania in the Kilombero Rift Valley, overlying the Karoo Supergroup, the Red Sandstone Group, which includes the Galula Formation and the Nsungwe Formation, contains pedogenic calcretes (Roberts et al., 2004, 2010). In the mid-Cretaceous Galula Formation are soil carbonates (Stage I–III of Gile et al., 1966) occurring in mudstone paleosols with termite trace fossils, root traces, and backfilled burrows. Together with channel fills, crevasse splays, and other floodplain deposits these suggest a large braidplain system (Roberts et al., 2010). Clasts of pedogenic carbonate are also found in debris flows of the Galula Formation (Roberts et al., 2010). Within the overlying Nsungwe Formation (Oligocene), pedogenic carbonate nodules occur in sandstones and conglomerates of alluvial fans that likely were deposited following a phase of rapid uplift of the rift walls in the late Paleogene (Roberts et al., 2010).

Near Lake Nakuru, the Upper Pleistocene sediments in the Nderit drift and Makalia River contain calcrete (kunkar) at their top. The sediments are diatomite at the base, grading up into reddish sands, silts and gravels (McCall et al., 1967).

Towards the northern extension of the rift valley in Ethiopia, calcretes and terrestrial carbonate deposits are also found. The Pliocene Hadar Formation of the Afar depression in

Ethiopia contains a ‘calcareous slab facies’ that is 5–10 cm thick (Tiercelin, 1986). It is a facies within the Sidi Hakoma Member, which is interpreted to represent a lacustrine/palustrine/fluvial regime with rapid lake level fluctuations and much hydrological imbalance (Tiercelin, 1986). Abundant carbonate nodules (up to Stage II) in the paleosols (mainly vertisols) of the Hadar Formation indicate periods of emergence or seasonal drying (Hailemichael et al., 2002; Wynn et al., 2008; Behrensmeyer, 2008). Stable carbon isotopes from this paleosol give an estimation of 30–34% C_4 grasses, indicating much more humid conditions than at present, which explains why calcrete development only proceeded to stage II. A paleosol with stage II calcrete development in the Busidima Formation, which overlies the Hadar Formation, is associated with sediments that indicate saline and highly evaporative conditions (Wynn et al., 2008). Also at Afar are carbonate horizons that include carbonate nodules associated with roots within the clayey silt facies of the Hadar Formation located at the Middle Awash valley (Tiercelin, 1986).

A calcrete lies at the top of member K3 of the Middle-Pleistocene Kapthurin Formation, a succession of alluvial and lacustrine sediments and volcanic beds southwest of Lake Baringo (Fig. 2-6) (Tallon, 1978; Renaut et al., 1999). Hominin remains were found just above this calcrete, and the calcrete was likely a surface upon which the hominins travelled (Tallon, 1978). Also in member K3 a calcrete/calcareous paleosol is interlayered with tufa deposits representing subaerial exposure of a wetland area (Johnson et al., 2009).

Figure 2-6. – (Previous page) Calcrete from Kapthurin Fm (Middle Silts and Gravels Member of Tallon, 1978). Photo from R. Renaut.

2.2.4. Association with lakes

Some calcretes are closely linked with paleolakes and former lake margins. The Miocene Aka Aiteputh Formation in the Samburu Hills near Baragoi, Kenya, contains red paleosols with calcrete horizons up to 1 m thick (Sakai et al., 2010). The calcretes are laminated and contain root moulds up to 5 mm in diameter. The formation consists mainly of basaltic lavas and derivative red soils, with paleosols increasing in abundance towards the top of the formation. Also in the formation is a basal layer of conglomerate and coarse sandstone that is interbedded with the paleosols. The formation represents a change in 'lake type' from overfilled or balanced-filled (terminology of Bohacs et al., 2000) to underfilled in a semi-arid to arid climate, with the calcrete layers indicating seasonal precipitation and subsequent evaporation of shallow groundwater (Sakai et al., 2010).

Renaut (1993) described a late Pleistocene calcrete horizon on the Sandai Plain between Lakes Baringo and Bogoria in the central Kenya Rift. The calcrete, up to 20 cm thick, lies at the disconformity between the underlying fluvio-lacustrine Loboi Silts (zeolitized) and the overlying lacustrine and deltaic Bogoria Silts. This complex calcrete shows textures of both pedogenic and groundwater formation with three distinct phases: first a pedogenic phase which formed the bulk of the hardpan calcrete, then a groundwater phase when root pores and fissures were filled with coarser carbonate cement, and a later pedogenic phase that reworked the calcrete. Interestingly, the Ca source was likely not windblown Ca because the dust is low in Ca—the source is more likely from weathering but remains uncertain (Renaut, 1993).

Figure 2-7. - Calcrete from Sandai Plain. Calcite cements subrounded gravel. Photo from R. Renaut.

Also located between the Baringo and Bogoria basins is the Pleistocene Ilosowuani Formation. Within the formation a calcrete caps lake marginal zeolitized volcaniclastic silts (Fig. 2-8). The calcrete is presumed to be pedogenic and contains rhizoliths and concretions (Renaut, pers. comm.). The calcrete represents a period of aridity and a lack of sediment deposition.

Figure 2-8. - Calcrete from the Ilosowuani Formation. The calcrete is well cemented and has an upper layer rich in Mn-oxides. Photo from R. Renaut.

North of Kalacha in the Chalbi basin a calcrete 5–10 m thick covers an area up to 6 km wide, and overlies basalt dated to 2.5 ± 0.3 Ma (Nyamweru, 1986). A lake is postulated for the area at about ~2 Ma. The calcrete is presumed to result from weathering of the basalt, though some of the carbonate is pisoidal and possibly palustrine (Nyamweru, 1986).

2.2.5. Association with volcanic rocks

Volcanic activity is plentiful in the rift, and much of the bedrock is igneous. Calcretes may form on lavas and ash beds as they weather, particularly during dry climate regimes. At Lodwar, west of Lake Turkana, a small volcanic cone is covered in pea-sized carbonate nodules formed from the lava by surface chemical weathering. These nodules were later washed down the cone to amass at the foot to make a wide expanse of superficial limestone (Walsh and Dodson, 1969). In the South Horr area, to the south of Lake Turkana, rare secondary limestone precipitates in soils (kunkar) are exposed in river courses cut through solid lava (Dodson, 1963).

2.2.6. Non-rift East African calcrete occurrences

Calcrete occurrences are not limited to the rift valley. Thick calcretes (40–60 cm) underlie the eastern Serengeti Plain of Tanzania. During the rainy season the calcretes prevent free drainage, and due to the alkalinity of the soil, only alkali-tolerant short-rooted plants can survive there. Interestingly, the calcretes determine the vegetation of the plain: where calcretes are absent, woodland communities thrive (Anderson and Talbot, 1965).

Although climatic conditions are typically wetter and general geology is different in the western branch of the East Africa Rift, it is worth mentioning that calcretes occur there also. The Semliki Beds in the Semliki Valley (DRC) are capped by a major unconformity and complex carbonate paleosol, indicating a depositional hiatus (Brooks, 1995). The overlying Katanda beds contain three pedogenic carbonate paleosols, plus a sharply bounded calcrete implying high water tables during formation (Brooks, 1995).

2.3 Conclusions

This brief survey, which is not intended to be comprehensive, shows that calcretes in a variety of stages of formation are widespread in East Africa in Neogene to Holocene deposits. Many mantle the land surface, incorporating vertebrate fossils and artifacts and forming important discontinuity surfaces, some of regional extent. Typically they evince semi-arid conditions where precipitation is minimal and probably strongly seasonal. Because of the carbonatite volcanism in parts of the East African Rift, some calcretes form more quickly than they would elsewhere due to the abundant calcium carbonate in the tephra. Away from the semi-arid and alkaline conditions that characterize the Eastern Rift, the calcretes are less well developed and form in a variety of sediments.

3. PLEISTOCENE CALCRETES OF THE LAKE MAGADI AREA

3.1. Geological background

Lake Magadi, at the southern end of the Kenya Rift, occupies the deepest part of a half-graben, ~70 km wide, and is bordered on its western margin by the steep Nguruman Escarpment, which rises 1300 m above the valley floor. Magadi is a closed underfilled lake in a region of high evaporation potential and little rainfall, which has led to the lake becoming hypersaline and precipitating trona annually (Eugster, 1980). Several Quaternary volcanic centers lie within a few hundred kilometres of the lake, ranging from nephelinitic, phonolitic, trachytic and carbonatitic, to basaltic (Baker, 1975; Baker and Mitchell 1988; Baker et al., 1988; Peterson, 1989; Dawson 1992; le Roex et al., 2001; White et al., 2012). Tectonics and volcanic activity have strongly influenced the lake development during the Quaternary (Eugster, 1980; Yuretich, 1982; Behr and Röhricht, 2000) with climate often playing a key role in its sedimentary history.

3.1.1. Quaternary stratigraphy

The stratigraphy of the Magadi basin is complex because of limited exposure and the unusual lithology of many of the sedimentary rocks. The Quaternary sediments include lacustrine siltstone and mudstone, several types of chert, and evaporites. Relationships between the different chert-bearing units are especially difficult to decipher because some cherts are bedded within lacustrine sequences, whereas others intrude younger deposits (Behr and Röhricht, 2000). One consequence is that interpretations of the order of deposition have changed many times (Baker, 1958, 1963; Eugster, 1980; Behr, 2002). Four stratigraphic units are currently recognized (Behr, 2002): The Oloronga Beds, the Green Beds, the High Magadi Beds, and the Evaporite Series (Figure 3-1).

	AGE (y BP)
Evaporite Series	10,010[a] - PRESENT
High Magadi Beds	23,700[b] - 9,310[c]
Green Beds	98,000[d] - 40,000[e]
Oloronga Beds	780,000[f] - 300,000[g]
Magadi Trachytes	1,400,000[h] - 780,000[f]

Figure 3-1. Stratigraphy of the Magadi basin (after Behr, 2002). Sources: a) Butzer et al. (1972); b) Williamson et al. (1993); c) Tichy and Seegers (1999); d) Goetz and Hillaire-Marcel (1992); e) Williamson et al. (1993); f) Fairhead et al. (1972); g) Röhricht (1999); h) Baker and Mitchell (1976). The proposed age for the onset of the Evaporite Series (Butzer et al., 1972) is incompatible with evidence from elsewhere in East Africa. Most evidence shows that the climate in East Africa was more humid than today at ~10,000 y BP. Trona precipitation at Magadi probably began in the mid-Holocene, but the timing remains uncertain.

3.1.1.1. Oloronga Beds

The Oloronga Beds are mainly lacustrine volcaniclastic silts, carbonates -- including gastropod coquinas -- and beds of chert, some of which are diatomaceous (Baker, 1958, 1963; Eugster, 1980; Behr, 2002). In outcrops at the southwestern margin of Lake Magadi, these lacustrine sediments are underlain by fluvial trough-cross bedded sandstones that imply northward flowing perennial channels several metres deep (Renaut, pers. comm., 2015). The Oloronga sediments crop out discontinuously across the basin, with the best exposed sequences at the southern and northern ends of the two Magadi lakes. At these locations, they are up to 5 m thick in outcrop, but are thicker below the axis of the Magadi trough. North of Nasikie Engida, Oloronga sediments have been tilted westwards, implying that a phase of Pleistocene faulting and tilting occurred after sedimentation before deposition of the High Magadi Beds.

Paleolake Oloronga was the first lake to occupy the Magadi basin, both during and after the late-stage eruptions of the Pleistocene (Magadi) trachytes. The paleolake probably evolved during volcanism rather than after it had ceased. Lake sediments were being deposited during the mid-Pleistocene (a K-Ar age of 0.78 Ma was obtained from a glassy trachyte flow that interstratifies with the Oloronga Beds: Fairhead et al., 1972), and continued until about 300 ka (radiometric age from a hippopotamus tooth: Behr, 2002) or later.

During its highstands, Paleolake Oloronga was likely part of a larger lake that encompassed much of the modern Magadi-Natron basin. A group of lithologically similar sediments equivalent in age to part of the Oloronga Beds is preserved in a small graben at Lainyamok, 9.3 km west of Nasikie Engida (Shipman et al., 1983; Potts et al., 1988; Fig. 2-4).

Three generations of Pleistocene and Holocene stromatolites that formed along paleoshorelines of lake highstands were found at elevations of 698 m, 655 m, and 656 m, and dated to >200,000 y BP, 130,000-140,000 y BP, and 12,000-10,000 y BP, respectively (Hillaire-Marcel and Casanova, 1987). The third generation represents the highstand of the lake during High Magadi Beds time. The youngest stromatolites imply that lake level at those times was up to 50 m higher than at present, but the most prominent High Magadi Beds paleoshoreline lies at only + 13 m (~ 613 m elevation) (Eugster, 1980).

3.1.1.2. Green Beds

The Green Beds, proposed and discussed by Röhricht (1999), Behr and Röhricht (2000) and Behr (2002), were initially included in the Oloronga Beds (the ‘Chert Series’ of Baker, 1958). Eugster (1969, 1980) assigned them to the lower unit of the High Magadi Beds. However, the Green Beds are much older than the High Magadi Beds and were later dated at between 98,000 y BP (Goetz and Hillaire-Marcel, 1992) and 40,000 y BP (Williamson et al., 1993).

Behr and Röhricht (2000) recognized a lower massive chert and an upper bedded chert. Microbial textures such as stromatolitic laminae and silicified microbial mats are present in both cherts, as well as lenses of erionite silt. Some cherts may be bioherms. They are exposed along the southern and northeastern margins of Lake Magadi (Fig. 3-2 A) and the exposed bedded sediments are up to several meters thick. Behr (2002) proposed that precipitation of silica was accomplished through alteration of precursor colloidal silica sols and silica gel from the change of pH induced by microbial respiration. Preserved structures imply that the cherts were precipitated in shallow, evaporative, silica-rich alkaline brine pools in flat depressions that were

colonized by cyanobacteria and other microbes. Lake levels fluctuated during this period but probably did not reach those of the Oloronga and High Magadi paleolakes.

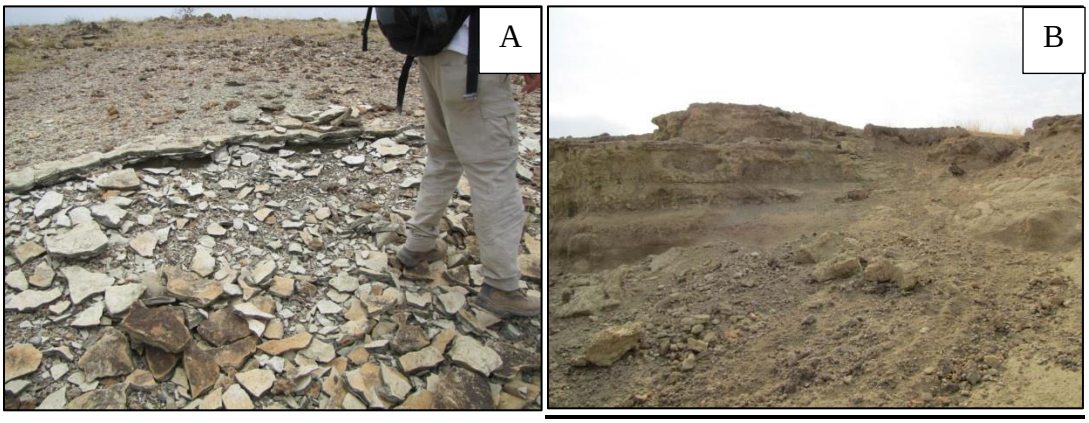

Figure 3-2. Photos of Lake Magadi sediments. A: Laminated chert facies of the Green Beds at the south lagoon. Broken pieces of the cherts frequently bear salt moulds, possibly from trona, calcite and gaylussite, along bedding planes. B: Photo of the High Magadi Beds at the Dry Lagoon. Section is approximately 3 m high.

3.1.1.3. High Magadi Beds

The High Magadi beds are exposed along the modern lake margin and overlie the Oloronga Beds and the Green Beds (Fig. 3-2 B). The High Magadi Beds, which are up to 9 m thick in outcrop, consist of finely bedded to laminated lacustrine volcaniclastic silts and clays. The upper unit is composed mainly of coarsely bedded, pale brown tuffaceous silts, the lower unit of dark brown to dark green, discontinuous laminites. In a study of the laminae, Damnati et al. (1992) identified a light layer consisting of detrital silicates, calcite, and authigenic magadiite (sodium silicate which alters to chert) alternating with a dark organic-rich layer containing diatom frustules, ostracods, and microspherules probably related to bacteria. These alternating laminae were interpreted to result from a 2–3 year variation in length of the rainy season.

Fish scales (*Tilapia* sp.) are found in the lower unit of the High Magadi Beds, and a prominent layer consisting of fish remains was ^{14}C dated to 9120 ± 170 y BP (Butzer et al., 1972). This coincides with lake records throughout East Africa indicating a wet climate starting in the late Pleistocene (Grove et al., 1975; Gasse, 1977; Gillespie et al., 1983; Roberts et al., 1993; Barker et al., 2002; Bergner et al., 2003). These conditions persisted until approximately 5000 years ago, coincident with the end of the African Humid Period that affected most of East Africa (Jolly et al., 1998; deMenocal et al., 2000; Berke et al. 2012; Garcin et al., 2012), when the climate became more arid and Lake Magadi produced primarily evaporites.

3.1.1.4. Evaporite Series

The Evaporite Series, up to at least 40 m thick, consists of alternating layers of trona and volcaniclastic silt and mud, representing 'cycles' of changing lake salinity with evaporite precipitation during the drier phases. Though trona is the dominant evaporite, the trona layers include minor nahcolite (Eugster 1980; Ogola and Behr, 2000; Darling, 2001). Other authigenic minerals appear as impurities in the trona, such as villiaumite, fluorite, gaylussite, calcite, zeolites, and sodium silicates (Ogola and Behr, 2000). Windborne impurities such as quartz, garnet, sillimanite, and actinolite from the Mozambique Belt are also present. Evaporites began forming after the last major wet period in Lake Magadi, some time after 9,120 y BP (questionable ^{14}C date from Nasikie Engida evaporites: Behr, 2002).

3.1.1.5. Calcretes

In his regional survey, Baker (1958) described a pisoidal calcrete overlying the Oloronga Beds (Fig. 3-3). He then used the calcrete layer as a stratigraphic boundary in determining extent of the Oloronga Beds. Subsequent researchers, including Eugster (1980), also used the easily identifiable calcrete to recognize the underlying Oloronga sediments. However, Behr and Röhricht (2000) later showed that the calcrete should not be used as a stratigraphic boundary unit because there are several calcretes in the basin; some are younger than the calcrete that overlies the Oloronga Beds. While Baker (1958) assigned the calcrete to the top of the Oloronga Beds, Behr and Röhricht (2000) assigned another, local calcrete to the base of the High Magadi Beds, capping the Green Beds. The most complete Magadi stratigraphy to date (Behr, 2002) includes at least two major calcretes: one above the Oloronga Beds that formed some time between ~ 300,000 y BP and ~ 98, 000 y BP, and one within the High Magadi Beds, that was dated to 14,515 y BP.

Figure 3-3 – Photo of the sampled calcrete north of Nasikie Engida. It shows a calcrete (center) overlying Oloronga Beds (greenish sediments, below). Calcrete layer (generally) is approximately 25–50 cm thick.

3.1.2. Basin hydrology

Lake Magadi is a hydrologically and topographically closed saline (up to 300 g/L TDS; Eugster, 1980), alkaline lake (pH range of 9.13–10.05 in lagoons: Wilson et al., 2004) with a Na-CO_3-Cl brine that currently precipitates trona ($Na_2CO_3 \cdot NaHCO_3 \cdot 2H_2O$). At ~600 m elevation, the lake occupies the axial depression of a half-graben bordered to the west by the steep north-south trending Nguruman Escarpment and to the east by a series of step faults. Together with Lake Natron in Tanzania it forms the Magadi-Natron basin. The two lakes were united periodically during the Quaternary. The lake is fed mainly by several groups of hot (~ 35–45°C) springs located along its faulted margins, and a few ephemeral streams that flow briefly during the rainy seasons. Most hot springs are recharged along the rift flanks; the springs to the west have solute concentrations similar to rainwater (Becht et al., 2006). However, the isotopic signature of the northern springs varies and may reflect groundwater input from freshwater Lake Naivasha 100 km to the north, though this theory remains controversial (Allen et al., 1989; Darling, 2001; Becht et al., 2006).

During the driest months (on average June to October) the lake is a saline pan with several perennial lagoons at its margins where the hot springs discharge. Seasonal rains flood the entire lake to depths up to ~1 m. Nasikie Engida (Little Magadi), which lies north of Lake Magadi, is a small separate saline lake with a similar ionic composition to Magadi but much

lower salinity. Nasikie Engida is perennial and is fed almost entirely by hot (up to 86°C) alkaline springs. It is probable that the two lakes were united at different times during the late Pleistocene and early Holocene.

The origin of the Magadi brines has been a focus of several studies (Eugster, 1970; Jones et al., 1977; Hillaire-Marcel and Casanova, 1987; Allen et al., 1989). Jones et al. (1977), using chloride as a conservative tracer ion, traced the fluids from their potential source in rainfall and runoff, through groundwater, to hot springs that feed the dense. They suggested that dense brines sink and mix with inflowing groundwater in complex fluid pathways that include recycling of evaporated fluids (Fig. 3-4).

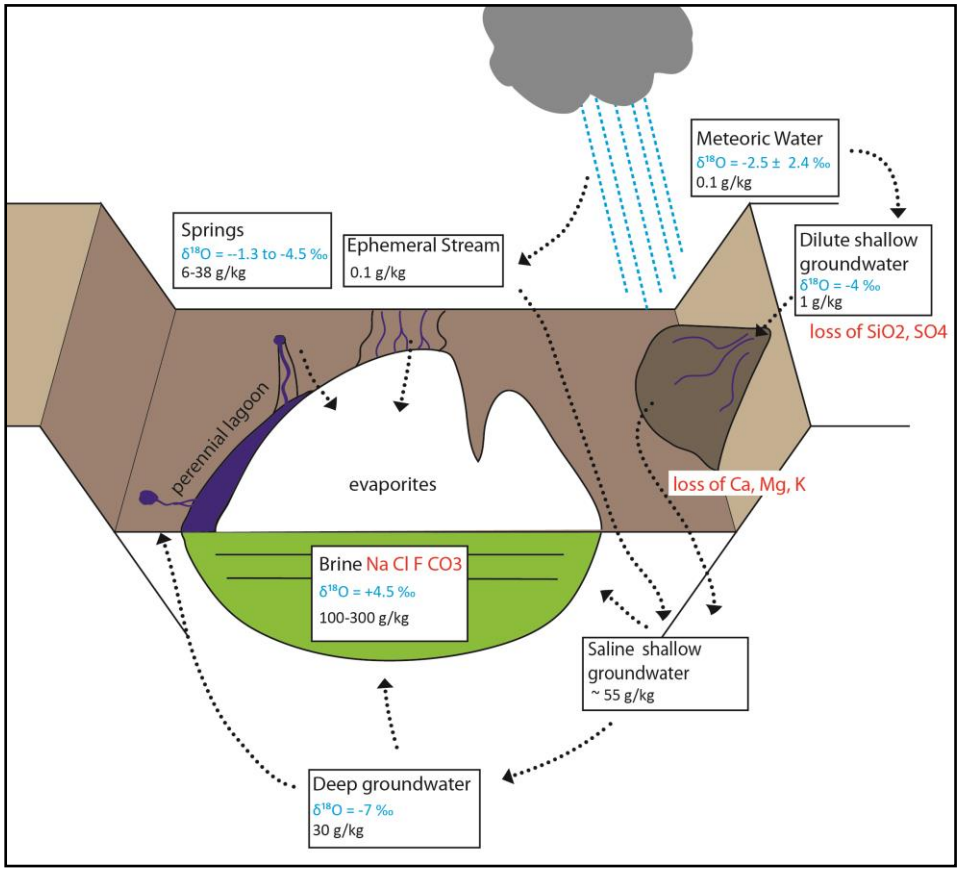

Figure 3-4: Fluid pathway, solute evolution, and stable isotope ranges for the Magadi basin. Based on Jones et al. (1977), and Eugster (1980). Isotope data from Hillaire-Marcel and Casanova (1987).

Meteoric water (runoff and shallow groundwater) weathers the trachytes mainly by silicate hydrolysis reactions, acquiring solutes including Ca, Mg, Na, K and Si, with bicarbonate

produced as a product of the reaction (Jones et al., 1977). Some of the silica and all of the SO_4 is lost from solution at an early stage, before the dilute surface water reaches the groundwater reservoir (Jones et al., 1977). The bedrock is relatively low in S and the SO_4 produced by oxidation is readily reduced by microorganisms. Ca and Mg are also removed early in the hydrological cycle, between the dilute and saline groundwater stages, either in sediments as cements or at the land surface where they form thin crusts by evaporative concentration. Ca forms carbonates, while Mg most likely forms sepiolite or other Mg-clays (Deocampo, 2004; Deocampo et al., 2010). Some K is lost by adsorption on volcanic glass. This leaves Na^+, HCO_3, CO_3^{2-}, and Cl^- as major ions when the water enters the lake. Thus the modern lake has negligible concentrations of Mg and Ca (Jones et al. 1977; Surdam and Eugster, 1976) but very high alkalinity and chloride.

Waters in the region have a very high F^- content: a spring at Lake Magadi contained 73 mg/L fluoride, far exceeding the 1.5 mg/L F^- value for safe consumption (Gikunju et al. 1992; Neilsen, 1999). Due to the lack of Ca in the waters, fluorite is an uncommon mineral except where dilute groundwater enters the lake towards the NE quadrant; however, F combines elsewhere with Na to create villiaumite. In core samples, fluorite and calcite are mutually exclusive (Surdam and Eugster, 1976). Other authigenic minerals in the lake sediments include the zeolite erionite, easily produced from trachyte with the addition of alkaline water (Surdam and Eugster, 1976), and other zeolites such as chabazite, phillipsite, and analcime. At different times, chert, magadiite and kenyaite have formed from the silica-rich fluids (Eugster, 1969, 1980; Behr, 2002).

3.1.3. Biota

Few aquatic organisms can thrive in the hot, briny, highly alkaline waters of Lake Magadi. A highly adapted species of tilapia fish (*Alcolapia grahami;* Seegers and Tichy, 1999) lives in the perennial lagoons. High concentrations of haloalkaliphilic archaea colour the brines—they produce C_{50} carotenoids which give a red colour (Mwatha and Grant, 1993; Fig. 3-5). Lesser flamingos, among other varieties of birds, feed on seasonal cyanobacterial blooms (mostly *Arthrospira fusiformis*) from the lagoons. Other species of cyanobacteria and green algae are also present, as well as bacteria (e.g. Davis, 2012). Tuite (1981) noted the importance of

benthic fauna in the primary production community, as cyanobacteria are comparatively diminished in number. Some actinomycetes are also in the present-day lake (Jones et al., 1998).

Fossil ‘tilapia’ much larger than the current species were found in the High Magadi Beds (Butzer et al., 1972). Behr (2002) reported fossil cyanobacteria of the morphotypes *Pleurocapsa Gloeocapsa*, *Entophysalis*, *Chroococcus*, and *Synechococcus*, as well as actinomycetes, within the Green Beds. Lake Oloronga had carbonate-secreting organisms that left gastropod shells (*Viviparus sp.*) (Baker, 1958) in limestone, some of which are silicified.

Diatoms were present during Oloronga and High Magadi times (Damnati et al. 1992; Barker et al. 1990). Mpawenayo and Mathooko (2005) reported several types of modern diatoms for the Magadi area but their sampling sites are unknown.

The vegetation around the lake is mainly dry, open semi-desert grassland and shrubland, with small *Commiphora* and *Acacia* trees (Trump, 1967; Vincens and Casanova, 1987). The local Maasai community uses the patchy grassland around Nasikie Engida for grazing by goats and cattle. Local wildlife includes gazelles, zebra, wildebeest, giraffe and occasional predators.

Soils are generally thin (< 15 cm thick), calcareous and stony except in valley floors containing sandy alluvium and silts.

Figure 3-5 - Brine pool at L. Magadi showing trona formation; red coloration is from Archaea. Note lack of vegetation at the shore. Typical regional vegetation and fault scarp are in the background.

3.1.4. Climate

Lake Magadi lies in a semi-arid tropical region (average annual temperature: 29.0°C; Climate Data, 2011) with high evaporation potential (>3,500 mm/year) and low annual precipitation (~ 500 mm/year). Monsoonal air masses from the Indian Ocean during March and April provide most of the precipitation, though the valley lies in the rain shadow of the eastern rift wall (Olaka et al., 2010). A secondary period of precipitation happens during December, resulting from the migration of the Inter-Tropical Convergence Zone (ITCZ), which causes moist air to flow northwards along the rift valley.

East African climate during the Neogene has been complex and has fluctuated from wet to dry, and hot to cool, due to a variety of influences (Gasse, 2000; Bobe, 2006). During the Quaternary, although the dominant trend has been aridification, the climate has been wetter for periods. Records from lacustrine stromatolites dated at some 100,000 years ago show a fluctuating wet/dry climate gradually becoming more arid to the present day (Hillaire-Marcel and Casanova, 1987). Palynological studies indicate vegetation corresponding to a humid environment at Magadi around 12–10 ka and ~17 ka (Vincens et al., 1990). The last major pluvial episode ended about 5000 years ago, about the time of the onset of Saharan desertification. Lakes elsewhere in the rift valley such as Turkana, Nakuru and Naivasha also show this trend (Roberts et al., 1993; Berke et al., 2012; Garcin et al., 2012).

3.2 Field observations at Lake Magadi

3.2.1. The Dry Lagoon

At the Dry Lagoon at the southeastern end of Lake Magadi, the High Magadi Beds and Oloronga Beds crop out together in vertical sections separated by a calcrete layer from 25 to 50 cm thick (Section C in Fig. 15-20 of Eugster, 1980; Site 1 in Fig. 3-6; Fig. 3-10 C). The calcrete can be traced discontinuously in sections along the northern margin of the Dry Lagoon over a lateral distance of ~ 250 m (Figs. 3-7 and 3-8). The calcrete unit rises eastwards with topography

by ~ 10 m in elevation over that distance, but maintains the same relative stratigraphic position.

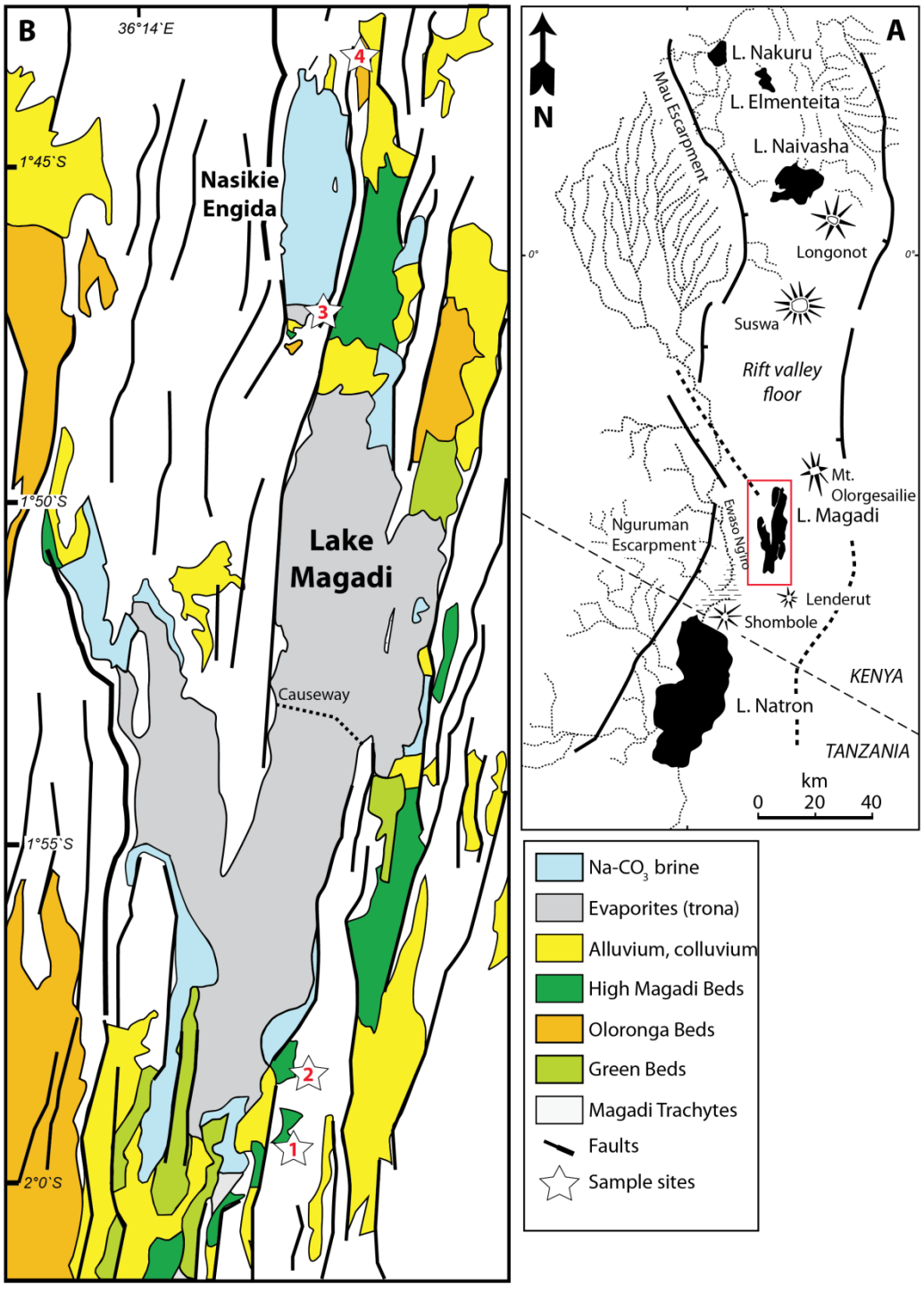

Figure 3-6. Geological map of the Lake Magadi area modified after (Scott, 2010 and Guth and Wood, 2013). Sample sites are denoted by a star, the number indicating site number. Sample site 1 is the Dry Lagoon. Sample site 2 is just above Graham's Lagoon. Sample sites 3 and 4 are discussed as south and north Nasikie Engida, respectively.

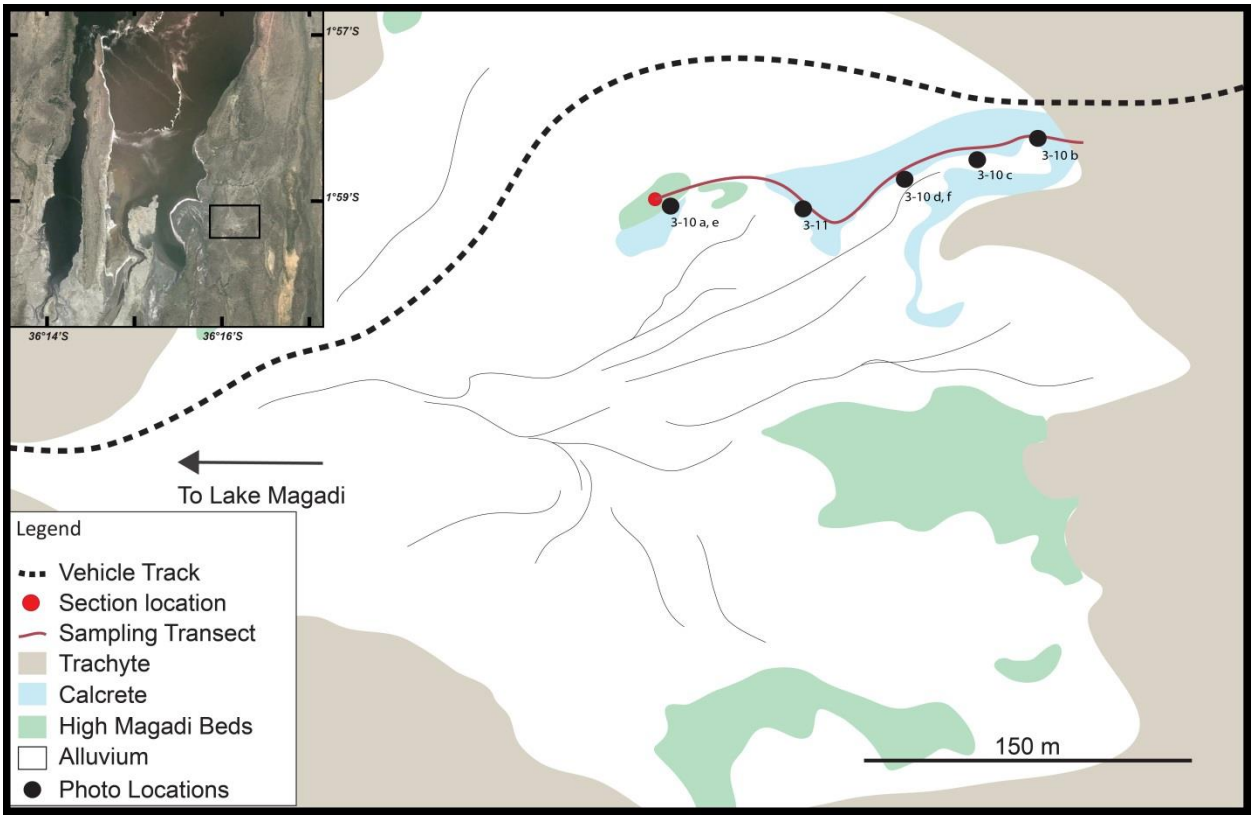

Figure 3-7 - Map of Dry Lagoon and sample locations. Line of sampling transect proceeds from the section location (Fig. 3.8, arrow) east to where calcrete is absent, following the best available exposure. Approximate photo locations for figures 3-10 and 3-11 are provided. The alluvium-filled valley slopes toward the lake. Top left image is from Google Earth©.

Figure 3-8. Photograph of the Dry Lagoon, looking east towards Lake Magadi. Arrow indicates the location of the stratigraphic section, which is at the same location as Figure 2 in Eugster (1986) . Discontinuous layer of calcrete in the foreground.

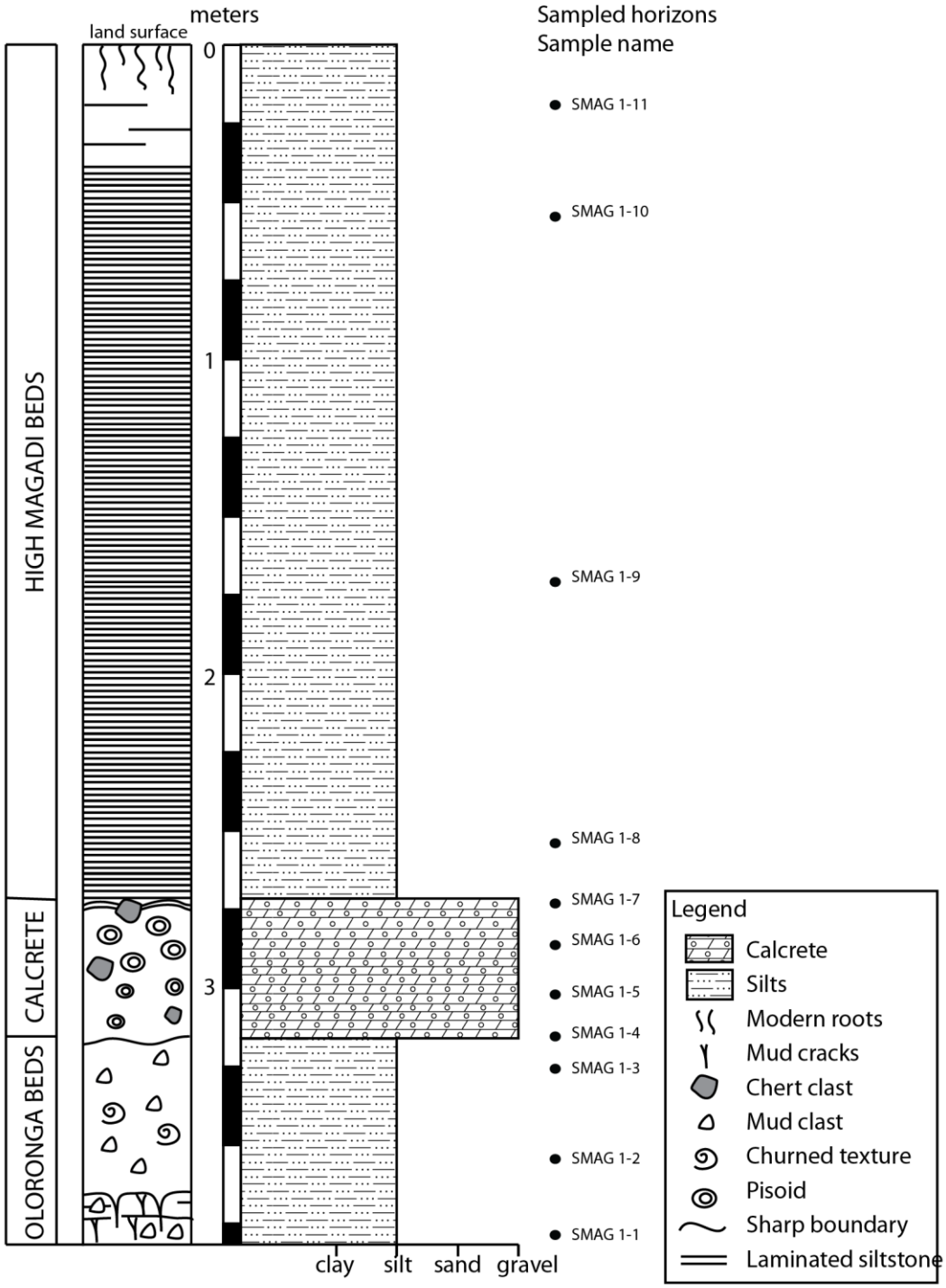

Figure 3-9. Stratigraphic section measured at the Dry Lagoon. See Figure 3-7 for location of section.

The Oloronga Beds at the Dry Lagoon consist mainly of faintly laminated green volcaniclastic silts and claystone containing the zeolite erionite (Fig. 3-9). The top of the Oloronga Beds, which are locally up to 2 m thick in outcrop, displays networks of cracks that are

1 mm to 2 cm wide by up to 30 cm deep (Fig. 3-10, A, D and E). The contact between the calcrete and the underlying Oloronga Beds is abrupt where these crack systems are present. Locally the cracks have a honeycomb framework (Fig. 3-10, C). Elsewhere, the top of the Oloronga Beds does not have these crack networks, but instead consists of green rounded zeolitized claystone pebbles surrounded by loose silt, which grade upwards into the calcrete layer (Fig. 3-10 C). These green pebbles, which are 0.5 to 10 cm long, are weakly lithified and are embedded in the uppermost sediments of the Oloronga Beds that display crack networks (e.g. mud intraclasts in the honeycomb cracks) and in the calcrete. The mud pebbles in the honeycomb cracks are 0.5 to ~2 cm in diameter.

The overlying High Magadi Beds, which are up to 2.5 m thick, are massive, bedded or laminated to weakly laminated, medium beige volcaniclastic siltstone. At the present land surface near the top of the section, vertical root moulds ~1 cm in diameter and horizontal pores ~1 mm diameter are present. The siltstones do not vary much in character throughout the stratigraphic section. The High Magadi Beds are in sharp contact with the underlying calcrete (Fig. 3-10 E).

Two types of calcrete are present in the Dry Lagoon: pisoidal calcrete, which overlies the Oloronga Beds, and laminar calcrete which caps the pisoidal calcrete and lies directly on unconsolidated silts with green clayey nodules, and trachytes at higher elevations (Fig. 3-11). Above the cracked surface the calcrete is pisoidal. Clasts of the Oloronga Beds are located in the lower portion of the calcrete and decrease in abundance upwards through the profile. Those clasts are commonly found as pisoid nuclei along with clasts of earlier calcrete and chert. Pisoids are ~ 0.5 to 1.5 cm in diameter and are spherical to subrounded. Pisoid laminae are discontinuous; some show thicker laminae towards one side of a pisoid that could be pendant laminae, but these are unaligned with other pisoids. Pisoid abundance increases upwards in the calcrete profile. Horizontal round tubules, up to 10 mm long and 2 mm wide, are present in lower parts of the calcrete. Above the poorly lithified sediments the calcrete is more vermiform with point-contact cemented smaller pisoids (~ 0.5 cm diameter) with a transitional boundary (Fig. 3-10 B and C). Where in contact with Magadi Trachyte, the calcrete is laminar and fracture-filling. The laminar calcrete is ~ 1 cm thick and includes detrital chert. The calcrete in the Dry Lagoon becomes very thin at ~ 639 m elevation.

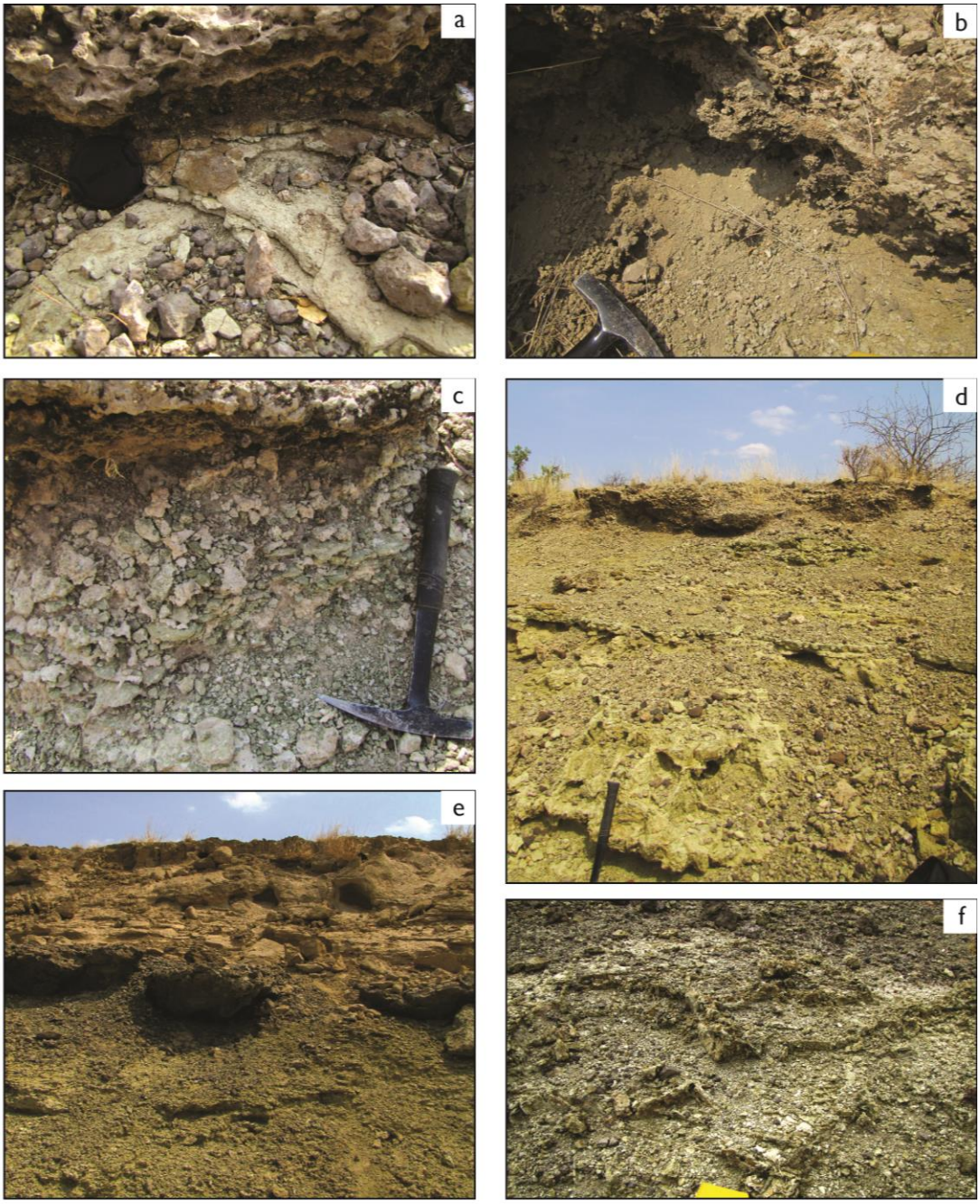

Fig. 3-10. Field photographs of calcretes at Lake Magadi. a) Sharp boundary between Oloronga Beds and pisoidal calcrete. Lens cap for scale (7 cm). b) Transitional boundary beneath calcrete. c) Transitional boundary beneath calcrete, with carbonate surrounding rounded green sediment clasts. Hammer is 32 cm in length. d) and f) Honeycomb texture in Oloronga Beds. In (f), notebook is 12 cm wide. e) Magadi calcrete section; Greenish Oloronga Beds below calcrete, High Magadi Beds above calcrete. Note sharp contact between High Magadi Beds and calcrete. Calcrete is approximately 50 cm thick.

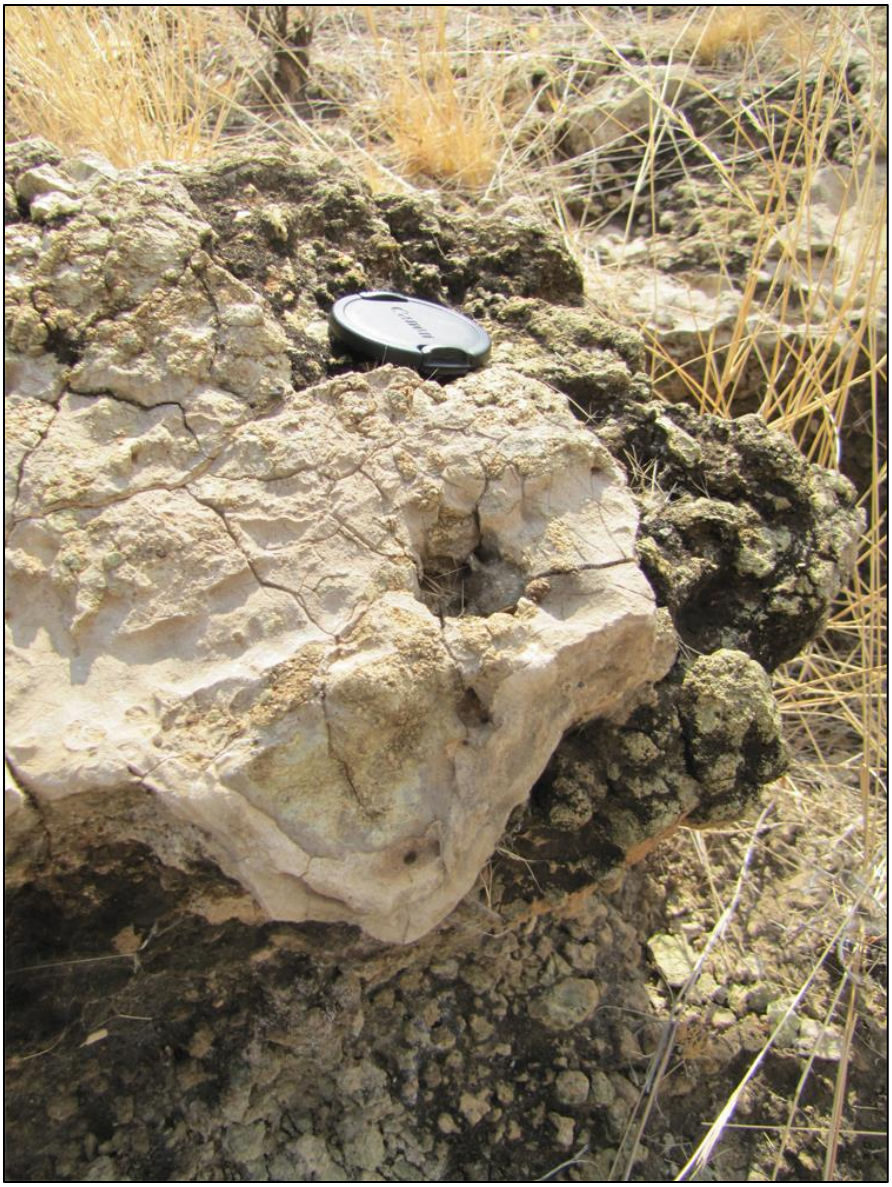

Figure 3-11. Photo of Oloronga-capping calcrete. Laminar calcrete (beige) overlies massive calcrete (dark grey). Lens cap is 7 cm in diameter. Approximate location given in Figure 3-9.

3.2.2. Laminar carbonates at Graham's Lagoon

Thin laminar calcretes coating volcanic rock surfaces are common near Lake Magadi. One area was chosen for study (Fig. 3-6, Site 2). At the SE corner of the lake at an elevation of ~ 640 m a (Fig. 3-12), up the hill north of the location of the magadiite type-section described by Eugster (1967), laminar carbonate coating up to 3 cm thick with detrital chert and volcaniclastic fragments directly overlies trachyte (Fig. 3-13). This laminar carbonate is similar to the laminar

carbonate which coats both the trachytes and the pisoidal calcretes at the aforementioned Dry Lagoon.

The calcrete is exposed in a 1 to 1.5 m wide very shallow ephemeral channel and is covered laterally by Holocene gravels (Fig. 3-13 B). Fine detrital material and pebble-sized chert fragments are present in the laminae. Rounded vesicular volcanic pebbles in the carbonate-cemented transitional zone are all trachyte. Two generations of carbonate cement are seen in outcrop: an early, yellowish, sparry, vesicle-filling cement, and a later patchy, powdery white cement, which has coated root tubules and other possibly biogenic structures. The white cement coats brecciated rocks that overlap the laminar calcrete. Cracks (shrinkage?) are present on the top surface of the laminar calcrete. The laminar calcrete is thickest (2–3 cm) in depressions and is thin or absent over sharp protrusions in the underlying trachyte. The carbonate fills cracks and vesicles within the volcanics, and also coats large volcanic clasts. Some gravel clasts are fully coated by carbonate up to 1 cm thick that contains discontinuous laminae.

Figure 3-12. General view of the laminar calcrete above Graham's Lagoon. Lake Magadi and Shombole volcano in the background. Calcrete lies on the floor of a small ephemeral channel (arrowed).

Fig. 3.13. Field photographs of laminar calcretes above Graham's Lagoon at south-east Lake Magadi. A) A laminar carbonate layer overlies a clast-coating, void-filling carbonate cement. B) Typical exposure of laminar calcrete in ephemeral runoff channel. Hammer is 32 cm long. C) Closeup of laminae. Pen is 13.5 cm long.

3.2.3. Nasikie Engida

Carbonate rocks are present north of Nasikie Engida and along its southeastern shoreline. These predate, and are separate from, the conglomerates described in Chapter 5. A pisoidal calcrete overlies Oloronga Beds in a N-S striking graben 1.4 km north of the eastern margin of the lake (Fig. 3-6, Site 4). The contact is sharp though irregular such that the calcrete appears to have locally filled depressions, possibly displacively, on the eroded Oloronga Beds surface (Fig. 3-3). The calcrete is ~ 30 cm thick where lying on a flat Oloronga surface. The calcrete is vermiform, medium green-grey, and well cemented at the top, but less cemented below. It lies on khaki porous siltstone with calcite crystal clasts. One sample was taken from this location and is included in the description and analysis of the Oloronga-capping calcretes at south Magadi.

At the southeast margin of Nasikie Engida (Site 3 in Fig. 3-6) a dark grey pisoidal carbonate is exposed at the land surface in a low area. It is adjacent to, and presumably overlain by, buff High Magadi Beds containing Magadi-type chert (Fig. 3-14).

Figure 3-14. Grey massive to pisoidal calcrete exposure to the south of Nasikie Engida (location 3 in Figure 3-7). Photo encompasses entire exposure. Hammer is 32 cm in length. This calcrete underlies the Magadi-type chert-bearing High Magadi Beds to the right of the photo.

3.3 Petrography

3.3.1. Oloronga calcretes

Oloronga calcretes consist of those at the boundary between the Oloronga Beds and the High Magadi Beds. Included in this analysis are samples from south Magadi and samples from north and south Nasikie Engida, respectively.

3.3.1.1. Microfabrics

Detailed petrographic analysis shows that both alpha and beta microfabrics (as in Wright, 1990) are present in the Oloronga calcretes with alpha textures dominant. The most common alpha microfabrics in the calcretes are circumgranular cracking (Figs. 3-15 B, 3-16 D), floating grain fabric (Fig. 3-15 B, D, F), dense microfabric (Fig. 3-15 B, D), and complex cracks (Fig. 3-

15 D). Others include nodular fabric (Fig. 3-15 A), crystal mosaic fabric (Fig. 3-15 B), and the presence of relatively rare rhombohedral calcite crystals (Fig. 3-15 E). Alpha textures also predominate within the laminar carbonates that formed on top of above mentioned calcrete and directly on the volcanic substrates, consisting mainly of dense microfabric and floating grain textures (Fig. 3-15 F).

Beta microfabrics are less abundant, commonly with only one example in any thin section. The most common beta microfabrics in the calcretes are microbial coatings (Fig. 3-16 B, top) and alveolar septal fabrics (Fig. 3-17 A, B). Needle fiber calcite is rare, but possibly overlooked or under-represented due to its fragile nature (Wright, 1986).

Much of the calcrete is formed of irregular micrite clumps ranging from 0.5 to 1 mm in size that are surrounded by sparite (Fig. 3-17 F). This clumped texture also forms pisoid cores.

Some of the larger calcite crystals have a columnar habit. They appear stacked and are usually associated with variably calcified and cemented clays (Fig. 3-15 D). In addition, calcite also rarely has a radiating fan shape (Fig. 3-16 E).

Volcaniclastic grains, clay particles, and solitary mineral grains are often coated by tabular calcite (Fig. 3-16 D). The coatings vary in thicknesses from 0.01 to 0.05 mm and are usually isopachous. Corroded and cracked grains, microspar haloes around grains, and extensive supplantation of trachyte grains indicate pervasive replacement by calcite (Fig. 3-15 B, C).

Aggrading neomorphism is evident in some samples where patches of microspar are replacing the micrite in nodules and matrix, but is not common.

The Dry Lagoon calcretes are composed of varying amounts of pisoids, each from 0.5 to 2.5 cm in diameter with micritic to microsparitic laminae. The pisoid cores vary in the amount of calcification, but are generally consolidated fragments of the underlying sediment, including claystone, volcaniclastic fragments, or pieces of older, highly calcified, reworked calcrete. Many pisoids show evidence of autobrecciation around their concentric rims to form circumgranular cracks (Goudie, 1983). These cracks do not necessarily encompass the entire pisoid but create ‘pockets’ where potentially younger spar cement grows closer to the core than older cement.

Former and open root-hair pores and cracks are cemented by successive layers of micrite and/or sparite, filled with fine detrital matter, or lined with clays. Those cracks not associated with roots are commonly filled with sparite, micrite, or detritus.

Examination under SEM revealed the presence of organic filaments. While most samples showed micritic calcite cement and detrital K-feldspar grains with replacement textures, rare bundles of microbial filaments and/or fibres are also present. These correspond with root-related microfabrics found in thin section. However, based on their lengths and diameters, the filaments likely represent both root hairs (Fig. 3-18 B, E) and fungi (Fig. 3-18 D, F) (fungi: 0.5–10 μm; actinoymycetes: 0.1–2 μm; root hairs: 5–17 μm; Klappa, 1979). A few deflated fungal spores of indeterminate genera and their associated hyphae (Fig. 3-18 D, F) are in one sample.

Rare spherulites that resemble those described by Wright (1989) and Verrecchia et al. (1995) were seen in thin section. These are typically seen in laminar calcretes and are thought to be related to cyanobacterial mats. Conversely, in the Oloronga-capping calcrete samples they occur in the massive calcrete and not in the late laminar sections.

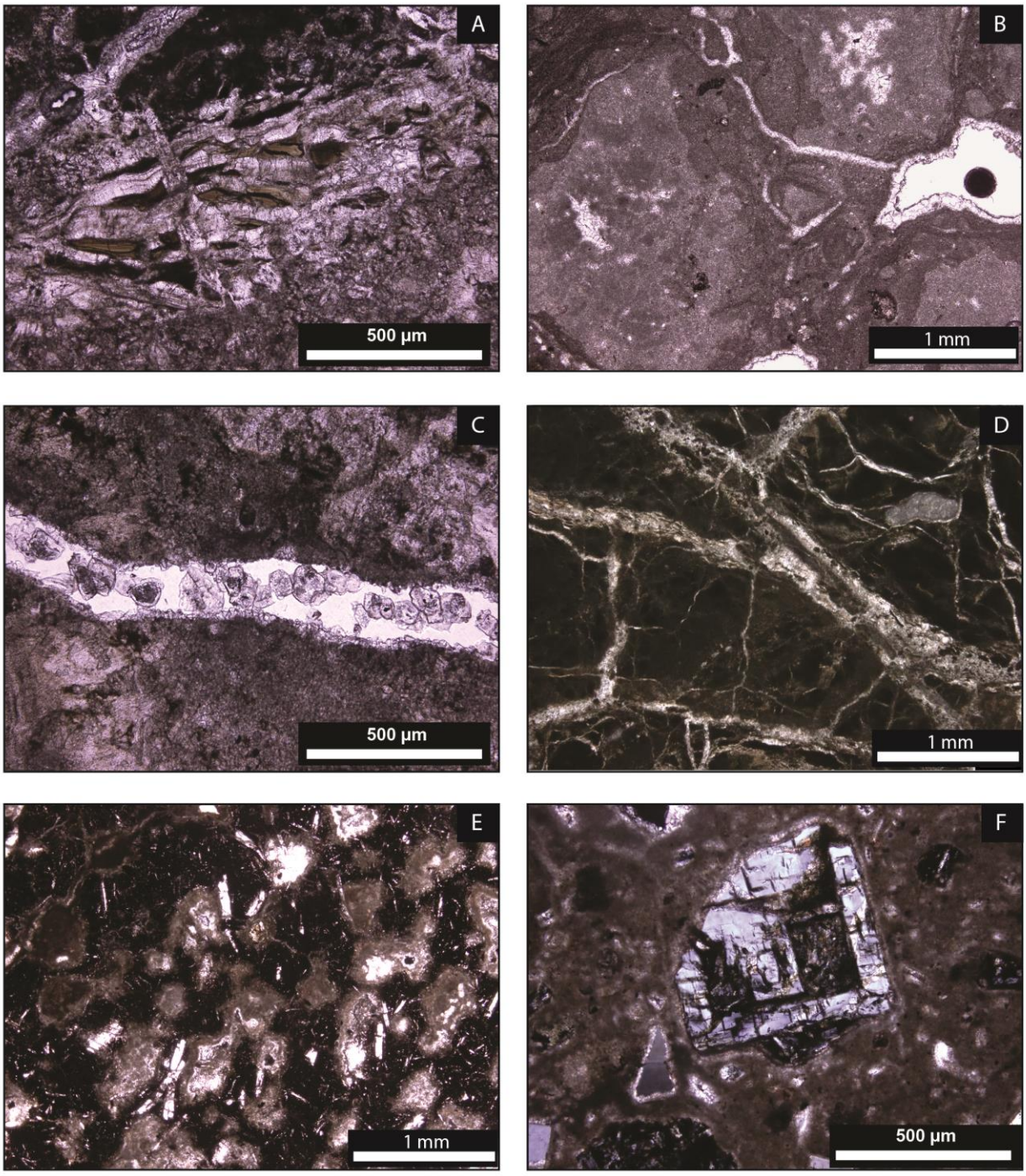

Figure 3-15 – Photomicrographs of alpha microfabrics in the Oloronga-capping calcrete. A) Prismatic calcite associated with clays. B) Photomicrograph in plane polarized light (PPL) of a thin section from the Dry Lagoon calcrete showing alpha textures such as crystal mosaic fabric and nodularization. C) Carbonate subhedral grains in an open fracture in a calcrete. D) Complex cracks filled with sparite in micrite-replaced sediment. E) Insular replacement by calcite of a trachyte grain. F) Cross polarized light (XPL) photomicrograph showing calcite replacing K-feldspar

(sanidine). Former borders of the crystal, and some surrounding fragments, are visible in variations in micrite. Note floating grain fabric.

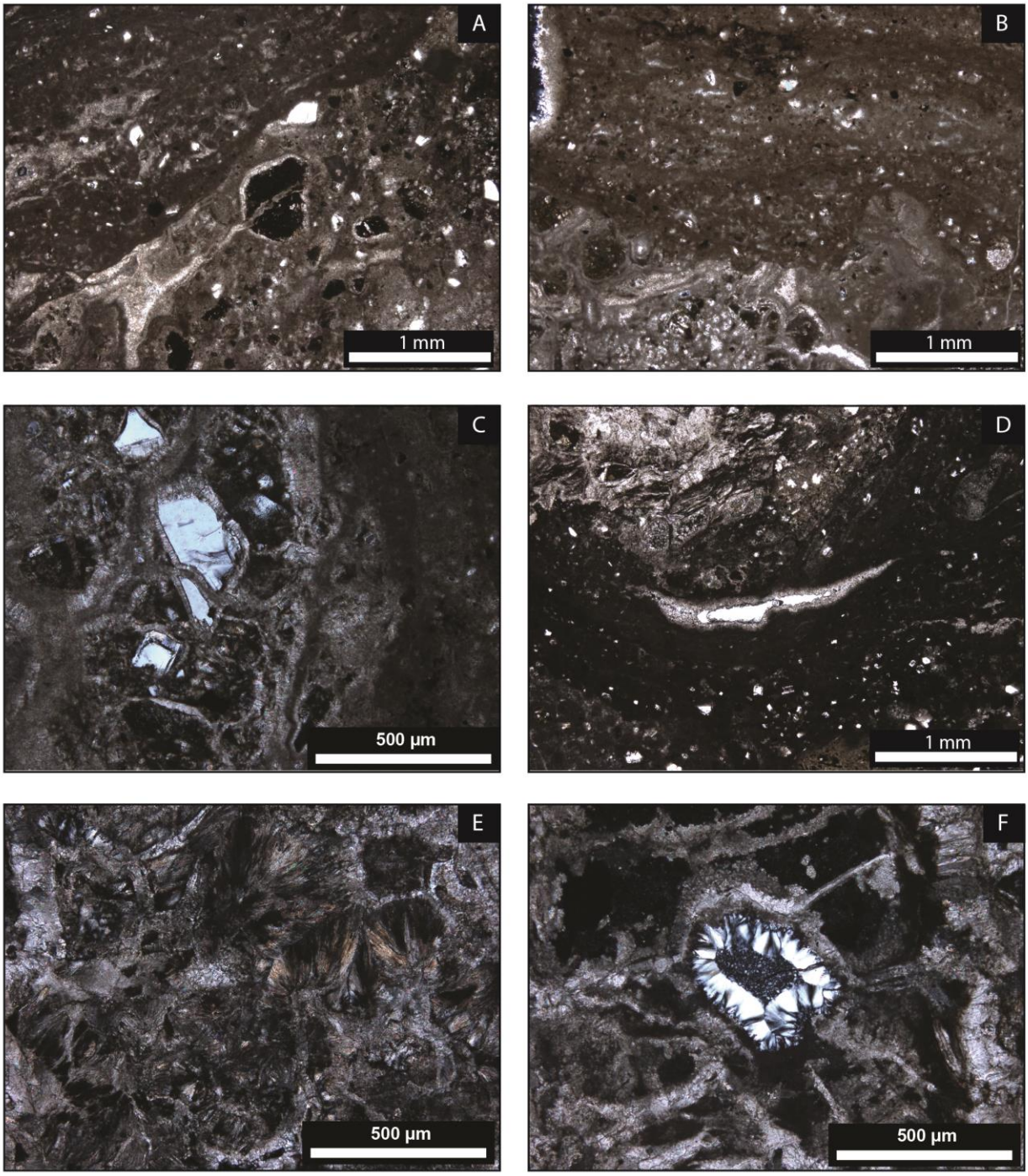

Figure 3-16. Photomicrographs of Oloronga-capping calcrete. (A) Massive calcrete below laminar calcrete. The laminar calcrete has fenestral voids thought to result from roots and root hairs. PPL. (B) Similar to A. The laminar calcrete overlies an irregular, jagged surface. PPL. (C) Tabular calcite surrounds fractured and displaced grains as well as filling other fractures. XPL. (D) A circumgranular crack occurring within the pisoid boundary. PPL. (E) Radial calcite replaces former erionite. XPL. (F) Silica cements a void potentially left by a root or root hair. Two phases of silica are present: early botryoids are in contact with equant silica crystals. XPL.

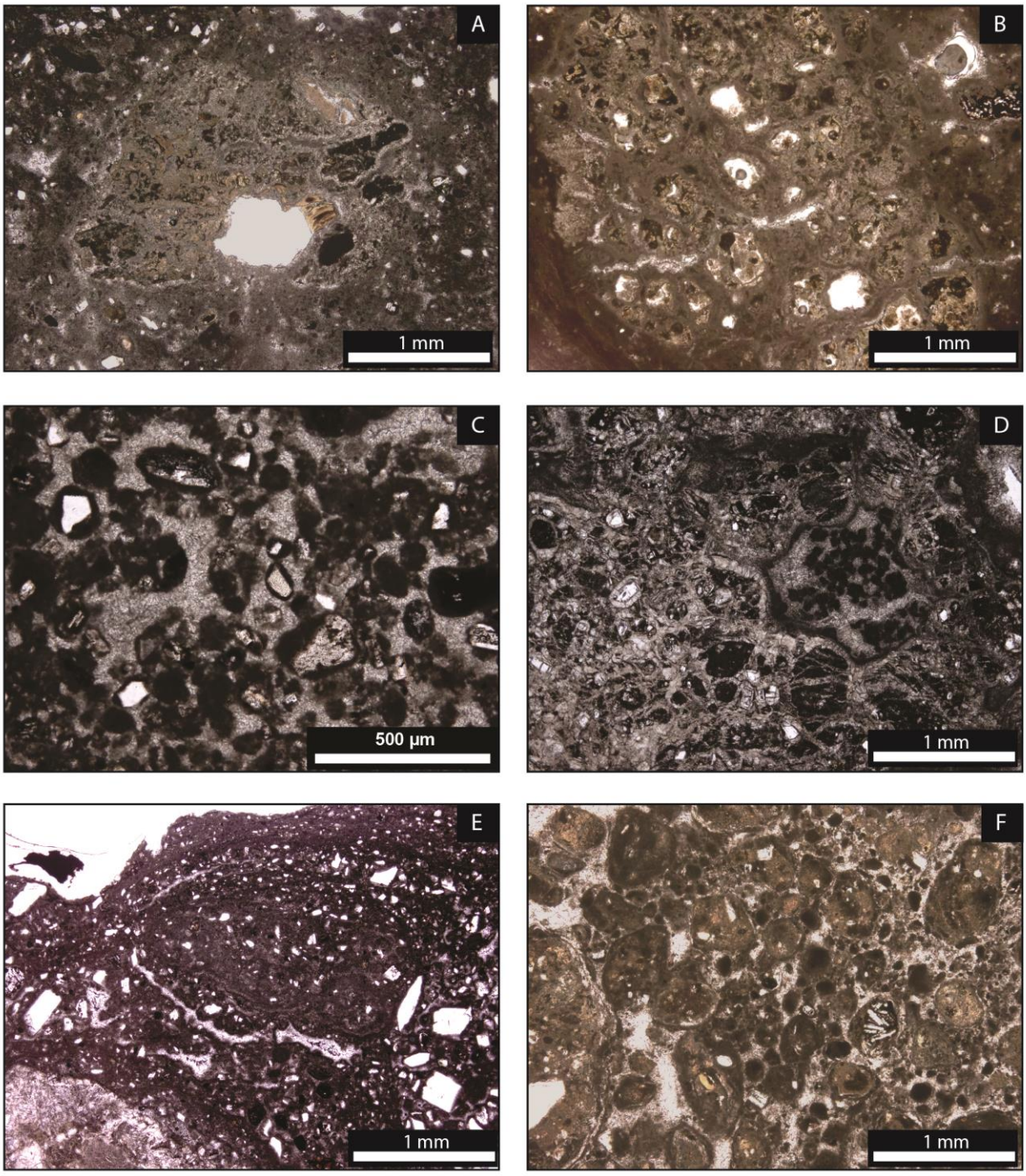

Figure 3-17. Beta microfabrics in the Oloronga-capping calcretes. A) The darker grey micrite septae surround clay-filled chambers in alveolar-septal microfabric. B) Another example of alveolar-septal microfabric. C) Micrite envelopes around mineral and micrite grains. D) Micritic peloids cemented by spar. E) Laminar calcrete shows some fenestral microfabric indicative of root mats. F) Clays and micrite make up peloids to create clotted texture.

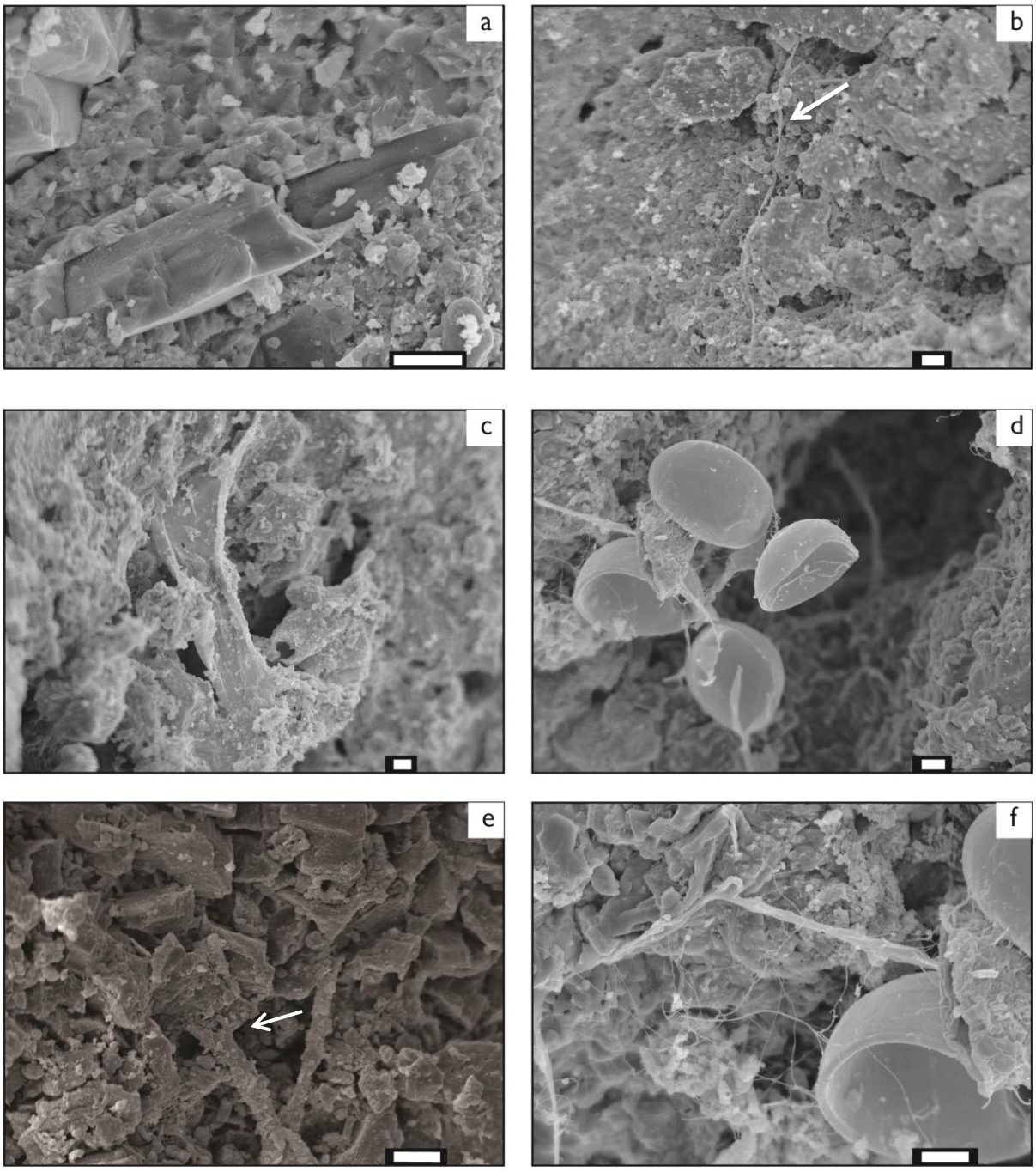

Figure 3-18. Scanning electron microscopy images of fresh fractured surfaces of the Oloronga-capping calcrete. A) A feldspar grain surrounded by micrite. Similar textures to this make up most (>80%) of the observed samples. B) Organic linear formation in micritic matrix (arrow). C) Desiccated organic material. D) Deformed smooth, globular fungal spores. These do not appear cemented into the calcrete and likely post-date calcrete formation. E) Calcified tubules (arrow) that may represent either root hairs or fungal hyphae. Compare with structure in F. F) Close-up of (D). Fungal hyphae net around the spores. All white scale bars are 10 µm.

3.3.1.2. Mineralogy

Calcium carbonate is present as micrite, spar, and euhedral fine sand sized grains. Subhedral to euhedral calcite crystals, 0.25–0.5 mm in size, are interspersed in the micritic matrix and differ in character from the authigenic cement. These crystals are light under backscattered electron (BSE) imagery (Fig. 3-19) unlike the normal micrite; this implies a higher concentration of atoms of a high atomic number, possibly Ba or Sr. These disaggregated calcites are present in the youngest, partially cemented, matrix material and have been recrystallized to micrite at the rims. They are associated with clinopyroxenes and K-feldspars (mostly sanidine).

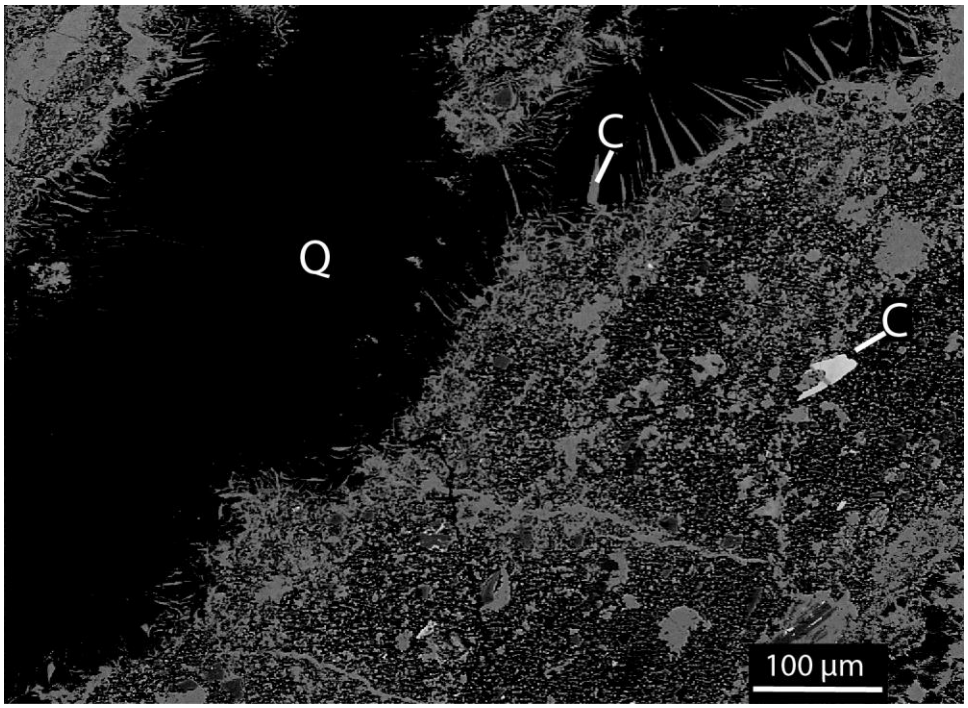

Figure 3-19. Back-scattered electron image of calcrete with calcite replacing a chalcedony vein. Within the micritic matrix is a solitary calcite crystal.

Clays are present as cutans around pores as a secondary mineral, acting as a cement in some samples. Clays are otherwise restricted to small linear fragments often associated with columnar calcite growth.

Barite was identified using BSE imagery with an energy-dispersive X-ray spectroscopy (EDS) sensor. Barite crystals within the transition zone where silica is being replaced by calcite

range from 1 to ~ 25 µm, and are subhedral to anhedral (Fig. 3-20). These crystals form aggregates up to 50 µm in diameter.

Detrital volcanic fragments are interspersed in the pisoid rim cements and the overall matrix cement. These fragments are typically trachytic with felted sodium-rich feldspar crystals in a glassy groundmass with porphyritic clinopyroxenes. Other detrital minerals in the matrix include clinopyroxene (aegerine-augite type), Na-amphibole, and minor plagioclase. Minor ilmenite, magnetite, titanite, and apatite are also present, mostly associated with clinopyroxenes or amphiboles.

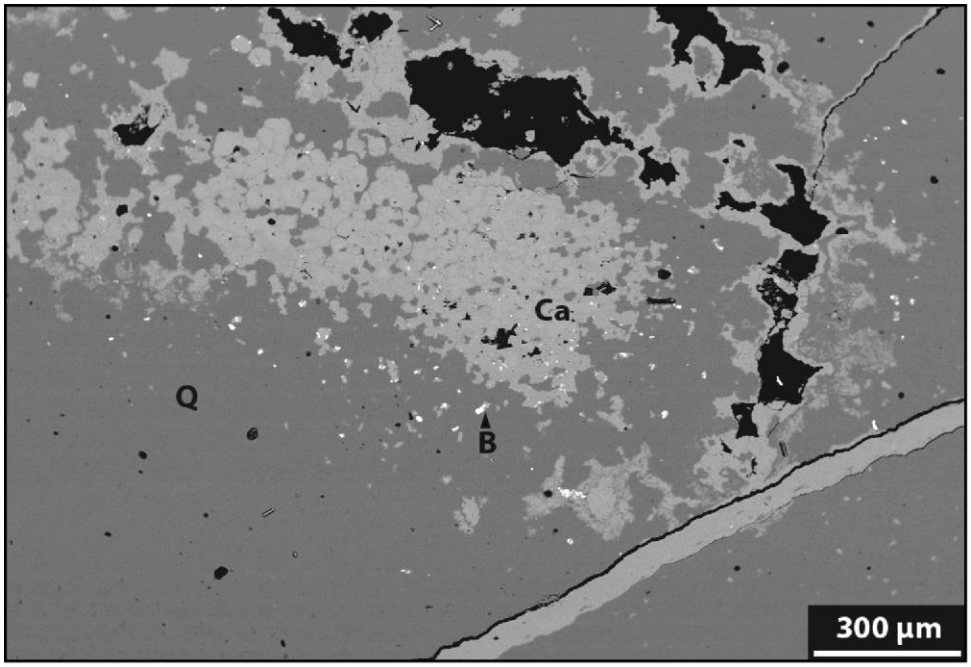

Figure 3-20. Back-scattered electron image of Oloronga-capping calcrete from the south shoreline of Nasikie Engida. Silica (Q) in the form of opaline spherules is being replaced by the lighter grey calcite (Ca), which adopts spherule shape. Barite (B) occurs in the zone of replacement. Note that calcite replacement occurs near voids and fractures (black).

Also noted in the matrix material are opaque laths and tabular isotropic minerals about 0.05 to 0.1 mm long. For the most part, all minerals in the matrix are subhedral to euhedral and are being replaced by micrite or have a tabular calcite corona.

Some of the calcrete contains clasts with irregular fibrous, chalcedony spherules. These are variably replaced by calcite which adopts the initial spherulitic texture. Replacement varies from very little to complete. In some samples it is only possible to determine that there was

precursor silica from the spherulitic pseudomorphs seen in the calcite. The silica has an alteration rim of opaque white material in thin section. Additionally, silica cements oval to spherical voids, potentially former root holes, as well as former circumgranular fractures in some samples, though overall this is rare (Fig. 3-16 F). Most samples have calcite pseudomorphs of erionite (e.g. Fig. 3-16 E).

3.3.1.4. Host sediments

A sample taken of the contact between the calcrete and the Oloronga Beds shows a clear delineation with calcrete overlying an erosive surface. Calcite is a minor cement in the sediments, filling only the still-open voids. Chalcedony spherules post-date the calcite. Erionite seems to be the principal cement (as determined petrographically), with amorphous silica. The zeolitic sediment was cemented prior to calcrete development, since calcite is present only in the most recent set of fractures that open from the contact boundary. Directly below the interface is a horizon with horizontal tubiform structures infilled with zeolite (likely erionite) (Fig. 3-21 B, G). These structures appear uniform in diameter and are possibly a trace fossil or representative of a root mat; because such a small sample was taken, it is hard to say with certainty what they represent. Below this horizon are horizontal laminated lacustrine deposits that include two distinct layers of radial calcitic ooids 0.5–1.5 mm in size (Fig. 3-21 A and C).

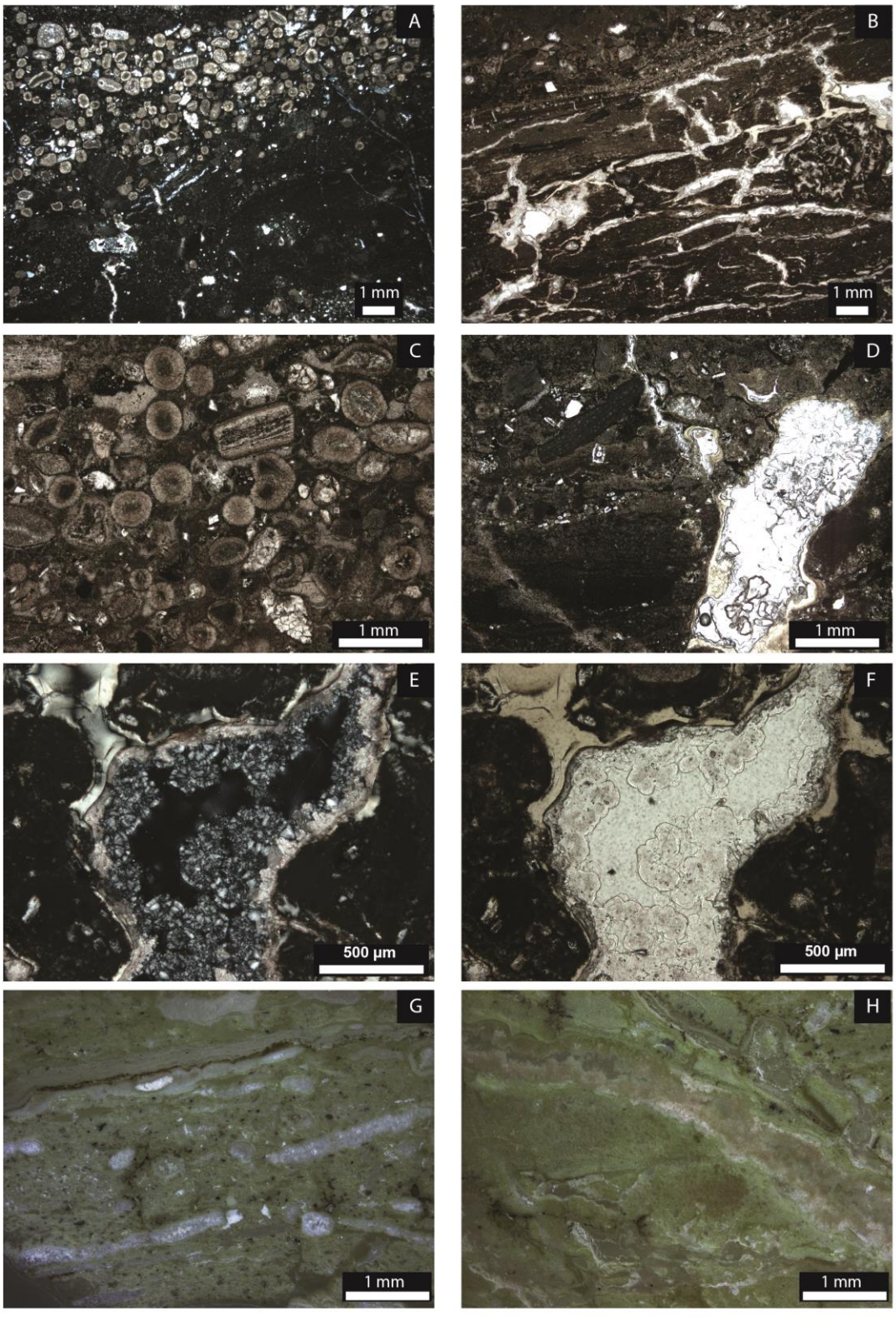
A
1 mm
B
1 mm
C
1 mm
D
1 mm
E
500 µm
F
500 µm
G
1 mm
H
1 mm

Figure 3-21 (previous page). Photomicrographs of some of the sediments underlying the calcretes. A) XPL photomicrograph of layer of ooids about 3-4 mm thick. B) Complex cracks partially filled with calcite spar, silica and amorphous silica cements. C) Close-up of ooids. Most are radial. D) Non-ooid layers. Note plant fragment fossil in upper left. E) XPL and F) PPL of the succession of cements: first amorphous silica, next spar to microspar, and finally chalcedonic spheres in the open pore. G) Photomicrographs using the white-card technique (Folk, 1987) showing tubules in cross-section and longitudinal section. H) Same technique as (G) showing a large crack partially infilled with acicular calcite cement.

3.3.2. Laminar calcretes

Laminar calcretes at Graham's Lagoon consist of a 0.01 to 2 cm thick layer of laminated micrite directly overlying the Magadi trachyte. Laminae are discontinuous and contain many micro-unconformities (Fig. 3-22 A, B). Laminae are typically of submillimeter thickness and are parallel to the substrate. Silt-sized detrital particles, mostly K-feldspars derived from the trachytes, are scattered within the laminae. Towards the top of the laminae layer, horizontal cracks present along lamina planes are open or filled with sparite. The laminae thicken in cm-scale depressions and thin over higher microtopography. Laminae are generally horizontal but some are subvertical following the trachyte surface. The micrite appears dense and light brown in plain polarized light (PPL), though alternates from lighter to darker. Some of these alternations reflect subtle changes in grain size (larger = lighter). Recognizable biologic microfabrics are absent. At hand sample scale many minute (sub-millimeter) round pores cross through the laminae.

Carbonate also replaces and fills the voids in the underlying trachytes (Fig. 3-22 F). Micritic pellet-sized particles within large pores are cemented by spar to create a pelletal microfabric (Fig. 3-22 F). In places the laminae resemble stromatolitic laminae; these sections are not laterally traceable and are no more than 0.5 cm in length (Fig. 3-22 C, E).

Floating grain microfabric dominates, though there are few instances of replacement by calcite or of calcite growth around a nucleus. Where a visible band of calcite surrounds a grain, it is thicker towards the bottom, indicative of vadose cementation (Fig. 3-22 D).

Detritus is derived from the host trachyte as well as rare chert fragments from older sediments. The source of the chert grains is unknown.

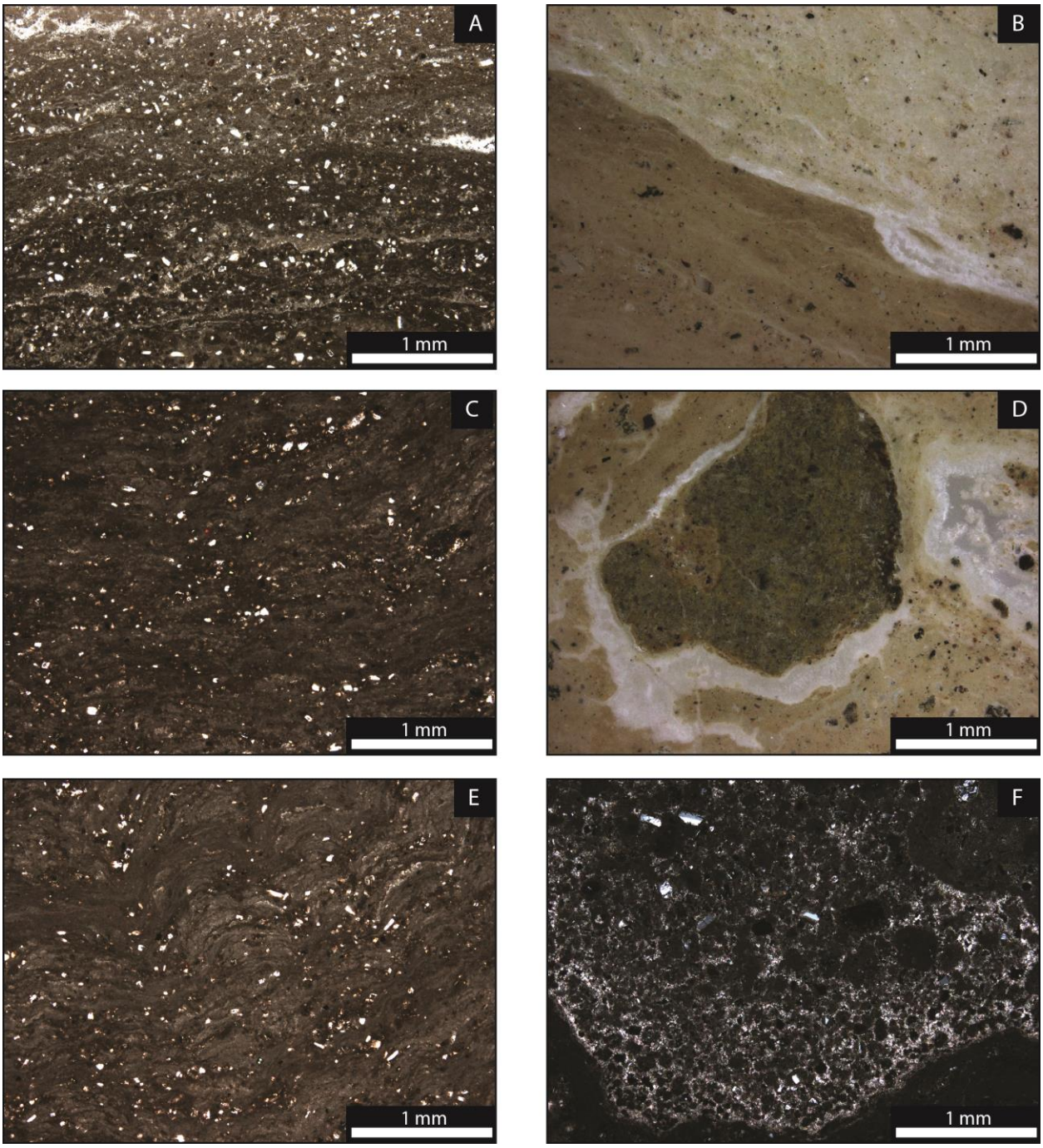

Figure 3-22. Photomicrographs of the laminar calcrete at Graham's Lagoon. A). General view of laminae. Note erosive surfaces and lack of light/dark laminae. Also note profusion of fine debris. There are a few instances of alveolar texture towards the top of the picture. B) Shows a micro-unconformity with two different laminae sets. C) Contrasted with A, slightly wavy laminae with fewer inclusions. D) Vadose cementation of calcite around a trachyte clast. E) Wavy laminae showing pseudo-stromatolitic texture. F) Spar cementation of fine grains collected gravitationally in a dip.

3.4 XRD analysis

XRD analysis of three calcrete samples determined they consisted predominantly of low-Mg calcite, with minor feldspars (albite, anorthoclase, and minor anorthite) and zeolites (including erionite and analcime). Analysis of the green clayey sediment underlying some of the calcrete in the Oloronga Beds yielded a predominance of erionite, opal C-T, quartz and calcite. A sample of the Oloronga Beds was analysed and its composition includes a variety of feldspars (anorthoclase, albite, and anorthite), clinopyroxene and minor orthopyroxene, low quartz, feldspathoid, and magnetite. The minerals detected in a sample from the High Magadi Beds are slightly different with albite as the dominant mineral with anorthoclase, clinopyroxene, zeolite(s), and quartz.

Analysis of two samples of Oloronga-capping calcrete near Nasikie Engida (one to the north, one to the south) indicates a dominance of low-Mg calcite. The southern sample also includes sanidine, quartz, and orthopyroxene. The northern sample contains albite, anorthoclase, feldspathoid, and zeolites.

The SE Magadi laminar calcrete sample analysed gives a dominance of low-Mg calcite with minor albite and zeolites.

3.5 Bulk rock geochemistry

The results of bulk rock geochemical analyses can be helpful in determining sediment source and diagenetic history (e.g. Lentz, 2003; Fralick, 2003; Owen et al., 2011). Sixteen samples of the Magadi calcrete and surrounding sediments were analysed for major and trace elements. Most of the samples came from the Dry Lagoon with two calcrete samples from south and north of Nasikie Engida. Additionally, two samples of the laminar calcretes above Graham's Lagoon were analysed.

	SiO_2	Al_2O_3	Fe_2O_3(T)	MnO	MgO	CaO	Na_2O	K_2O	TiO_2	P_2O_5	LOI	Total
Average Calcrete	22 ± 7.6	4.6 ± 1.3	2.6 ± 0.59	0.11 ± 0.033	0.81 ± 0.16	35.8 ± 5.6	1.7 ± 0.69	1.7 ± 0.51	0.30 ± 0.076	0.11 ± 0.055	30.2 ± 4.3	99.892

Table 3-1. Composition of average Magadi calcrete (n=8) in wt. %. LOI = Loss on ignition.

3.5.1. Major elements

The calcretes of Magadi have similar element distributions to the underlying Oloronga Beds but not the overlying High Magadi beds. As expected, most of the major elements show an inverse relationship with Ca, including Mg and P. For most samples, Mg becomes less abundant with calcrete formation (Fig. 3-23).

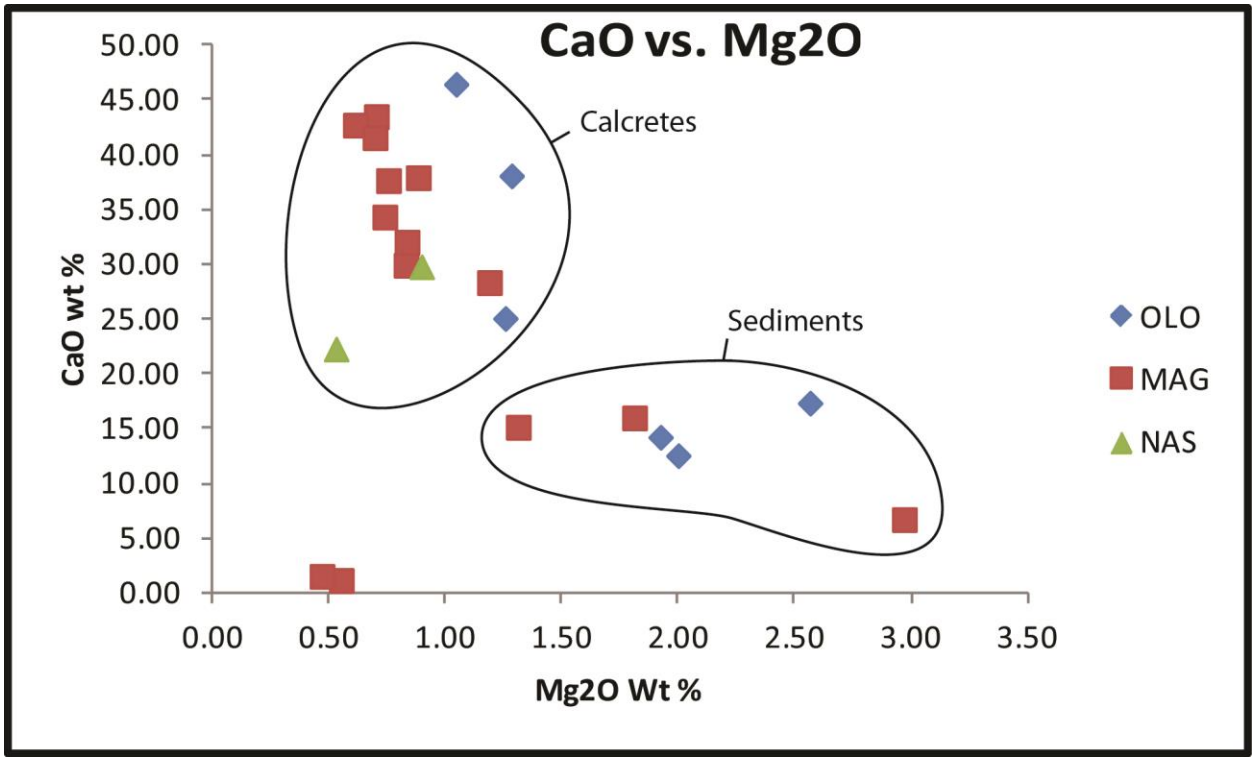

Figure 3-23. - XY Plot of CaO vs. Mg_2O wt.% in calcretes and associated sediments. While Ca increases, Mg decreases, indicating that Mg is taken up with Ca into the calcite. The two MAG samples with low concentrations of both species are from the upper High Magadi Beds and post-date calcrete formation. OLO: Olorgesailie (see Ch. 4); MAG: Magadi; NAS: Nasikie Engida (see Ch. 5).

The compositions lie within the range of calcrete samples analysed from near the Magadi town site by Baker (1958), as well as with calcrete samples from Tanzania (Hay and Reeder 1978) (Fig. 3-24). The calcretes of Baker (1958) have calculated calcite values of 70–72 wt % while samples from this study have a greater range (50–76 wt. %). Calcrete samples in the lower end of this range are more porous and less of the sediment has been replaced by calcite.

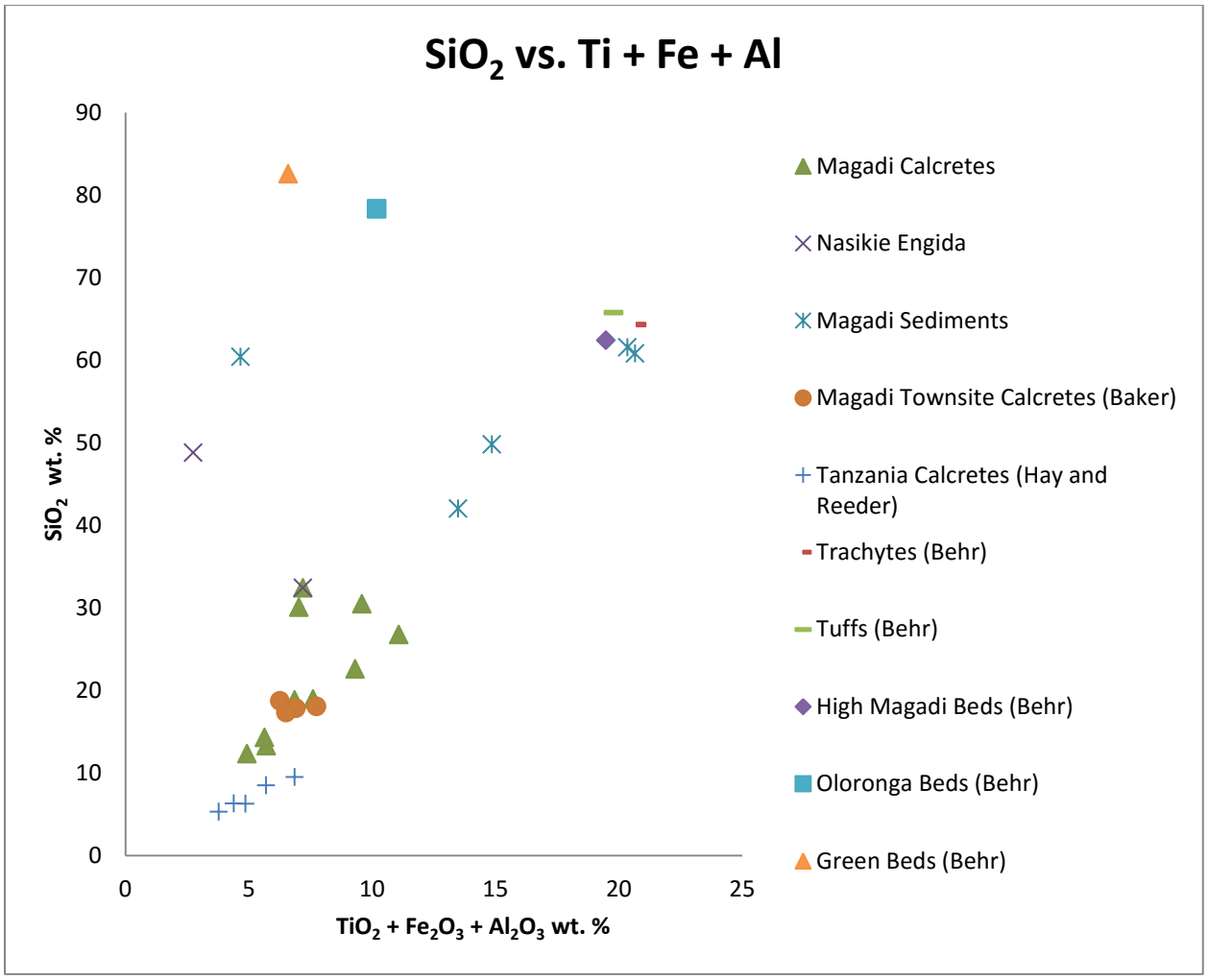

Figure 3-24. XY plot of major oxides comparing samples from this study and those of previous studies. Data from Baker (1958), Hay and Reeder (1978), and Behr (2002).

Two samples, one from the south of the Nasikie area and one from the Dry Lagoon, do not plot along the same trends as the rest of the samples. Their silica content is much greater while Ti and Al are much less, indicating secondary silica growth and not addition of detrital silica. Silica content varies from 12 to 32 wt. %.

There was a high loss on ignition (LOI) in all samples. This correlates well with Ca content and is likely the CO_2 from calcite (Fig. 3-25 f).

Calcretes range from 28 to 43 wt. % CaO. The highest values are in the most indurated calcretes. Calcretes have a calculated calcite concentration, assuming all or most Ca is from calcite, of 50–76 wt%. In general the trachytic sediments are calcium-poor; in thin section, Ca-bearing minerals are rare. The calculation was done under the assumption that if Ca is present in

minerals other than calcite, its contribution to the overall value is negligible. Calcium oxide concentration in the associated sediments varies from 1.14 to 15 wt%, with the higher percent probably indicative of secondary calcite cementation. The laminar calcretes average 66% calcite and are fairly low in silica (13–30 wt. % SiO_2). They also have slightly lower Na_2O wt. % than the average Oloronga-capping calcrete.

Figure 3-25. (Next page) Harker-type diagrams for whole-rock analyses of sediments and calcretes. Silica is not conservative so Al_2O_3 and TiO_2 are used instead. Note the separation of source areas using Ba.

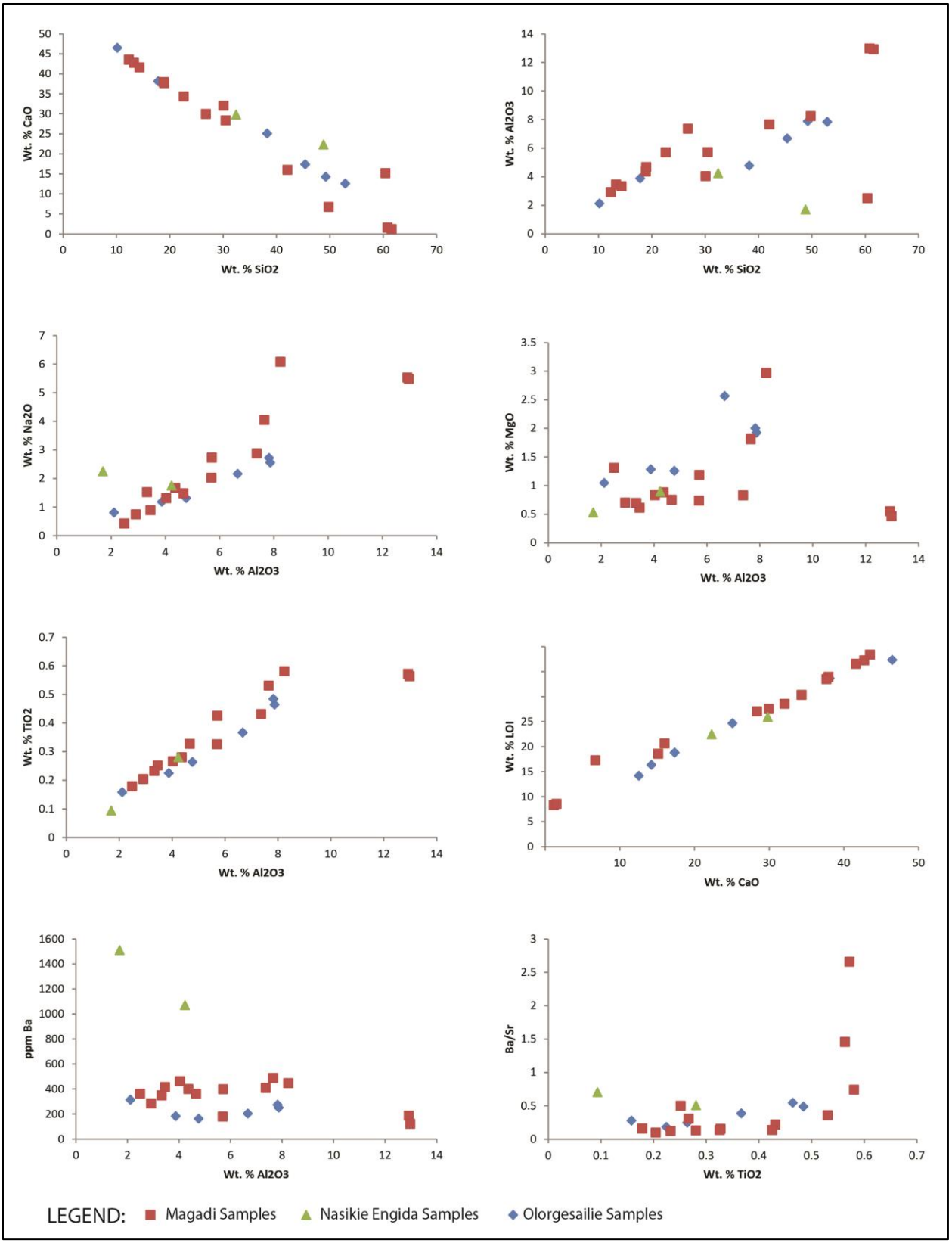
Wt. % CaO
Wt. % SiO2
Wt. % Al2O3
Wt. % SiO2
Wt. % Na2O
Wt. % Al2O3
Wt. % MgO
Wt. % Al2O3
Wt. % TiO2
Wt. % Al2O3
Wt. % LOI
Wt. % CaO
ppm Ba
Wt. % Al2O3
Ba/Sr
Wt. % TiO2
LEGEND:
Magadi Samples
Nasikie Engida Samples
Olorgesailie Samples

3.5.2. Rare Earth Elements

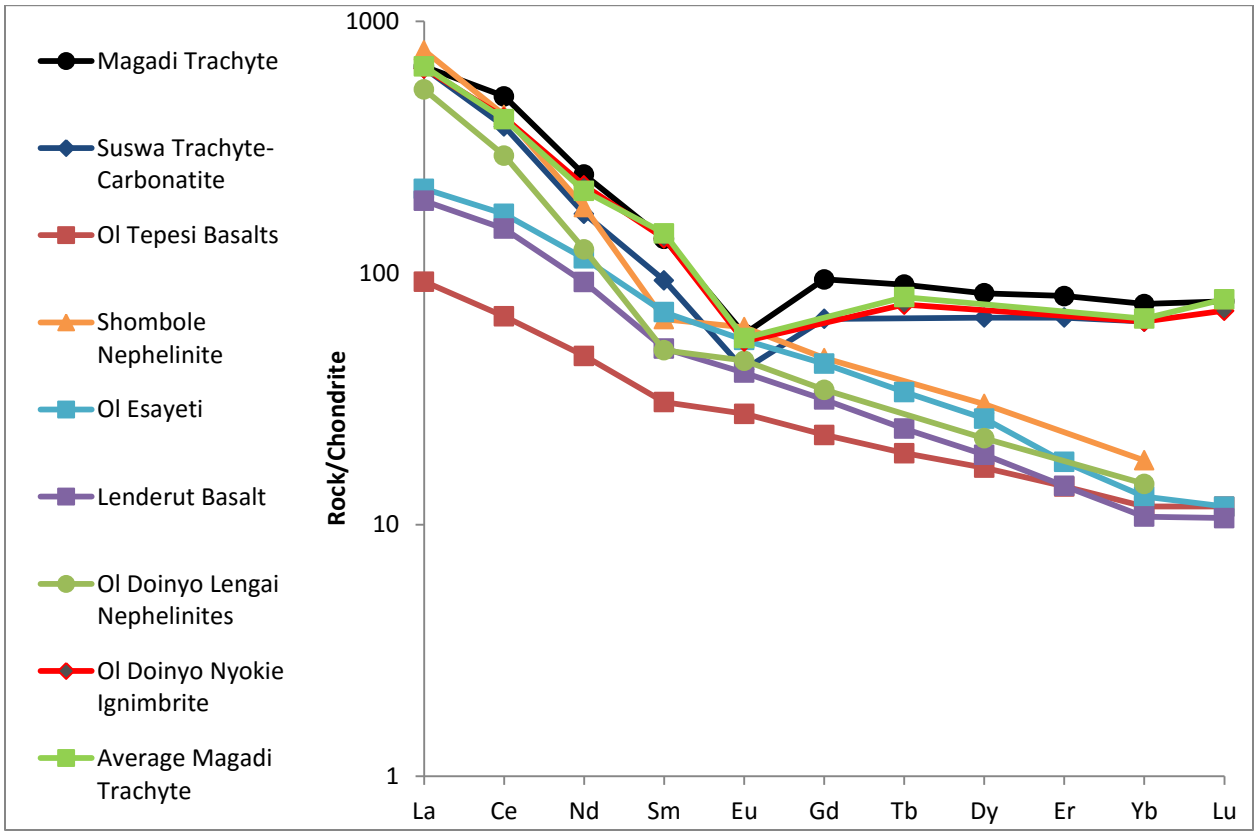

Figure 3-26. Regional REE distributions for a variety of rock types. The Magadi Trachytes have a significant Eu anomaly. The average Magadi calcrete plots very similarly to the Magadi trachytes. Magadi Trachyte data (black) is from leRoex et al. (2001). The Average Magadi Trachyte was collected beneath Ol Doinyo Nyokie ignimbrites, from Baker (1975). Data is from Baker (1975); Peterson (1989); Macdonald et al. (1993); and le Roex et al. (2001). C1 Chondrite data is from Sun and McDonough (1989).

Compared to regional host rocks, samples from Magadi show similar elemental distribution trends to the Magadi Trachytes. Normalized to C1 chondrite (Sun and McDonough, 1989), they show enrichment in REEs with a negative Eu anomaly as compared to the local basalts and nephelinites. Figure 3-26 shows local potential source rocks with the trachytes showing the pattern seen in the Magadi sediments.

Calcrete REE diagrams normalized to continental crust (Taylor and McLennan, 1985) show uneven enrichment, having a higher concentration of HREEs, while maintaining a negative europium anomaly (Fig. 3-27). Compared to their source sediments, however, the calcretes are less enriched overall. Sediments from below the calcretes (the Oloronga Beds) show a nearly identical pattern to the overlying sediments of the High Magadi Beds (Fig. 3-27 C).

Several differences in REE composition are noticeable between the sediments and the calcretes. In the laminar calcretes, it appears that while LREE are less concentrated than those in the sediments, Ce appears to be even less concentrated. In the Oloronga-capping calcretes, the LREE distribution aside from La is nearly flat, suggesting that more Sm, or perhaps less Nd, is lost from the sediments upon calcretization. The Eu-Tb join has a much shallower slope in the calcretes than in the sediments. Additionally, it appears that while the LREE and MREE have decreased in concentration in the calcretes, the HREE have increased beyond proportionally.

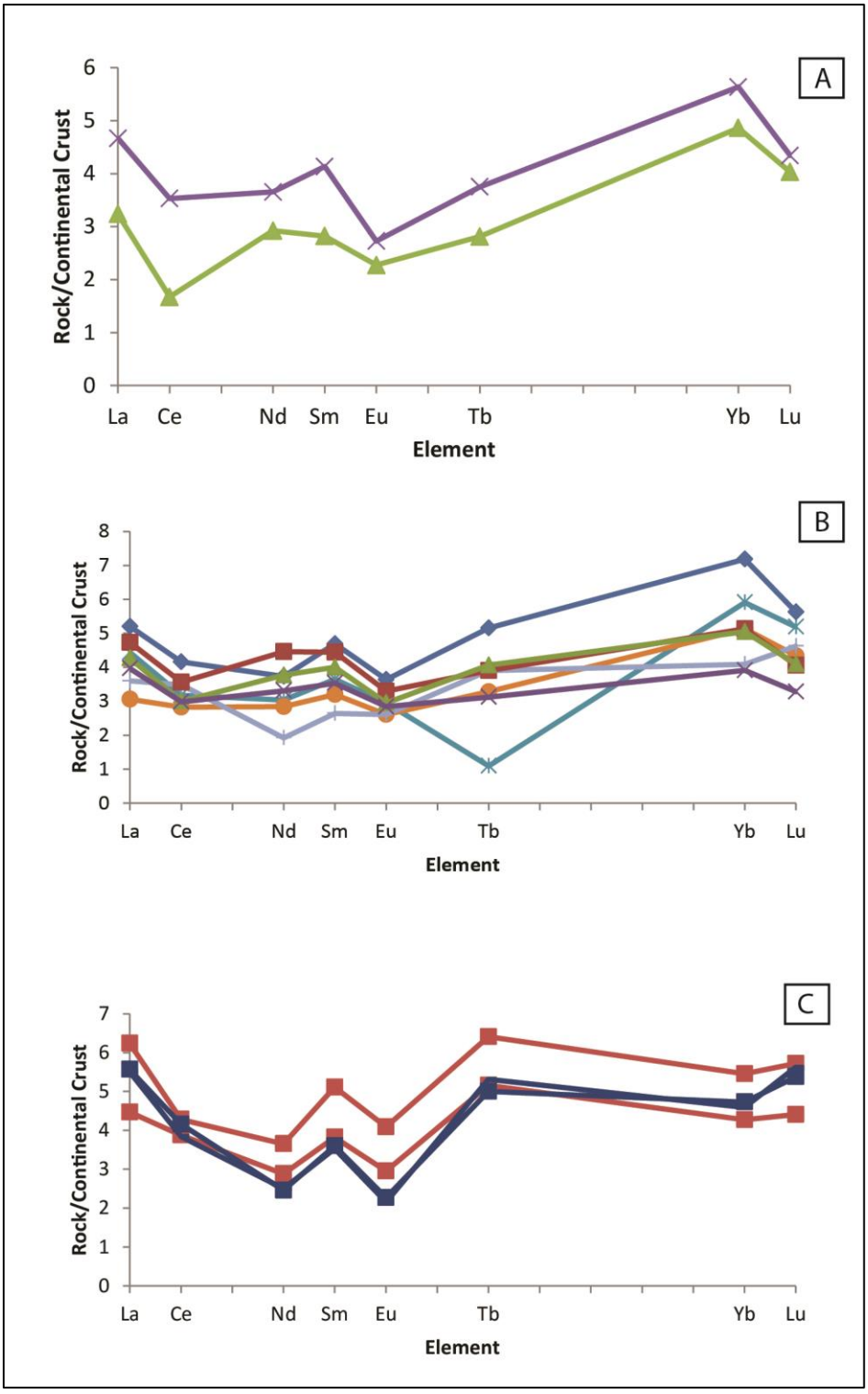

Figure 3-27. REE distribution in Magadi samples relative to continental crust (Taylor and McLennan, 1985). A) Laminar calcrete samples showing enrichment in HREE. B) Oloronga-capping calcrete. One sample shows an anomalous concentration of Tb. C) Sediment samples of the High Magadi Beds (in red) and the Oloronga Beds (in blue).

Europium and cerium anomalies were calculated using the formulas $(Sm^2Tb)^{1/3}$, and $(La^2Nd)^{1/3}$, respectively, where data for Pr and Gd is unavailable (McLennan et al., 2003). When plotted against each other there is a clear separation of source areas (Fig. 3-28). Suswa and Magadi Trachytes show negative anomalies for Eu, while the rift basalts, Shombole, and Oldoinyo Lengai all show minor positive deflections in Eu. Europium partitions into plagioclase; the Magadi and Suswa trachytes are plagioclase-poor and thus have less Eu. Similarly, sediments from Magadi show negative Eu anomalies, indicating their trachyte source. The sediments at Magadi also generally show an increased Eu/Eu* with decreasing Ce/Ce* as compared to the trachytes. The calcretes plot similarly to the trachytes, though in comparison to the sediments, are lower in Eu/Eu* and higher in Ce/Ce*.

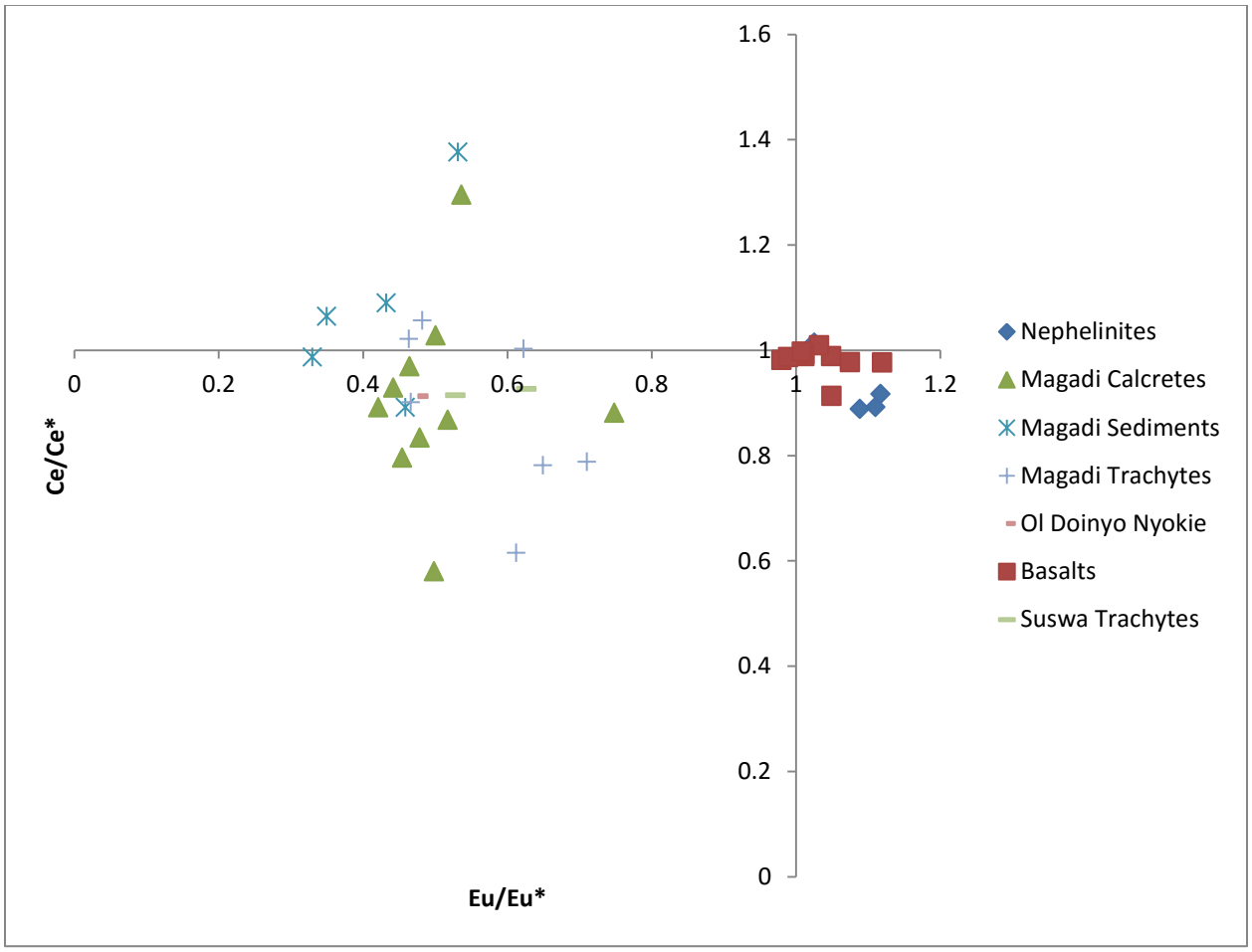

Figure 3-28. Europium anomaly vs. cerium anomaly for Magadi calcretes, sediments and volcanic rocks. While the basalts and nephelinites plot closely, the Magadi Trachytes are more scattered. Suswa Trachytes and the Ol Doinyo Nyokie Ignimbrite plot similar to the Magadi Trachytes. The Magadi sediments generally have a higher Ce/Ce* than

both the trachytes and the calcretes. Data from: Baker (1975); Peterson (1989); Macdonald et al. (1993); and leRoex et al. (2001).

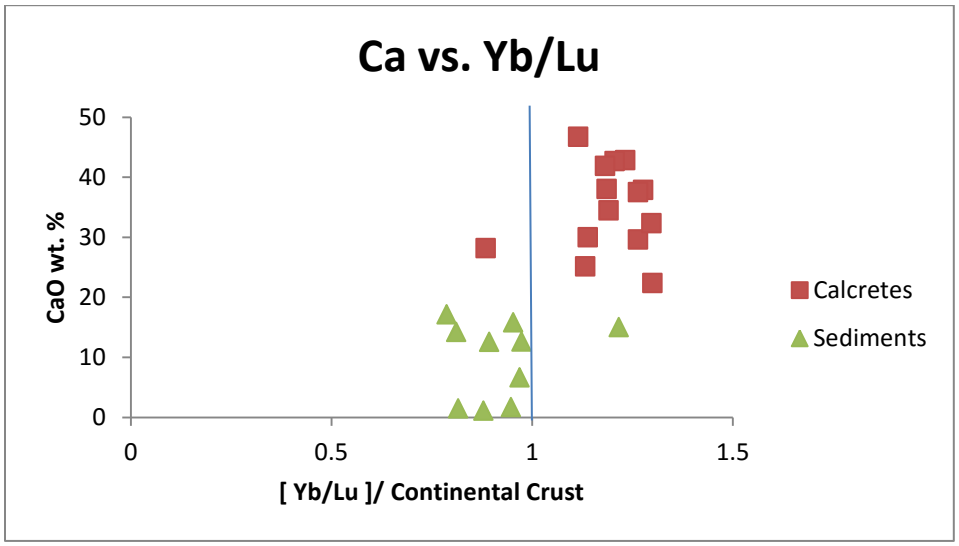

Figure 3-29. Graph of CaO wt % vs. Yb/Lu normalized ratio for calcretes and associated sediments. Almost all samples of calcrete had greater Yb amounts relative to Lu as compared to the sediments. The anomalous calcrete contains a large amount of sediment. The anomalous sediment sample has been highly altered and consists of zeolites, opaline silica, and calcite.

When normalized to continental crust the laminar calcretes show negative cerium and europium anomalies, and are enriched in HREEs, the latter being typical of calcretes (Ramakrishnan and Tiwari, 1998; Compton, 2003; Prudêncio et al., 2003, 2011).

An association between Ca content and Yb/Lu content was noted (Fig. 3-29) for all samples of calcrete and sediments studied, including the Olorgesailie site (see Chapter 4).

Calcrete samples show increased HREE compared to the sediments. In the stratigraphic section from Dry Lagoon, the sediments showed a greater concentration of REE than the associated calcrete, though their respective HREE remained at about the same concentration. The increase in the HREE may be due to carbonate formation from alkaline concentrated water. Weathering of the sediments to produce the Ca for the carbonate would also release the REEs, explaining their less enriched values in the calcrete. Because the HREEs are have high affinity for carbonates (Johannesson and Lyons, 1994), their concentration would stay the same, or nearly so, and the LREEs would be slightly lower as they are more likely to be removed in solution.

3.5.3. Trace elements

One sample of the laminar calcrete from Graham's Lagoon showed twice the sulfur content as the average Magadi calcretes (Table 3-1), and much lower vanadium. Both samples of the laminar calcrete have a higher Ba/Sr ratio than the Oloronga-capping calcrete (two points at 0.5 Ba/Sr, Fig. 3-39).

Based on element ratio diagrams, all sediment samples are enriched in Sr compared to their parent rocks. Strontium is mobile and is preferentially incorporated into calcite, substituting for Ca^{2+}. There is no good statistical relationship between amount of Ca and Sr in the Magadi calcretes or sediments, though there may be for those from Olorgesailie (Figure 3-30).

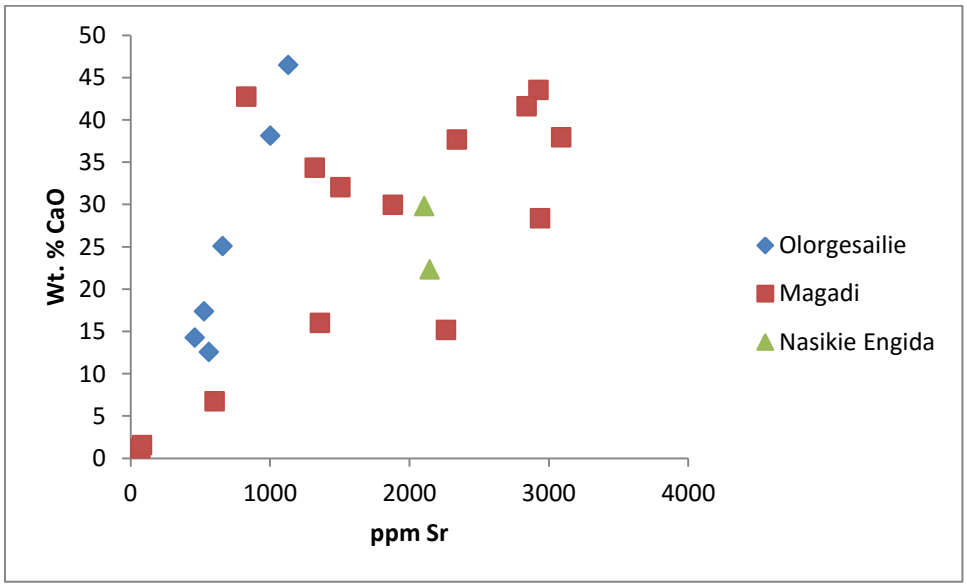

Figure 3-30 - Graph comparing calcium concentrations to strontium in Magadi calcretes and related rocks.

The laminar calcretes on volcanic rocks (indicated in Fig. 3-30) do not have the same Sr trend as the other calcretes and show that Sr enrichment is weaker in the laminar calcretes than the pisoidal calcretes.

The ratio of Ba/Sr is used as an indicator of amount of weathering in surficial deposits (Bestland and Retallack, 1993; Retallack 1994) because Sr is more soluble than Ba in a typical surface environment. Barium ranges from ~ 200–500 ppm in all Magadi samples, apart from two at SE Nasikie Engida which have Ba > 1000 ppm matched by an increase in Sr. There is little difference in Ba content between calcretes and sediments, whereas Sr varies considerably in all

samples. In Figure 3-31, Ba/Sr is plotted against CaO to show that non-calcrete sediments (i.e. those with low CaO wt. %) have higher Ba/Sr ratios, which implies more weathering. The High Magadi Beds have the highest values of Ba/Sr while the Oloronga Beds have lower values. The calcretes have extremely low values because of the uptake of Sr during calcite precipitation.

Most calcretes are enriched in Br compared to the sediments. A high Br/Sc ratio has been reported in biological precipitation of calcite (Prudêncio et al., 2011). Calcretes at Magadi range from 1.9 to 5.8 Br/Sc.

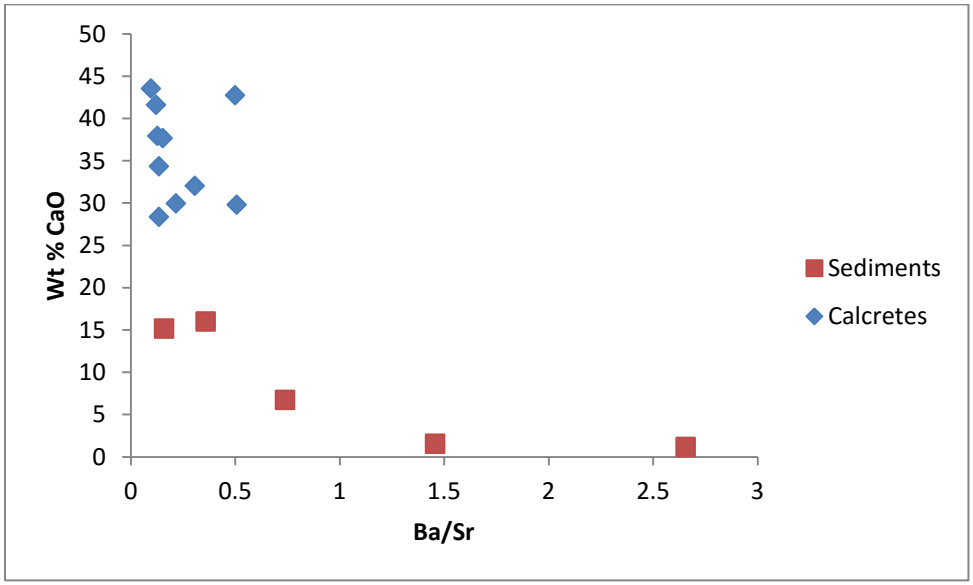

Figure 3-31. CaO wt % vs. Ba/Sr ratio for sediments, Oloronga-capping calcretes and laminar calcretes at Magadi.

3.5.4. Observed trends in the stratigraphic section at Dry Lagoon

The sampled section at Dry Lagoon (Fig. 3-7) shows an upward increase in calcite concentration, culminating in the calcrete at 68 mol% $CaCO_3$. The overlying High Magadi Beds sediments are very calcium poor, with concentrations of 1.5 and 2 mol% CaO. Mn, P, Ba, S, Sr, and Mg increase in the calcrete, though there is internal variation (Fig. 3-32).

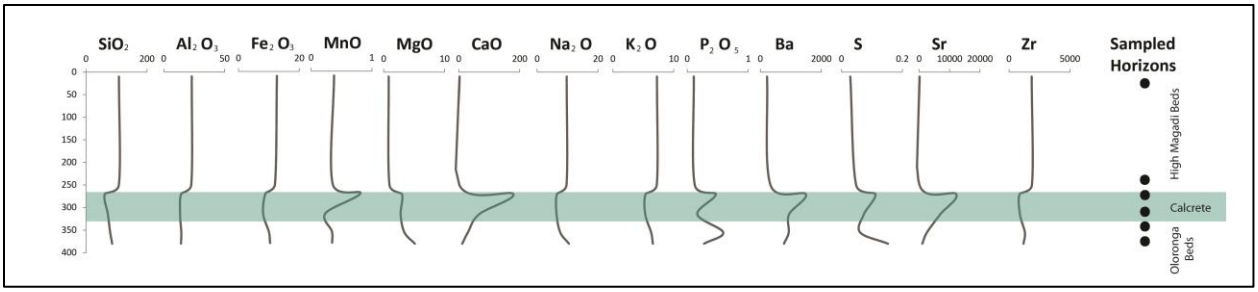

Figure 3-32. Depth plots depicting relative abundances of certain major and trace elements in the section measured in the Dry Lagoon (Fig. 3-9). All elements are relative to TiO_2 to mitigate detrital component influence. Colored horizon is the calcrete layer. Depth is in cm below the land surface.

3.6 Stable isotope geochemistry

Carbon and oxygen isotopes show covariance ($R^2 = 0.5195$) in the Magadi calcretes, and show a slight inverse relationship in the host sediments (Fig. 3-33). Both $\delta^{13}C$ and $\delta^{18}O$ values are enriched in the calcretes with respect to the underlying or overlying sediment – more so for ^{13}C. Possible contamination from carbonatite ash ($\delta^{13}C$: -6 to -8‰; $\delta^{18}O$: +5.5 to +7.5‰$_{SMOW}$) would cause the values to be more depleted in ^{13}C (Keller and Zaitsev, 2006). As the values are significantly higher, it is unlikely that there is much contamination from this source.

For the Oloronga-capping calcretes, $\delta^{13}C$ ranges from -2.01 to +2.82‰ VPDB: +0.74 to +2.82‰ in calcretes and -2.01 to +1.64‰ in sediments. The range for $\delta^{18}O$ is -3.16 to +3.69‰ VPDB, with values of -1.32 to +3.69‰ in calcretes and -3.16 to +1.46‰ in sediments.

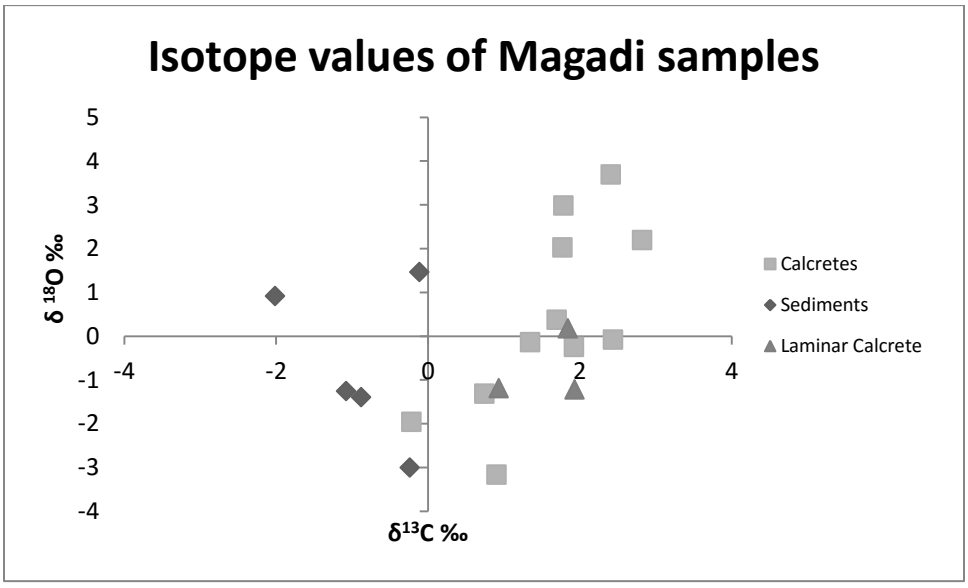

Figure 3-33 (previous page). C and O isotope values of Magadi samples, showing enrichment in $\delta^{13}C$ of calcretes over sediments and, similarly, an increase of $\delta^{18}O$. The two sediment samples with high $\delta^{18}O$ (>0‰) are from the High

Magadi Beds, which overlie the calcretes. Calcretes in the figure refers to the Oloronga-capping calcretes. Laminar calcretes are those above Graham's Lagoon.

At the Dry Lagoon the δ ^{18}O profile shows an upward increase in ^{18}O content—the calcrete is not enriched relative to the High Magadi Beds above (Fig. 3-34). δ ^{13}C increases in the calcrete with a typically positive **‰** value compared to the related sediments which have negative **‰** values The High Magadi Beds have a decreased δ ^{13}C compared to the calcretes.

The laminar calcretes above Graham's Lagoon range from +0.94 to 1.93 ‰ δ ^{13}C and -1.22 to +0.17 ‰ δ ^{18}O, with averages of +1.57‰ δ ^{13}C and -0.75‰ δ ^{18}O.

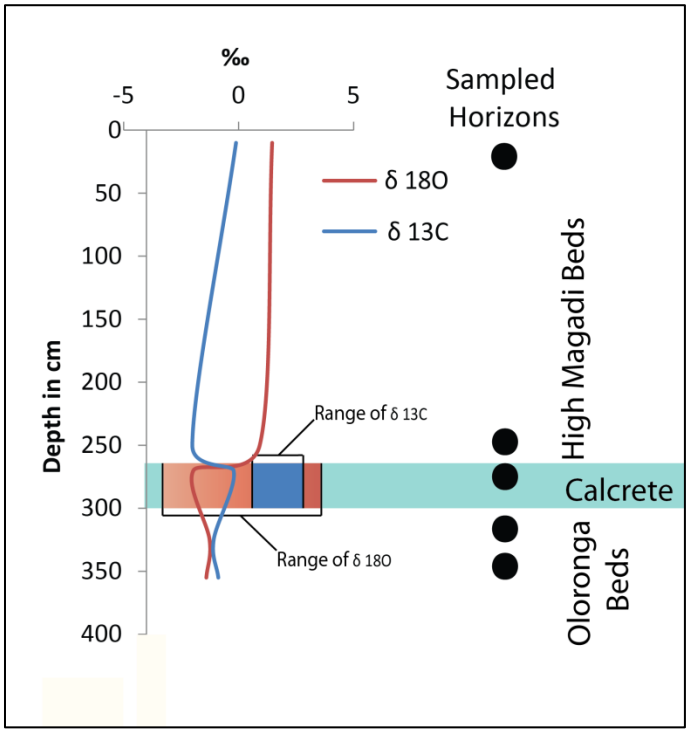

Figure 3-34. δ ^{18}O and δ ^{13}C of the sampled stratigraphic column of the Dry Lagoon. In the calcrete there is a marked decrease in δ ^{18}O and an increase in δ ^{13}C. C and O isotopes are reciprocally covariant in this stratigraphic section but isotopes for all calcretes show a positive covariant relationship. Ranges for the isotope values are given with the red box, which indicates the range of δ ^{18}O, and the blue box, which shows the range of δ ^{13}C. Because the sample from the stratigraphic section shows δ ^{13}C at the very lowest end of the range of all samples, the result for the calcrete sample from the section may be erroneous.

3.7 Processes of calcrete formation

3.7.1. Water source

In the Kenya Rift Valley, the carbonate-bearing water can be lake water, spring water, groundwater, circulating geothermal fluids, or surface runoff including rainwater. Since the calcite shows no evidence of deposition from a large body of water, it is not of lacustrine origin. The underlying sediments contain layers of ooids, though the calcrete clearly post-dates these. While there may be a few textures possibly related to springs within the calcrete, these are rare and the overall abundance, stratigraphic position, and widespread distribution preclude subaerial spring water as a major source. Thus, the calcrete has been supplied with either regional groundwater or percolating runoff for its formation.

One potential indicator of water source is the presence or absence, and abundance of alpha microfabrics, as well as indicators of vadose or phreatic precipitation, such as pendant and meniscus carbonate cements. Typically, calcretes that formed in the vadose realm are more micritic, with pendent and meniscus cements, and textures that imply near-surface processes and rapid crystallization. Crystal size commonly varies within a single calcrete (McLaren 2004; Stokes et al., 2006). Additionally, fine micritic calcite mosaics may recrystallize to microsparite or sparite over time (e.g. Carozzi, 1993), and may destroy primary microfabrics. Differences in primary crystal sizes and their relative crystallinity are related to the parent fluids. Micrite usually indicates precipitation in a rapidly evaporating (or diminishing) fluid, while coarser sparite indicates precipitation from an enduring fluid replenished in Ca^{2+} and CO_3^{2-}, though crystal size can be influenced by other factors, such as impurities (Braithwaite, 1983). Changes in crystal size can reflect whether the calcrete was formed during periodic inundation (in the vadose realm) or from groundwater. For example, Stokes et al. (2006) studied a calcrete that showed two phases of growth: first, pedogenic formation, with grain-coating and glaebular micrite, followed by groundwater cementation, evinced by pore- and void-filling microsparite and sparite.

Micrite, microspar and sparite are present in the Oloronga-capping calcrete. Dense micrite is present as nodules, peloids, matrix, and laminated layers. Drusy sparite fills cracks and voids; tabular sparite forms circumgranular rims around volcaniclasts and solitary feldspar crystals. Much of the micrite is replacive and preserves relict textures from the host material.

Pendent and meniscus cements are rare and not present in most samples; instead, sparite cements multiple generations of cracks and pores. One sample showed build up of micrite on the tops of nodules (Figure 3-35), similar to the thickened laminae on pisoids towards the top of the Olduvai calcretes (Hay and Reeder, 1978), and may be related to temperature and gravitational flow of water. This may indicate a fluctuation in groundwater or calcite precipitation within descending meteoric fluids. These nodules are small and indicate that rotation of grains did not occur during their formation.Textural evidence points towards a predominant groundwater source of water (and thus carbonate) with cementation occurring at or near the groundwater table with periods of dryness.

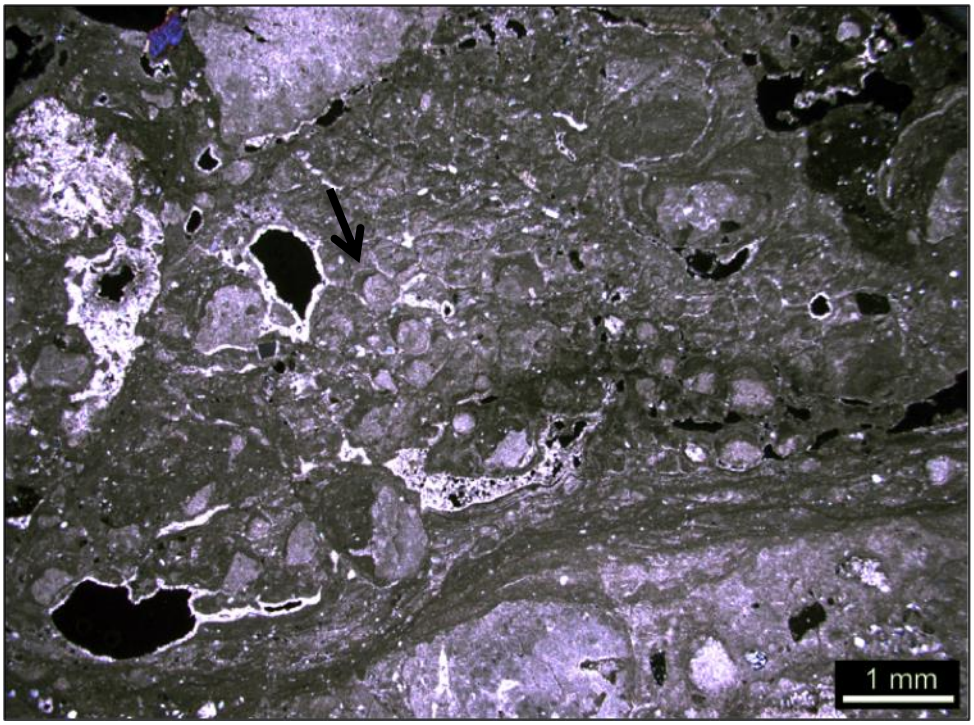

Figure 3-35. Oriented photomicrograph of the Oloronga-capping calcretes showing dense micrite at the tops of nodules (arrowed). XPL.

Additionally, silica precipitated as cement in fractures and voids of the calcrete. Detrital chert clasts are also common in the calcrete. Silica has precipitated at Magadi several times as Al-Si gels and as Magadi- and other types of chert (Eugster, 1967, 1969, 1980; Eugster and Jones, 1968). Locally, opaline cements in the calcretes were precipitated following chemical corrosion of detrital silicate grains. Silica could not remain in solution when the pH was lowered, or when Ca-depleted, Si-rich spring fluids at the surface or feeding subsurface waters underwent cooling. Silica precipitation occurred in the green waxy claystone in the Oloronga Beds;

elsewhere the silica remained in solution as monosilicic acid or as ions, and flowed towards the lake. High aqueous silica implies a pH > 9, which is compatible with most lake and ground-waters in the basin.

Tandon and Andrews (2001) showed that it might be possible to infer the source of the waters using stable isotopes, but care must be taken to assess the impact of diagenesis. Covariance in isotopes can result from a pedogenic environment (Cerling, 1984; Cerling and Hay 1986) or a hydrologically-closed lake environment (Talbot, 1990). However, pedogenic carbonates are typically less enriched than the closed-lake carbonates, which experience more evaporative concentration (Cerling and Hay, 1986). The isotopes measured for the Magadi calcretes increase in both $\delta^{18}O$ and $\delta^{13}C$ when compared to the host sediments, indicating evaporative concentration (Fig. 3-32), and the calcretes show textures that imply precipitation from groundwater, as discussed above.

Modern springs at Lake Magadi have $\delta\,^{18}O$ values of -4.4 to -1.3 $‰_{VSMOW}$ (Hillaire-Marcel and Casanova, 1987) and the spring-fed lagoons have slightly more enriched values of -3.1 to -0.1 $‰_{VSMOW}$ (Darling et al., 1996; Darling, 2001) The average Kenyan meteoric water, regardless of elevation, is -2.5 ± 2.4 ‰ for $\delta\,^{18}O_{VSMOW}$ (Levin et al., 2009). Theoretical isotope values calculated using $1000\ln\alpha_{calcite\text{-}water}=29.08$ (Coplen, 2007) for calcite precipitated from modern meteoric water at typical East African temperatures (~25°C) do not yield values compatible with those for the analysed calcretes. Those values, from meteoric water values of -3.8 ‰ (Hillaire-Marcel and Casanova, 1987) and -2.5± 2.4 ‰ (Levin et al., 2009) are +24 and a range of +23.4 to +28.4 $‰_{SMOW}$, respectively. Calcite precipitated in modern lake water would give a value of +33‰ and modern brines a value of +38‰ (Hillaire-Marcel and Casanova, 1987). The measured values of the calcrete give an equivalent range of +28 to +35 $‰_{SMOW}$ using the conversion calculation of Friedmann and O'Neil (1977). This implies that the calcite precipitated from a solution within the range between meteoric and lake water, which agrees with the hydrochemical model of Jones et al. (1977).

Isotopic evidence for the Magadi carbonates does not support calcite precipitation from dilute meteoric water, but rather from concentrated fluids. Although there might be problems with the alpha values used in the calculations (e.g. Coplen, 2007), these values imply that the calcite precipitated from waters more concentrated than meteoric water.

Temperature and pH both have a significant impact on the fractionation factor of the calcite-carbonate-water equilibrium. The temperature estimate might not be appropriate. In a study of modern soil temperatures in Kenya, Mace (2012) showed that grasslands and bushlands had soil temperatures at 0.25 m depth that were 2–6 °C higher than the air temperature. At Magadi, the pH of the lake waters is typically high (pH > 9: Jones et al., 1977), which reflects evaporative concentration and the alkaline trachytic bedrock, which would decrease the fractionation factor (Dietzel et al., 2009). The fractionation factor is also affected by the rate of precipitation (Dietzel et al., 2009; Gabitov et al., 2012), which in turn influences crystal size and shape. Calcite crystals in the calcrete vary from micrite to sparite, and thus rates of precipitation likely varied during calcrete formation. The bulk samples analysed give only an average value for the precipitation rate, lessening its impact as a factor controlling the crystal size. Many processes control precipitation of the calcite.

The relationships between the carbonate and water oxygen isotopes of the calcretes are uncertain because the fractionation factor changes with temporal changes in temperature, pH and precipitation rate. Calculations between water and calcite $\delta^{18}O$ using fractionation factors calibrated for equilibrium in another setting may not yield useful results (Dietzel et al., 2009). It may therefore be better to compare isotope values qualitatively with values obtained from calcretes in similar environments (e.g. Talma and Netterberg, 1983; Cerling, 1984).

Studies have shown that evaporation has little to no effect on isotopic composition in soil water below about 50 cm depth (Retallack, 2004). As mentioned, the Magadi calcretes are inferred to have precipitated from fluids that underwent significant evaporation from fluids at depths < 50 cm below the contemporary land surface. Potentially, those fluids were not in equilibrium with contemporary atmospheric CO_2, or the carbonate-bearing solutions were isotopically enriched groundwater.

The $\delta^{18}O$ values for the Oloronga-capping calcretes are variable with values from -3.16 to +3.69 ‰ VPDB. This might be explained by spatial differences, reflecting differences in water source because the calcretes with the highest $\delta^{18}O$ values were sampled in more northern locations than those to the south. Cerling and Hay (1984), Hillaire-Marcel and Casanova (1987), and Nehza et al. (2009), however, note that wide variations in isotope values are common in closed-lake environments, especially where separate lagoons (i.e. very local groundwater sources) develop. Although the calcrete values are variable, calcrete samples from the Dry

Lagoon stratigraphic-profile follow the same trend as the profile sediments, using higher $\delta^{18}O$ values as an indicator of increasing aridity (Cerling and Hay, 1984; Nehza et al., 2009). Thus, from the time of the Oloronga Beds to the present, the $\delta^{18}O$ values imply increasing aridity (Fig. 3-33). The enriched $\delta^{18}O$ values of the calcretes, when compared to those of the host sediments, imply that the dominant mechanism of calcite formation was evaporation from evaporatively concentrated water.

Subhedral to anhedral clusters of barite were found in some samples using BSE and an EDS sensor. Without an in-depth study it is difficult to determine the source of the barite in the studied calcretes. The barite is not derived from the host material, nor does it seem to be detrital. It is located both in zones of replacement and in calcite-filled microfractures, implying that it is authigenic. Two possibilities are that 1) barite precipitation is physicochemical, or 2) barite precipitation is biomediated. Barite has been linked to precipitation as a response to biological processes (biomediated) including adsorption onto microbial surfaces and extracellular polymeric substances (EPS: Bonny and Jones, 2008a, 2008b; Brock-Hon et al., 2012). Because the barite was found primarily at sites of calcite replacement of silica, it is likely the chemical conditions caused barite formation. Though unusual, barite has been found in other calcretes (Brock-Hon et al., 2012). Barite may also form from saline groundwater in some calcretes (Khalaf, 2007).

Given the evidence, a shallow-groundwater origin for most of the calcrete is likely, with cementation taking place at or near the water table under a drying climate.

3.7.2. Source of Ca

When CO_2-charged rainwater weathers and erodes the trachytes it gains Ca and Mg as well as other solutes. Although they have low wt.% Ca, the trachytes contain Ca-bearing minerals (augite, aenigmatite, Na-Ca amphibole, and minor amounts of apatite). Water from the Ewaso Ngiro River and dilute groundwater contains up to 24 mg/L Ca (Jones et al., 1977), which at present is the most concentrated fluid with respect to calcium. After the groundwater is further concentrated by evaporation in a semi-arid environment, Ca and Mg are the first cations to precipitate as carbonates. As the water moves from meteoric precipitation to groundwater to lake water, it follows a chemical evolution path that leads to Na, CO_3^{2-}, and Cl^- as the dominant ions in the lake brine (Jones et al., 1977). The high evaporation and low rainfall retard the movement

of runoff and rainwater into the lake, and Ca and Mg are often depleted before the evolved groundwater enters the lake or is discharged as spring water. Under a moister climate regime and during the rainy season, some calcium may enter the lake; oncoids dated at 5000 y BP (Seegers and Tichy, 1999), which is coincident with the onset of aridification of the Sahara and broadly north-east Africa and the end of the African Humid Period (deMenocal et al., 2000; Berke et al., 2012), formed at the south end of Magadi and may still be forming today (Casanova and Tiercelin, 1982). Additionally, layers of ooids are present in the sediments (Oloronga Beds) that underlie the calcretes, indicating times when Ca was, at least locally, present in the lake water.

Sampled Rock	SiO_2,	Al_2O_3	Fe_2O_3	MnO	MgO	CaO	Na_2O	K_2O	TiO_2	P_2O5	LOI	Total
Magadi Trachyte	61.38	13.66	8.53	0.31	0.63	1.95	5.46	4.66	0.92	0.14	1.17	98.80
Kirikiti Basalt	47.12	14.36	12.98	0.20	6.89	11.31	2.82	0.74	2.01	0.36	0.88	100.09
Ol Tepesi Basalt	46.90	14.69	12.73	0.20	6.49	11.84	3.11	0.67	1.94	0.32	0.71	99.86
Ol Esayeti Basanite	44.22	9.46	12.77	0.19	9.98	13.52	3.89	0.98	2.89	0.44	1.51	100.20
Singaraini Basalt	47.18	15.34	11.93	0.19	6.60	12.86	3.04	0.57	1.85	0.32	0.37	100.45
Lenderut Mugearite	49.97	15.38	12.18	0.17	3.86	7.04	4.61	2.10	2.54	0.51	0.31	99.09

Table 3-2. Average wt. % values (n=3) of Magadi Trachyte, Kirikiti Basalt (n=6), Ol Tepesi Basalt (n=3), Ol Esayeti Basanite (n=2), Singaraini Basalt (n=3), and Lenderut Mugearite (n=4). LOI = Loss on ignition. Data from Le Roex et al., 2001.

The surficial zone of relative Ca-enrichment (Carlisle, 1983) is seen in the form of the laminar calcretes that cover the trachytes. Rain falls on the trachytes, chemical weathering (silicate hydrolysis) takes place, and a thin layer of calcite forms as the water evaporates. Efflorescent crusts, of both calcite and, towards the lake, trona, thermonatrite and/or nahcolite, are common results of precipitation and subsequent evaporation and are seen throughout the Magadi area.

Calcium for replacement of the amphiboles, pyroxenes, and feldspars may come from the breakdown of the volcanic rock fragments (VRFs) with the addition of high pH waters, which is possible if the groundwater is alkaline. However, high values of Sr and Ba within the calcretes

may indicate a natro-carbonatite source of the Ca (Dawson, 1964). Ba, which is the more soluble of the pair, is still more concentrated in the calcretes than the associated sediments.

Redistribution of Ca in dust is thought to play a large role in calcrete development in many places (Goudie, 1983; Chiquet et al., 1999; Capo and Chadwick, 1999; Naiman et al., 2000), though Hay and Reeder (1978) found that for the calcretes in Tanzania, wind-blown dust was a minor Ca source when compared to locally abundant carbonatite ash. However, dust-devils are common in the dry southern Kenyan rift valley and likely bring and redistribute much detritus, which may have provided a significant Ca input for the Magadi calcretes. The amount of calcium within the trachytes is much lower than the calcium in the rift-flanking basalts across the region, and although the shallow regional drainage passes only through the trachytes, wind may distribute basaltic detritus within the rift.

3.7.3. Role of biota

Alveolar septal texture (Wright, 1986) from fungal presence in root voids indicates a rhizosphere community. This does not necessarily indicate a pedogenic origin for calcrete because roots may penetrate to shallow groundwater tables. Root-related microfabrics are dominantly horizontal to sub-horizontal indicating a high or perched water table, which can signify that these are groundwater-based calcretes instead of pedogenic. Elsewhere in the rift valley, root systems are vertical from the paucity of accessible water; near rivers, root systems are mainly horizontal (Cohen, 1982; Mount and Cohen, 1984). Horizontal root structures also indicate horizontal flow of water, such as would occur near the top of the calcrete once it became too cemented for water to easily pass through, which can create laminar calcrete (Esteban and Klappa, 1983). However, the root textures throughout are sub-horizontal, not just at the top of the calcrete.

It is common for there to be a microbial presence along roots. Given the paucity of preserved filaments, roots were possibly a major biological agent in forming these calcretes, but root-related textures are not pervasive and most of the calcrete formation is probably due to physicochemical processes. However, given the estimated age of the calcretes, forming any time between 300,000 and 98,000 years, fragile components such as micobial filaments and root hairs may not have been preserved because of the frequent recrystallization of calcite, and their record might have been lost (Wright, 1986).

It is difficult to distinguish primary calcite crystallization from calcite recrystallization particularly in calcretes that have a wide range of microfabrics and crystal sizes. In most samples, small micritic nodules are surrounded by microsparite and sparite. Because micrite recrystallizes to sparite over time (Carozzi, 1993), it is unlikely that there has been a significant amount of recrystallization, but it cannot be discounted. A few examples of microspar to sparry calcite patches within micrite nodules were observed, implying recrystallization, but these are uncommon. The role of microbes in the calcrete development is unclear because of the lack of preserved evidence.

In pedogenic calcretes, the $\delta^{13}C$ content of soil carbonate is related to soil-respirated CO_2, and in turn, the metabolic pathway of the adjacent vegetation, be it the C_3, C_4, or CAM pathway (Cerling, 1984). Estimation of percent of C_4 vegetation (arid-environment adapted pathway) for Kenya today is ~98% (Cerling, 1977, 1992). The end-member for 100% C_4 plants at 25°C is about +2‰ $\delta^{13}C$ VPDB. Although the calcretes at Magadi are not fully pedogenic, the $\delta^{13}C$ analysis may yield pertinent results. The $\delta^{13}C$ range for calcretes is from -0.22 to 2.82 ‰, which broadly indicates a dominance of C_4 vegetation. This implies a climate similar to today, with mostly C_4 grasses with few C_3 *Acacia* trees. However, some workers suggest ^{13}C values may also be related to changes in groundwater (Raidla et al., 2012). Instead of being related to soil carbonate and soil-respirated CO_2, groundwater C is related to the carbonate-bicarbonate-carbon dioxide chemistry. Groundwater-sourced C isotope values do not affect the interpretation of the laminar calcretes, but they may be relevant for the Oloronga-capping calcrete. The disparate values could reflect local differences in groundwater composition instead of reflecting type of vegetation then present. Including the ^{18}O values, the isotopes are generally coeval; both values may be explained by evaporative concentration. Because most textures can be attributed to precipitation from groundwater, it is more likely that the isotope values reflect physical, rather than the biological, processes. Some calcrete formation might have occurred in the rhizophere, as shown by examples of alveolar-septal microfabric and rare fenestral fabric, but these were not the dominant mechanisms of carbonate precipitation.

3.7.4. Pisoid formation

Pisoids in calcretes have been attributed to growth within a soil on a slope (Wright, 1989), and growth within calm, shallow open waters (Nash and McLaren, 2003), as well as forming from pedoturbation or microbial coating (Brasier, 2011). Hay and Reeder (1978) suggested that pisoids of Olduvai Gorge calcretes formed where older clay coatings on grains were replaced by calcite, but explaining the concentricity of the calcite laminae around the pisoids remains difficult (Braithwaite, 1983).

Growth of pisoids in open water is unlikely because there are no contemporary aqueous sediments near the pisoids, and most pisoids retain an irregular shape, which over the long-term (tens to hundreds of years), is unlikely in calm water. Pisoid rotation through pedoturbation is feasible, but clear indicators of fabrics and diagenetic processes linked to roots are rare or absent in the calcretes. Calcrete development on a shallow slope is possible and the pisoidal nature of the calcrete varies topographically in the Dry Lagoon, where the more pisoidal calcrete occurs nearer the lake than the more massive calcrete, which is several hundred metres higher and distal from the main section; however, the post-Oloronga calcrete is widespread and all evidence of an overlying soil is gone. Nonetheless, the calcrete was studied in small area so the basin-wide variations are unknown.

It is unlikely that the pisoids formed through microbial processes. The calcite laminae are discontinuous and irregular, similar to microbially attributed oncoids. However, for many pisoids an important genetic process seems to have been the mechanical rotation of grains, possibly from pedoturbation from repetitive wetting and drying of the clays and zeolites, with micritic laminae precipitating from near-surface evaporating fluids during periods of shrinkage and drying. The observed differences in the laminae appear to reflect staining of grains, whereas microbial influences in laminae often produce a light (organic poor)/dark (organic rich) pattern representative of cycles of microbial growth and die-off. Moreover, microbial filaments and needle fiber calcite, which is thought to be the result of microbial activities, were not seen in the pisoid laminae.

The pisoids in the calcrete are randomly oriented. Although in some pisoids laminae seem to thicken downwards, indicating vadose drip cements, closer inspection shows that those laminae only appear thicker because the pisoid has a core (nucleus) of laminar calcrete. Many laminae do not enclose the entire pisoid but are the infilled remnants of lunate (in two

dimensions) cracks—the circumgranular cracks of alpha microfabrics. These cracks appear to be related to the formation of nodules in that, under pressure, the matrix will crack preferentially before the more compact nodule. These cracks fill with fluid and are occluded by the growth of isopachous microsparite. Cracks occur both outside and within former laminae, which may explain the origin of some of the micritic laminae. A microprobe line-scan through one of the pisoids revealed no symmetry in the contents of Mg, Mn, Fe or Sr: elements that, if sourced from the same fluid, should precipitate in similar concentrations if the laminae are truly concentric. Additionally, because of the high seismicity of the area in the late Pleistocene (Ibs-von Seht et al., 2001; Behr, 2000), evidenced by the extensive grid-faulting after deposition of the Oloronga Beds (Baker, 1958), the possibility that the cracks and partial rotation of the pisoids occured due to seismic jostling of the sediments cannot be discounted. Owen et al. (2012) found evidence for contemporary seismic disturbance in sediments of the Olorgesailie Formation, and Behr and Röhricht (2000) showed that the formation of some of the intrusive cherts at Lake Magadi was linked to seismotectonics.

In some samples the pisoid nuclei are internally fractured. These fractures do not extend into the outer laminae or the matrix yet are not completely cemented. This may be because the dense cementation of the pisoid cortical laminae has completely blocked the pisoid core (nucleus) from fluids. Fracturing within pisoid cores implies repeated wetting and drying (Tucker and Wright, 2009).

Pisoid formation might also be related to underlying substrate. Two significantly different sediments were identified directly below the Oloronga-capping calcrete using both field observations and chemical analyses. At the measured section in the Dry Lagoon (Figure 3-10), infilled mudcracked beds and zeolitized nodular silica-rich sediments are present. The zeolitized nodular sediments vary in induration. Calcretes that overlie the mudcracked beds and the hardest zeolitized sediments have a sharp contact, whereas the contact between the calcretes and the less-cemented sediments is transitional. The basal boundary of the calcrete depends on the substrate. Where the host beds are more cemented, the delineation is clearer. Moreover there is a difference in the character of the calcrete: calcrete that overlies tightly-cemented horizons contains more pisoids than calcrete that formed on, or in, loosely cemented sediments. Movement in a softer substrate would be less pronounced than movement on a hard surface, as the forces would not be diffused through/absorbed by the sediment, hence the greater degree of pisoid development in

calcretes directly overlying well cemented sediments. This indicates that pisoids were formed abiotically and not through calcite accumulation by microbes. Possible reasons for movement are root action, gravity, earthquakes or repeated wetting and drying. The latter process is the only one with direct evidence (pisoid cores) and it almost certainly played a role, though seismicity is also possible.

3.8. Discussion and implications of calcrete formation at Magadi

3.8.1. Stratigraphic context and age estimation of the Oloronga-capping calcretes

The Oloronga-capping calcretes formed during the interval between deposition of the lacustrine Oloronga Beds and the High Magadi Beds. Two different calcretes, however, have been placed at the top of the Oloronga Beds (Baker, 1958) and at the bottom of the High Magadi beds (Behr, 2000). A local calcrete overlies the Green Beds SE of the lake. Fairhead et al. (1972) dated a trachytic obsidian flow that covered the Oloronga Beds, which were capped by about 10 cm of calcrete (Eugster, 1980), to 780,000 y BP, so some calcrete had formed by then. This age is improbable for all of the Oloronga-capping calcrete, and this thin calcrete is probably part of the Oloronga Beds. As discussed, there are several stages of calcrete formation and not all calcretes discussed are necessarily of the same age (Eugster, 1980; Behr, 2002).

Pisoids with cores of reworked calcrete indicate there have been many stages of calcrete formation, indicating a long period of calcrete-forming conditions. Machete (1985) suggested that stage VI pedogenic calcretes (those that include reworked older calcrete) can take up to 100,000 years to form. Since the Oloronga-capping calcretes did not form as part of a soil profile, the timing of formation is likely different than Machete's idealized sequence. Groundwater calcretes form faster than pedogenic calcretes (Nash and Smith, 1998; Kaemmerer and Revel, 1999; Nash and McLaren, 2003; McLaren, 2004). It is likely the calcrete formed within a period of 1000s of years, similar to groundwater calcretes and the Olduvai Gorge calcretes, which formed relatively quickly due to bountiful Ca from nearby carbonatite volcanism (Hay and Reeder, 1978).

As the location of the chert fragments within the laminar and underlying calcrete is higher in elevation (639 m) than any other known chert occurrences in the basin from the High

Magadi Beds (Eugster, 1980), the chert must be from an older source, such as the Green Beds or Oloronga Beds (Behr and Röhricht, 2000). Cherts were not found *in situ* within the High Magadi Beds in the Dry Lagoon, but chert gravel locally forms a residual lag on the floor of the Dry Lagoon. The chert is unlikely to be from the Green Beds due to its elevation. Behr (2002) suggested that the Green Beds paleolake could have extended beyond the present outcrops and have been higher, but this is unlikely. The Green Beds cherts are confined mainly to low lake-marginal areas, but intrusive cherts injected along faults lie several metres above the height of most outcrops (e.g. margins of Magadi townsite horst). The Oloronga Beds contained chert, reached higher than the studied elevations, and so the chert within the calcrete is likely from the Oloronga Beds. This suggests that the laminar calcretes above Graham's Lagoon, and possibly calcretes elsewhere in the basin, have preserved Oloronga cherts while the Oloronga Beds have worn away. While the cherts are likely from the Oloronga Beds, they may have been deposited during any post-Oloronga flooding phase.

The Oloronga-capping calcrete, though probably a composite, marks an unconformity and can be used to identify a time range throughout the basin, though care must be taken to ensure the sediments below are the Oloronga Beds. Previously, Baker (1958) suggested using it to help identify the Oloronga Beds but, because it is not present everywhere and calcretes in the basin are superficially very similar, this is discouraged. The laminar calcretes SE of the lake are of indeterminate age, though they must have formed a) after the trachytes and b) after major block faulting, based on location. It may be possible to match the types of chert embedded in the laminar calcretes with cherts of different ages to allow for an accurate measure of age. The laminar calcrete associated with the Oloronga-capping calcrete is potentially much younger than the underlying pisoidal calcrete. There is an erosional surface between the two noticeable in the field and in thin section. Depending on the type of chert present in the laminar calcrete, it could be as young as High Magadi Beds time.

3.8.2. Sediment source and basin dynamics

Due to the active tectonism and volcanism of the area, changes in basin hydrology and drainage patterns are not unexpected. Identifying the sediment source through geochemical methods within a stratigraphic column will provide details of changing drainage patterns, which may be linked to specific events. Similarly, climate may be inferred from sediment source

identification; the more humid Western rift valley drains predominantly axially whereas the semi-arid Kenya Rift drains, for the most part, perpendicular to the axis into several closed basins (Fordham et al., 2010). Axial drainage under a humid climate can bring sediments from farther away whereas under drier conditions the sediments will be more local. Heavy erosion along the rift scarps will provide the chemical signature of the older basalts and Precambrian rocks. Outcrops of the dominant source rock for the sediments, the Magadi Trachytes, are elongated N-S along the rift valley. This could mean that axial versus lateral drainage may not be easily identified and compared in the sediments.

Rare earth element (REE) spider diagrams are used as the signature of a specific rock (Kerrich et al., 2002; McLennan et al., 2003). As well, each rock type has specific patterns of immobile major and trace elements. The source rocks will be chemically modified during weathering, but this happens in a predictable way and the geochemical composition of sediments is still useful though they may have undergone leaching. For example, it is difficult to decipher the REE pattern for the calcretes, as calcretes tend to incorporate more of the HREEs than the LREEs (Fig. 3-27); this leads to questioning whether the sediments are truly from the Magadi Trachytes or whether the calcretes are displaying misleadingly high HREE concentrations from a different source. When taken with the major and other trace element data, and with mineralogy, however, it becomes clear that the main source is indeed the Magadi Trachytes (Figs. 3-24, 3-28).

The proximity of Shombole, a phonolitic volcano to the southwest in the catchment area, to the Magadi area makes it a potential sediment source. This is unlikely, as the lake sediments show a clear negative Eu anomaly, and the Shombole phonolites and nephelinites instead show a positive anomaly. The evidence that it is not a sediment source indicates that basin hydrology during Lakes Oloronga and High Magadi time has remained similar to present day, in that Shombole runoff drains into Ewaso Ngiro, which enters Lake Natron. Unfortunately REE data for Pleistocene sediments of Lake Natron are unavailable.

Additionally, the mineralogy of the Oloronga Beds and the High Magadi Beds sediments is very similar but the High Magadi beds in the Dry Lagoon show less concentrated trace elements, indicating that the source is the same, but the degree of weathering is greater in the youngest deposits. This makes sense, since the High Magadi Beds are likely reworked Oloronga Beds. The calcrete samples from the northern area, however, are slightly different; they contain

some feldspathoid minerals, which possibly come from the nephelinitic and phonolitic volcanic centers to the north.

The stable isotopes are of interest. In the north, the $\delta^{18}O$ values are much higher than for all other calcretes, and equivalent to the much younger Nasikie Engida conglomerate (see Chapter 5). Two samples of Oloronga calcrete from north and south Nasikie Engida show high $\delta^{18}O$ values (+3.69 and +2.89 respectively). This suggests that, if time equivalent, the water towards the north was more ^{18}O rich than the south, indicating more fresh water input towards the south. This could be because of different drainage patterns during deposition. Alternatively the difference could reflect poor mixing of groundwater from different sources (springs, streams, etc.). Because there is little evidence for fresher water input at the south (aside from potential mixing with fresher Natron lake waters during high lake levels), discrete groundwater inputs seems more likely as an explanation.

Calcretes are generally made up of low-Mg calcite, and XRD analyses confirm that the calcretes from Magadi are no different. Although Mg is lost at the same brine evolution stage as Ca, Mg uptake by clays becomes greater in alkaline, saline conditions (Hay and Kyser, 2001; Deocampo, 2004). So while Ca is precipitated as calcite, most of the Mg is incorporated in clay minerals. While dolomite formation is possible, and occurs in similar deposits such as the Olduvai calcretes (Hay and Reeder, 1978), dolomite was not detected in the Magadi calcretes.

Because of the calcium-poor nature of the Magadi trachytes (1.72–2.09 wt%; le Roex et al., 2001), it is unlikely that the calcium deficiency in the High Magadi Beds as compared to the Oloronga Beds is due to leaching, and is simply a reflection of the sediment source and hydrochemistry. This implies that during the latter part of High Magadi Beds time, there was very little calcium in the lake, as at present.

The gradual decrease in calcite downward through the sampled Oloronga sediments indicates that the calcrete does not have a truly sharp boundary as indicated in outcrop. This may result from downward percolation of Ca-bearing fluids from calcium input prior to calcrete formation. This seems likely, as the boundary between the calcrete and sediments is for the most part sharp.

Normalized to the average Magadi Trachyte of Behr (2000), most of the major elements are depleted, as one would expect from weathering. Slight increases in SiO_2 and Fe_2O_3 in both Oloronga Beds and High Magadi Beds sediments are explained by the minor silica cements and

iron oxide staining from weathering, respectively. These increases were recorded at higher concentrations only in the most recent sediments (i.e. the most weathered). Because the High Magadi Beds analysed in this study have lower concentrations of CaO than all other sediments of the area except for tuffs, perhaps most High Magadi Beds in this study are tuffs, or a tuff-derived portion of the High Magadi Beds. When compared with previous analyses, , the laminar calcretes are the most chemically similar to laminar calcretes tested in Tanzania by Hay and Reeder (1978). The sediments underlying the calcrete are similar to the Oloronga Beds and Green Beds of Behr (2000), but have less SiO_2, which is possibly a dilutory effect from an increase in CaO content from carbonate.

That the sediments between Oloronga and High Magadi times in the Dry Lagoon do not have differing sediment sources is important; at both times this area of the lake would have had similar, predominantly local drainage patterns and little influx from the north. The sediments studied are a small sample of a complex area; more samples are needed to have a more definitive result.

3.9. Paleoenvironment and models of calcrete formation

3.9.1. Oloronga-capping calcrete

In determining a model for formation of the calcrete one must look at the evidence for each of the end members: groundwater and pedogenic. Because the Oloronga calcrete is neither thick nor lens-shaped, and includes a variety of microfabrics not of the alpha type, it is unlikely that the Oloronga calcrete is a ‘valley calcrete’ as defined by Carlisle (1983). Likewise, the scarcity of soil features, ped structures, beta microfabrics, and horizonation indicates that it is not purely a pedogenic calcrete either. The calcrete contains characteristics of both groundwater and pedogenic calcretes and during formation was influenced by both phreatic and vadose processes. It could be considered a groundwater calcrete because of its sharp boundaries between the supra- and subjacent sediments, the presence of isopachous void-filling spar cement, and its consistent presence throughout the basin. It could also be considered a pedogenic calcrete because of the presence of many root textures (though these can also be present in groundwater calcretes where the water table is high), clay textures related to pedogenesis (e.g. cutans), and its moderate variability in texture across small distances.

In support of the idea that it is a groundwater variety, the calcrete is present both in the south and north of Lake Magadi. Samples of calcrete from both areas are chemically, texturally and stratigraphically very similar and differ only in the minor mineral components of the detrital fragments in the calcrete, indicating the differing drainage patterns of their source areas. (In the north there is more feldspathoid in the calcrete than the south.) From the analyses done in this study it is not possible to prove that these two calcretes are truly time-equivalent but the chemical data implies that they are similar and might be contemporary.

No calcrete was found in any recent core samples taken from the lake (Lowenstein et al., 2015; Rabideaux et al., 2015); though there are calcite cements, these are probably not related. It may be that the lake has always been present and has never fully dried. The calcrete is then lake-marginal, developing when the lake levels are very low. The presence of a contemporary lake in the depocenter is supported by the groundwater cement signatures and microfabrics in the calcrete.

Because the calcrete shows textures of both groundwater and pedogenic origin, it is probably polygenic, similar to the calcretes discussed by Renaut (1993), Bustillo and Alonso-Zarza (2007), and Khalaf (2007). After the Oloronga Beds were deposited, they underwent zeolitization, which can occur in trachytic glass with the addition of alkaline water (Surdam and Eugster, 1976). Some zeolitization took place while the Oloronga Beds were exposed periodically, judging by the abundant root textures in the layer directly underlying the calcrete. The Oloronga Beds had also experienced alternating periods of wetting and drying, as seen by the several generations of infilled crack networks below the calcrete. The calcrete formed within the Oloronga Beds: it is chemically similar to them and includes clasts of the Oloronga Beds, but none of later deposits. It is possible that the calcrete formed under somewhat wetter conditions than the cracked beds underneath; the $\delta\ ^{18}O$ values in the stratigraphic profile suggest a somewhat wetter environment than the over- and underlying sediments. Thus it is most likely that the calcrete was at first produced through pedogenesis and, after the water table rose, became a shallow groundwater calcrete. The later calcite from the groundwater cement provides the dominant chemical signature and overprinted the pedogenic beginnings. The majority of calcrete formation took place under shallow groundwater conditions at or near the water table with the minor influence of plant roots. After the horizon became plugged, the laminar cap began to form (as discussed by Wright, 1989).

The calcrete must have been influenced by groundwater at some time. It was developed before the High Magadi Beds were deposited in a lake that covered most, if not all, of the Oloronga calcrete occurrences. Additionally, other high lake level events are thought to have occurred since Oloronga time (Hillaire-Marcel and Casanova, 1987; Behr 2002). Up until the formation of the Green Beds, no sediments have been recognized from these intermediate highstands because the basin is sediment-poor (subsidence from the rifting outpaces sedimentation) and past deposits are cannibalized. The calcrete, along with zeolitisation, helped to protect some of the Oloronga sediments from these periods of erosion. The time period between the latest recorded deposition of the Oloronga Beds at 300,000 y BP (Röhricht, 1999) and the next recorded highstand at ~130,000–140,000 y BP (Hillaire-Marcel and Casanova, 1986) makes the most sense as the period of formation for the Oloronga-capping calcrete. Lake Naivasha to the north also records a high lake period at ~130,000 y BP (Trauth et al., 2010). Other calcretes in the basin formed during other lowstands or when the sediments became subaerially exposed. It is unlikely the calcrete took the entire intervening 150,000 years to form, though the brecciation and recementation of the calcrete suggests calcrete-forming conditions were maintained for a long period. As a corollary, a long period of semi-arid climate may, in a rift valley setting, imply minimal regional volcanic and tectonic events during this time.

Once the calcrete had formed, any Oloronga Beds that had been on top of the calcrete were stripped. This happened any time after calcrete formation due to erosion, or perhaps due to sediment reworking during the next lake highstand. Additionally the calcretes were subject to erosion themselves as they are absent from many places despite their being widespread. The laminar calcrete may have acquired some chert clasts from younger deposits including the earliest High Magadi Beds and could have remained forming until their deposition.

3.9.2. Laminar calcrete

Laminar calcretes are widely discussed in the literature, with formation resulting from rhizogenic activity (Alonso-Zarza, 1999; Alonso-Zarza, 2003; Wright et al., 1988), microbial

influence (Krumbein and Giele, 1979; Wright et al., 1988; Verrecchia, 1996), or abiogenic processes (Wright 1989).

In the laminar calcretes from SE Magadi, the laminae are discontinuous and irregular, showing micro-unconformities as would be expected of non-stromatolitic laminar calcretes. The surface is often smooth with irregular crack networks indicating shrinking during desiccation or perhaps movement of the substrate. This is indicative of abiogenic precipitation resulting from periodic runoff and subsequent evaporation, probably at the rock/air interface. While plants may have sporadically inhabited this laminar carbonate surface, indicated by the few instances of horizontal spar-filled root tubules in the laminae (fenestral texture), the majority of the carbonate was precipitated directly from meteoric runoff under the influence of evaporative concentration, as shown by the high relative ‰ of the $\delta^{18}O$ values as compared to the meteoric water from which the carbonate would have precipitated (albeit not likely in equilibrium). Carbonate-encrusting microbes, which would thrive briefly in the runoff, especially in micro-ponds, might have also played a role in calcrete development, and there is some evidence for hemispheric stromatolite-like laminae, though these are rare and minute.

The laminar calcrete was preceded by carbonate cementation of the underlying trachyte. Most of this cement is spar though shows meniscus and pendant cements and was probably related to surface water infiltrating the vesicular trachytes. Carbonate formed as the trachyte was weathered by meteoric water, converting some of the trachyte to zeolites and releasing Ca. Once cementation made the surface impermeable, the laminar calcrete began to form. Large pieces of chert washed in during the ephemeral rainfall and became cemented into the calcrete.

It is difficult to ascertain the origin of these chert clasts. It is possible they are from the Oloronga Beds cherts but they could also be from the Green Beds cherts, which are locally abundant. A High Magadi Beds origin is unlikely due to the high elevation of the laminar calcrete relative to present High Magadi Beds outcrops. However, the horst that hosts the laminar calcrete was developed by Green Beds time: Green Beds silica was injected along the marginal faults due to tectonic activity (Behr and Rohricht, 2000; Behr, 2002). The Green Beds paleolake was unlikely to have been that high (Behr, 2002). Lake Oloronga, which may have existed before the faulting, certainly was deep enough to encompass the horst and may have deposited cherts nearby, though there is no evidence. Another possibility, though less likely, is that the cherts are not lacustrine but from silica spring deposits that have been eroded.

Determining the source of the cherts would help to determine the age of the laminar calcrete; for now it is assumed that they have formed some time after uplift due to faulting and the present.

3.10. Summary

The Lake Magadi area has at least three distinct calcretes: a pisoidal variety that overlies the Oloronga Beds; a local grain-coating calcrete that overlies the Green Beds; and a laminar calcrete that coats the Magadi Trachytes. There are likely more, but basinwide stratigraphy is difficult to discern and not all areas are accessible. The predominant calcrete, the Oloronga-capping calcrete, has been used as stratigraphic marker to recognize the underlying Oloronga Beds. Because calcretes can look similar, they should be used as a stratigraphic marker only when the identity of the underlying beds has been confirmed. The Oloronga-capping calcrete is >100,000 years old, and probably formed within the range 300–200 ka, though it likely took much less than 100,000 years to form. This calcrete marks a time when the Oloronga Beds were exposed during low lake levels. The calcrete was formed from both pedogenesis and groundwater cementation and diagenesis, making it a polygenic. The laminar calcrete at the SE of Lake Magadi was formed predominantly by physicochemical processes, particularly high evaporation. Its age is unclear; it could be up to 300,000 years old but is likely much younger.

4. CALCRETES OF THE POST-OLORGESAILIE FORMATION SEDIMENTS

4.1. Geological setting and paleoenvironment

About 30 km to the northwest of Lake Magadi, the Olorgesailie basin is bounded by N-S trending horsts of flood trachytes and basalts to the east and west, and to the south by Mt. Olorgesailie, a Pliocene phonolitic volcanic center. Quaternary volcanic centers include Ol Doinyo Nyokie and Suswa. Ol Doinyo Nyokie, a trachyte ignimbrite complex about 20 km to the south-west, formed at 0.66 Ma and contains thick layers of obsidian (Baker, 1975). Suswa is 30 km north of Olorgesailie and includes trachytes, nephelinites, and phonolites, and was active between 240 and <100 Ka (Baker et al., 1988; White et al., 2012).

The Olorgesailie sediments were deposited on an eroded surface of Magadi Trachytes, which were extruded from 1.4–0.8 Ma, and the older Ol Tepesi (1.6–1.4 Ma) and Ol Keju Nero flood basalts (Baker and Mitchell, 1976). After deposition of the Olorgesailie Formation the region was grid-faulted and locally uplifted to make the Legemunge and Ol Tepesi Plains. Present drainage is dominated by the Ol Keju Nyiro River and tributaries, which have downcut and exposed the Olorgesailie Formation (Fig. 1-2).

The Pleistocene Olorgesailie Formation consists of up to 80 m of mainly lacustrine and wetland sediments interlayered with volcaniclastic deposits, calcretes and other paleosol deposits, representing a series of paleolakes of early to mid-Pleistocene age (1.2 to 0.5 my ago; Deino and Potts, 1992).

The Olorgesailie Formation records the repeated expansion and contraction of many former lakes (Owen et al., 2008, 2011), fed mainly by rivers and groundwater discharge, though springs might also have contributed during the later parts of the basin history (Owen et al., 2011; Lee et al., 2013). During phases of regression, the lacustrine sediments were subaerially exposed and variably modified by pedogenesis, which, during the later stages of basin history, included formation of cherty, opaline, and carbonate rhizoliths in wetland sediments. Some sediments were incised and eroded. The reworked sediments were then transported ~ 20–25 km southwards along the Ol Kejo Nero paleodrainage system and some were possibly deposited in the Koora

Graben. Studies of these sediments have provided a mid-Pleistocene climate record for the basin, but interpretation has been complicated by syndepositional tectonics (Owen et al., 2008, 2011).

Unlike many paleolakes in the rift valley, Olorgesailie has little evidence of zeolitic alteration, although Owen and Renaut (1981) reported minor analcime. The paucity of zeolites implies low salinity during most of the lake sediment deposition (Isaac, 1978) and minimal alteration during early diagenesis. In constrast, a zeolitic interval is present in a core recovered from Koora Graben in 2012 that spans the mid Pleistocene (Rabideaux et al., 2016).

4.2. Stratigraphy

The Olorgesailie Formation, as defined by Isaac (1977), has 14 members comprising about 80 m of sediments in outcrop. Member 1 contains a fossil-bearing paleosol 10–30 cm thick named UM1p. This paleosol is a smectitic vertisol (Deocampo et al., 2010), which consists of pedogenically altered lacustrine silts and sands interbedded with diatomite and reworked tuffaceous sands (Potts et al., 1999). The presence of rootmarks, burrows and footprints indicate a stable land surface that formed over about 1 kyr (Potts et al., 1999). Also in Member 1 are ash beds which were dated to 0.992 Ma (Potts et al., 1999). Member 2 is mostly lacustrine silty diatomite with some calcrete and includes the Evaporative/Carbonate (EC) marker horizon, interpreted as a secondary replacement of a salt crust during lake contraction, used in lithostratigraphic correlation across the basin (Potts et al., 1999). Owen et al. (2011) suggest that this unusual horizon with carbonate-filled crack networks is linked to a paleoseismic event.

Description of the following members is summarized from Owen et al. (2008). Member 3 is mostly tuffaceous diatomite. Members 4 and 10 are primarily pumiceous sands and gravels of fluvial origin. Members 5–8 are mostly diatomaceous silts and clays which have been pedogenically modified. Within Member 7 is another paleosol of archeological interest, termed UM7p (Potts et al., 1999). This paleosol, up to 1 m thick, consists of a waxy dark green claystone (Owen et al., 2008), including carbonate nodules with MnO_2 staining. About 190,000 years was proposed for formation of UM7p, but this is likely an overestimation (Potts et al., 1999). Though excavation of UM7p produced artefacts, the highest concentration of archeological finds came from paleosol UM1p.

Member 9 includes fluvial sands with layers of tuff, diatomaceous silt and clay, and diatomite with carbonate nodules of uncertain origin. Member 11 is similar to Member 9 though lacks tuffaceous layers and the sediments have undergone pedogenesis. Member 13 contains local red beds that resulted from spontaneous combustion metamorphism during extreme drought (Melson and Potts, 2002). These red beds are also present in Member 12 but combustion metamorphism occured some time after Member 13 deposition. Member 14 is composed of reworked diatomaceous silts and contains calcrete not included in this study.

A disconformity produced by a period of fluvial incision separates the Olorgesailie Formation from the overlying sediments, called "Steppe Limestone" by Isaac (1978). These sediments have recently been examined in detail and include several calcrete layers, one of which currently mantles part of the land surface of the Legemunge and Ol Tepesi Plains as a resistant unit. The three uppermost calcretes were chosen for study. The stratigraphic position and age of these sediments, which are younger than Member 14, is under review. In this thesis, they are referred to as "post-Olorgesailie Formation sediments".

The period after the Olorgesailie Formation is marked by recurring fluvial incision and deposition (Behrensmeyer et al., 2002), including wetland, shallow lake, and terrestrial deposits. These deposits are the post-Olorgesailie Formation sediments, which span the time from ~350 ka to 50 ka (Deino and Potts, 1990). These sediments are mostly volcanic silts, sands and gravels, but also have layers of volcaniclastics, tufa/travertine and calcrete, and some have experienced pedogenesis (Owen et al., 2014). Of note, CaO content increases upwards through the post-Olorgesailie Formation sediments, an indication of increasing evaporative conditions (Owen et al., 2014).

4.3. Paleontological and archeological significance

Paleontological excavations began at Olorgesailie in 1942 by L. and M. Leakey, continued by G. Ll. Isaac (1960s), and have been ongoing since 1985 by R. Potts. The formation has yielded Acheulean artifacts, such as handaxes, as well as mammal and hominin bones, in particular a partial cranium attributed to *Homo erectus* that is about ~900,000 years old (Potts et al., 2004). Though there are many Acheulian handaxes and other bifacial tools in the Olorgesailie Formation, hominin bones are rare. Potts et al. (1999) suggested this paucity is due to a tendency for the hominins to spend most of their time in the uplands, and going into the

lowlands only for food gathering. The area has been used by hominins for the past million years. There are many other fossil vertebrates within the formation (Isaac, 1977, 1978), including a species of baboon (Jablownski et al., 1982).

4.4. Field description

The studied area is an exposure on an east-facing downcut surface of an incised channel in the Olorgesailie Formation at (1°34’24.0”S, 36°25’14.30” E; sample site indicated in Figure 1-2). Layers of calcrete are apparent, with one forming the upper land surface (Fig. 4-1). The calcretes form resistant units that form shelves on the steep hillsides.

Three distinct calcrete layers are present in the sediments that overlie the Olorgesailie Formation (Post-Olorgesailie Formation sediments; Fig. 4-2). The lower two calcretes are pisoidal (refered to as Pisoidal A and Pisoidal B calcretes) whereas the calcrete forming the present land surface is laminar to massive (referred to as Capping calcrete). The entire section has a thickness of about 3.6 m. The bottom of the section is midway up the hillside; the Olorgesailie Formation is below.

A dark blue-grey, well-lithified siltstone unit with white vertical rhizoliths is overlain by a buff, poorly-lithified, bedded indurated silt with pebble-sized calcite crystal clasts. The upper surface passes transitionally vertically into the lowest calcrete, the Pisoidal A calcrete, which is 25 cm thick (Fig. 4-3 B, D). Another buff indurated silty unit 50 cm thick separates Pisoidal A from Pisoidal B calcrete. This silt has continuous root moulds 5 to 6 mm in diameter and several cm long. Pisoidal B calcrete, which is 10–15 cm thick, has a more transitional lower boundary into the underlying silt (Fig. 4-3 E). Overlying this calcrete is another beige indurated silt unit up to 60 cm thick, with coated grains and fewer detrital feldspar grains than lower silt units. This, in turn, is capped by a laminar to massive calcrete up to 10 cm thick (Fig. 4-4).

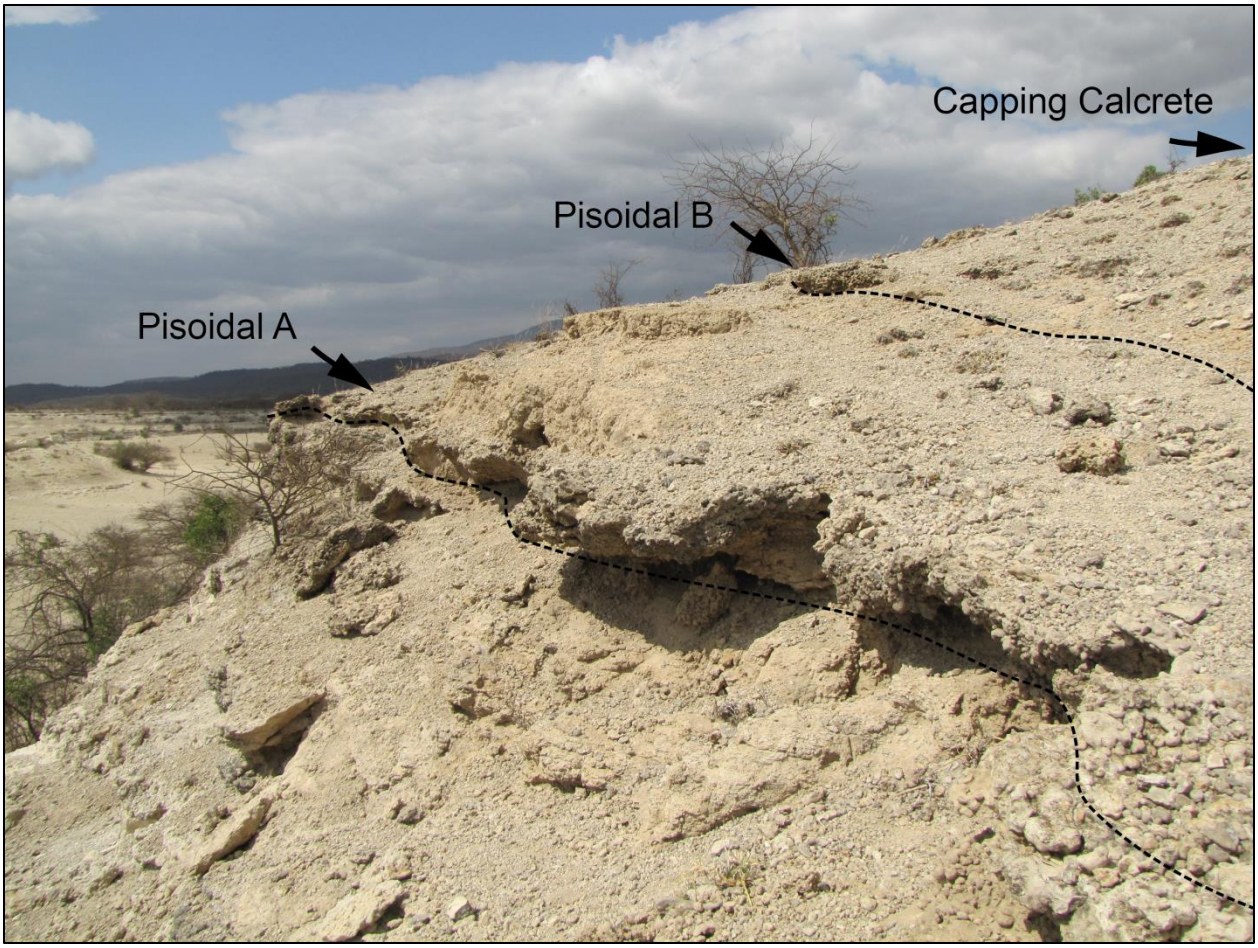

Figure 4-1. Photo of the stratigraphic context of the calcretes discussed in this chapter. Dashed line follows each calcrete. The capping calcrete is not prominent and the flat land surface that is mantled with calcrete begins where the arrow indicates.

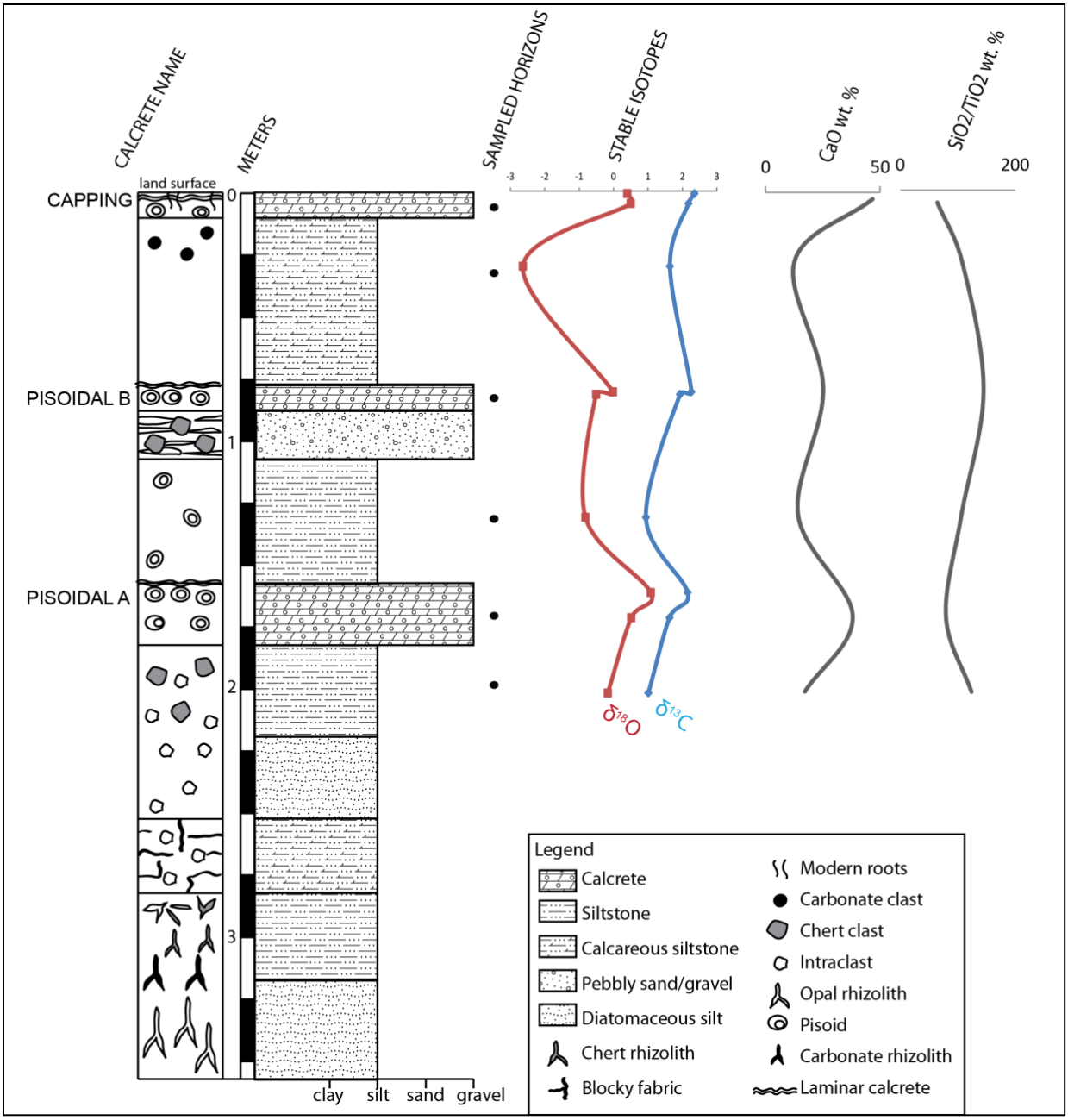

Figure 4-2. Stratigraphic profile of the Post-Olorgesailie Formation sediments and calcretes. Lithology and features are shown as well as the stable isotope profile, the CaO wt% and the SiO_2/TiO_2 wt%. Si has been normalized to Ti to mitigate detrital influence. An increase in Pisoidal B for authigenic SiO_2 is corroborated by the presence of silica cement.

The pisoidal calcretes are not fully cemented, and cementation is strongest at the top and weakest at the base of Pisoidal A, where the coated grains are surrounded by the lower silts (Fig. 4-3 B and C). The exposed ledge of Pisoidal A is covered in loose pisoids (Fig. 4-3 C), and in places is coated by a laminar carbonate no more than 1 cm thick. This laminar carbonate is

undulose, ‘stromatolitic’ in appearance, and has discontinuous layers. Pisoidal A is more compact than B, has an undulose lower contact, and consists mainly of carbonate, with little detrital material. Rare clasts include chert fragments and large feldspar grains. Horizontal pores 1 to 3 mm in diameter are present. The Pisoidal A calcrete, which consists of tightly cemented pisoids, is the thickest calcrete (25 cm), though its thickness is laterally variable. Uncemented pisoids are also located in the overlying sediments. Pisoids in Unit A range from 0.5 to 4 cm in diameter. The basal contact of this calcrete is sharp and irregular, as is the top contact with its thin (<0.5 cm) laminar coating.

Pisoidal B calcrete grades into the silty unit downwards, but is cemented only on pisoid contacts as opposed to Pisoidal A calcrete in which cement also fills the interstices. Vertical and horizontal round pores ~ 0. 5 mm in diameter are present together with minor detrital material. The pisoids are smaller than Pisoidal A calcrete with a range of 0.5 to 2 cm diameter. Cementation becomes weaker downwards (Fig. 4-4 E). A thin (0.5 cm) laminar carbonate coats the top of the pisoidal section of Pisoidal B.

The laminar capping calcrete that forms the land surface weathers white but has a dark grey interior, and is locally pisoidal. Its thickness ranges from ~ 1 to 5 cm. This calcrete is composed mostly of calcite, with rare feldspar grains, volcaniclastic grains and chert fragments. Horizontal 1 mm-diameter pores are present, and possible root moulds occur on the underside of the calcrete. Roots of modern and recent vegetation have penetrated the laminar calcrete (Fig. 4-4 C), which is present at the land surface in most places in the study area; faulting and erosion account for its absence elsewhere.

Loose detrital gravels on the capping calcrete surface are composed mainly of large angular pieces of carbonate and minor volcanic gravels; below the capping calcrete are pisoidal coated grains either reworked from previous calcretes or as part of the capping calcrete (Fig. 3-5 D and E).

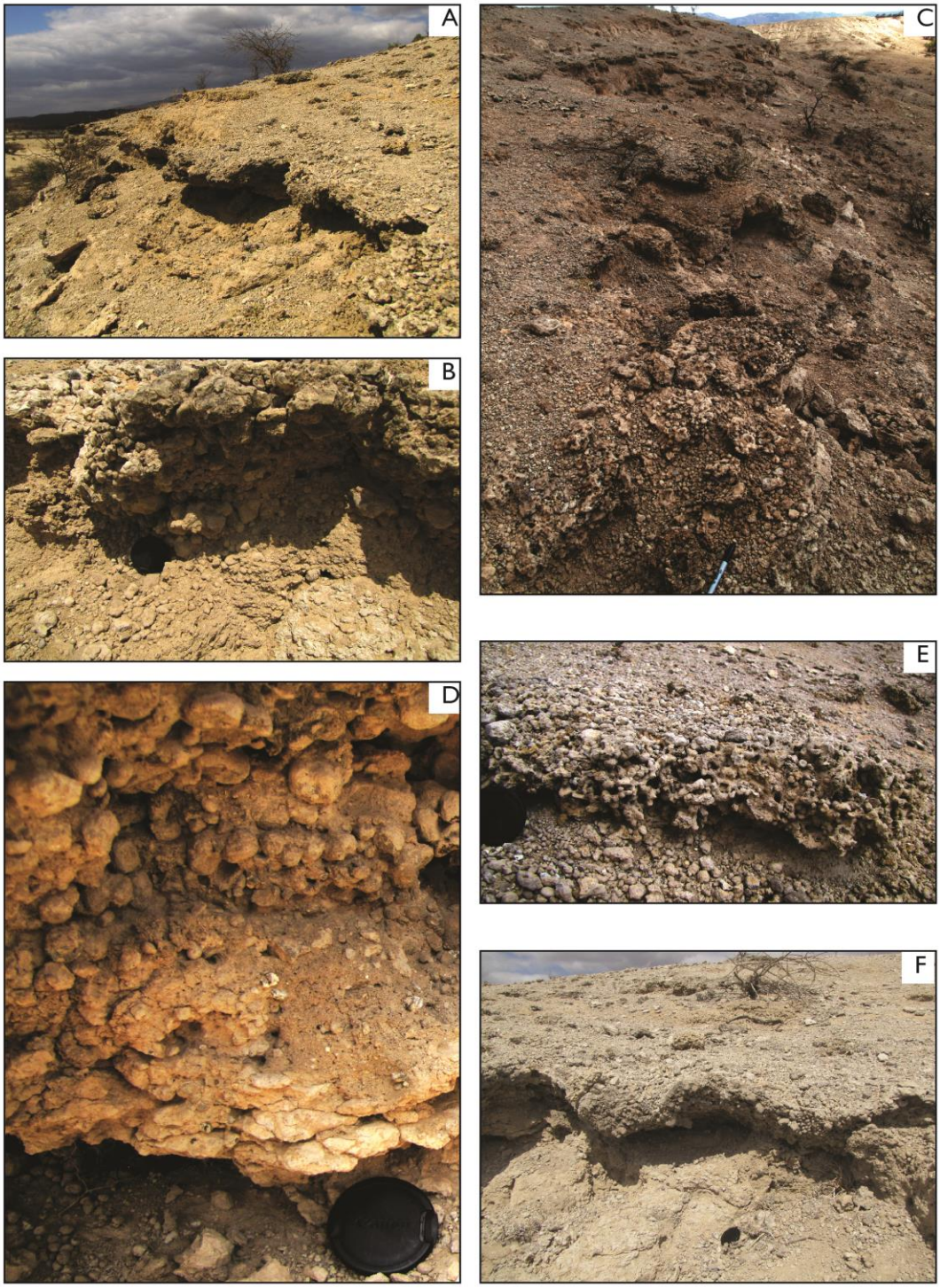

Figure 4-3. Field photos of the two lower calcretes at Olorgesailie, Pisoidal A and Pisoidal B. A) View of the Pisoidal A calcrete (exposed shelf) looking towards the south. B) A closeup showing the average thickness of the Pisoidal A calcrete. C) A photo of the Post-Olorgesailie sediments looking north. Pen is on top of the Pisoidal A calcrete, which

can be traced laterally in the photo. D) A closeup of the Pisoidal A calcrete showing the transition from calcrete down into sediment. E) A photo showing general appearance of the thinner Pisoidal B calcrete. F) A photo of the Pisoidal A calcrete showing undulations. Lens cap for scale is 7 cm in diameter.

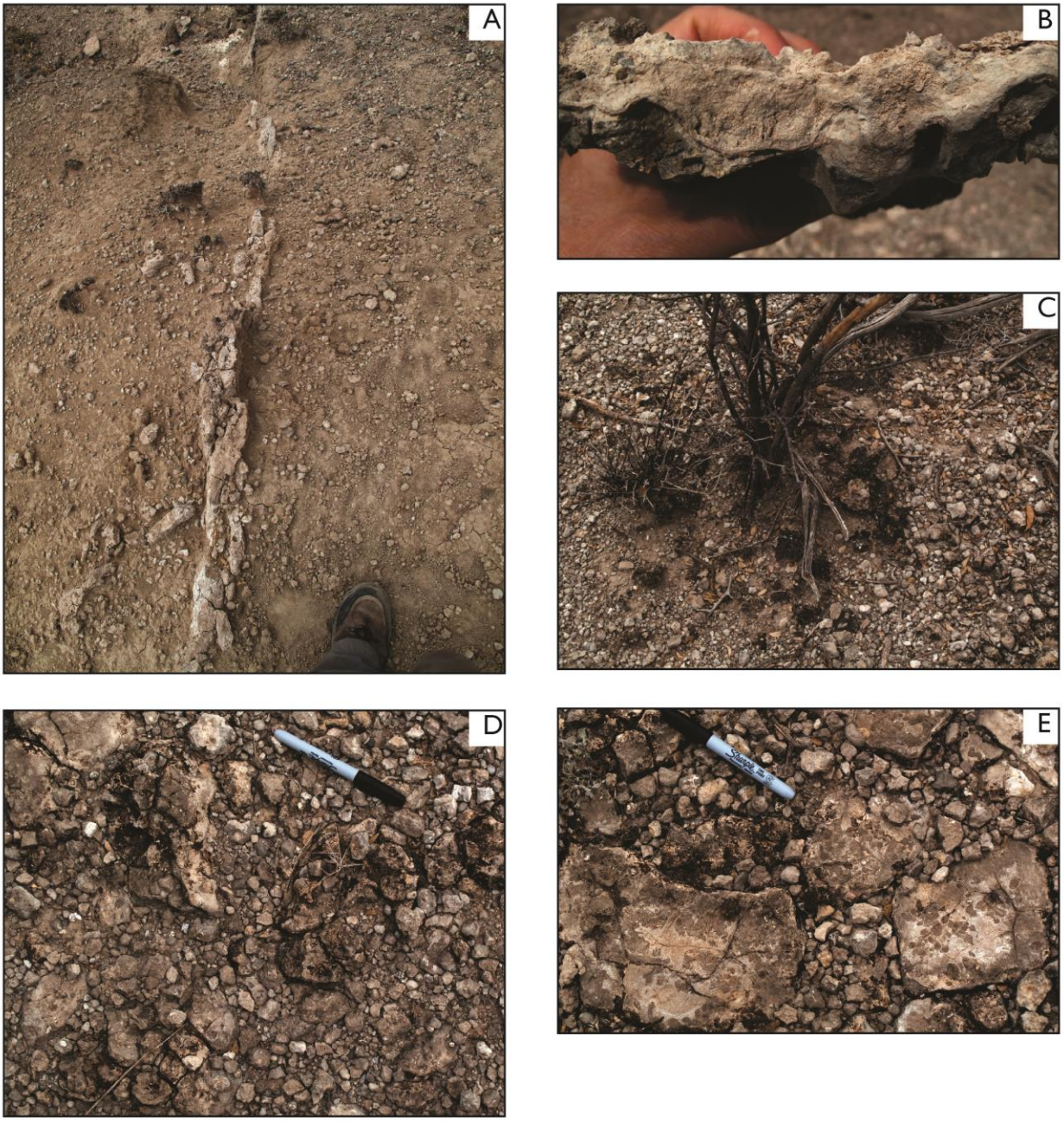

Figure 4-4. Field photographs of the capping calcrete of the Post-Olorgesailie sediments. A) A linear feature (crack-fill) at the top of the capping calcrete. B) A sample of the capping calcrete showing its general thickness. C) Plants grow through the capping calcrete. D) The capping calcrete has debris and scattered carbonate pieces on the surface. E) Photo shows platy character of the calcrete at the surface. Pen for scale is 14 cm long.

4.5. Petrography

4.5.1. Pisoidal A

Beta microfabrics predominate in the Olorgesailie calcretes, as well as root and root hair textures (Fig. 4-5). Dense micrite prevails in both the massive and laminar forms of this calcrete. The calcite is both replacive, mainly of easily weathered grains, and displacive, where a more stable form is present (e.g. varieties of quartz; Fig. 4-5 E, F, H). Clumped microfabric (see Ch. 2) is common with rounded micrite or clay clumps varying from ~ 0.1 to 0.5 mm in size. These clumps are cemented by sparite in the youngest matrix material or by microsparite where present in pisoid cores or massive calcrete. Within the pisoid cores are unfilled fractures, which do not pass into the cement (Fig. 4-6 A, B). These fractures were noted in all three calcretes, but not all pisoids. A gradation occurs between rounded clay masses (Fig. 4-5 D) and micritized clumped microfabric; clays have micrite envelopes with variable thickness (Fig. 4-5 D). There are incidences of alveolar-septal microfabric (Fig. 4-5 A and B) as well as fossil root hairs (Fig. 4-5 D) and filled root voids (Fig. 4-5 C).

4.5.2. Pisoidal B

Massive micrite microfabric predominates in the Pisoidal B calcrete. Small (0.5–1 cm) pisoids are common and have cores of reworked calcrete clasts (Fig. 4-6 A, C). Replacive textures are also common; monocrystalline clasts of K-feldspar and volcanic fragments provide a spectrum of stages of mineral etching and replacement. Instead of calcite sparite, however, microcrystalline quartz in the form of botryoidal chalcedony cements many voids (Fig. 4-6 B, G, H). Clays cement the youngest detrital material. The denser micrite-replaced areas have been cemented by chalcedony, whereas the poorly-cemented (in terms of micrite) lower and fracture-filling parts are mostly lined/cemented by clays (Fig. 4-6 E, F). Detrital chert fragments are angular and of coarse-sand size (Fig. 4-6 C).

4.5.3. Capping calcrete

The thin (15–20 cm) calcrete at the top of the section is predominantly massive (Fig. 4-7) though is laminar in the upper surface and is pisoidal in places (Fig. 4-7 F). Nearly all material

has been replaced by micrite grading into spar in the pore spaces (Fig. 4-7 A, D, G, H). Chert fragments are rare; most of the detrital component consists of K-feldspar and plagioclase. Root structures are predominantly horizontal and are original moulds infilled with volcaniclastic detritus and clays (Fig. 4-7 A, B, D), or are successively lined by undulating layers of micrite (Fig. 4-7 E). The dominant crystal shape of the void-filling sparite is acicular and drusy (Fig. 4-7 C) though in some voids in less-cemented areas the calcite has a needle-fibre sheaflike appearance. Microbial staining is common within pisoid laminae and other laminar features (Fig. 4-7 G and H)

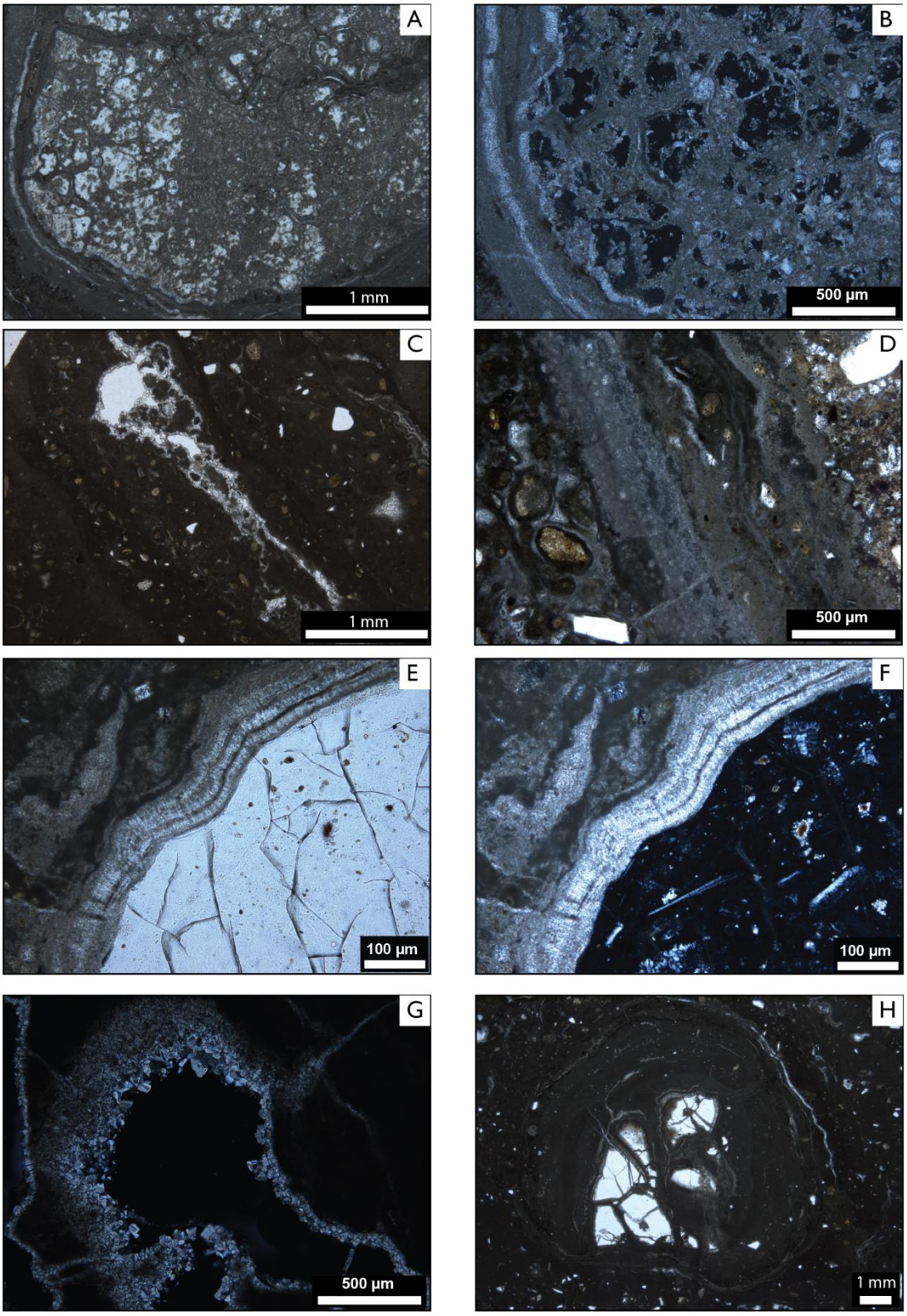

Figure 4-5. Photomicrographs of the Pisoidal A calcrete. A) A large root mould showing alveolar-septal microfabric. PPL. B) XPL closeup of (A). C) A root mould infilled with micrite cement and detritus. The pore space is lined with

sparite. PPL. D) Calcified plant material. Clay masses to the left. PPL. E) A chert clast with at least three generations of isopachous circumgranular calcite. PPL. F) Same as in (E) but under XPL, the chert shows complexity, possibly resulting from the silicification of volcanic grains. G) Sparite growing into pore space. XPL. H) A small pisoid with a fractured chert core. The laminae are uneven and are thicker on top. PPL.

Figure 4-6 (next page). Photomicrographs of the Pisoidal B calcrete. A) A partial view of a pisoid showing circumgranular cracking within the pisoid boundary. PPL. B) The irregular and non-continuous laminae of a pisoid. Some silica cement occurs close to the central part of the pisoid (lower center left). The crack in the center, micritic portion of the pisoid does not pass through the pisoid laminae. PPL. C) A fractured, angular chert clast surrounded by micrite. PPL. D) Silica pseudomorph of euhedral gypsum or titanite (?). Micrite forms a similar shape below. This was the only instance of this pseudomorph. XPL. E) Clays surround clasts. The majority of cementation is accomplished by clays. The calcite is confined to the nodules. PPL. F) XPL of (E) showing clay thickness and presence only at grain boundaries. G) Chalcedonic cement in elongate voids. XPL. H) Chalcedonic cements voids in microsparite matrix. XPL.

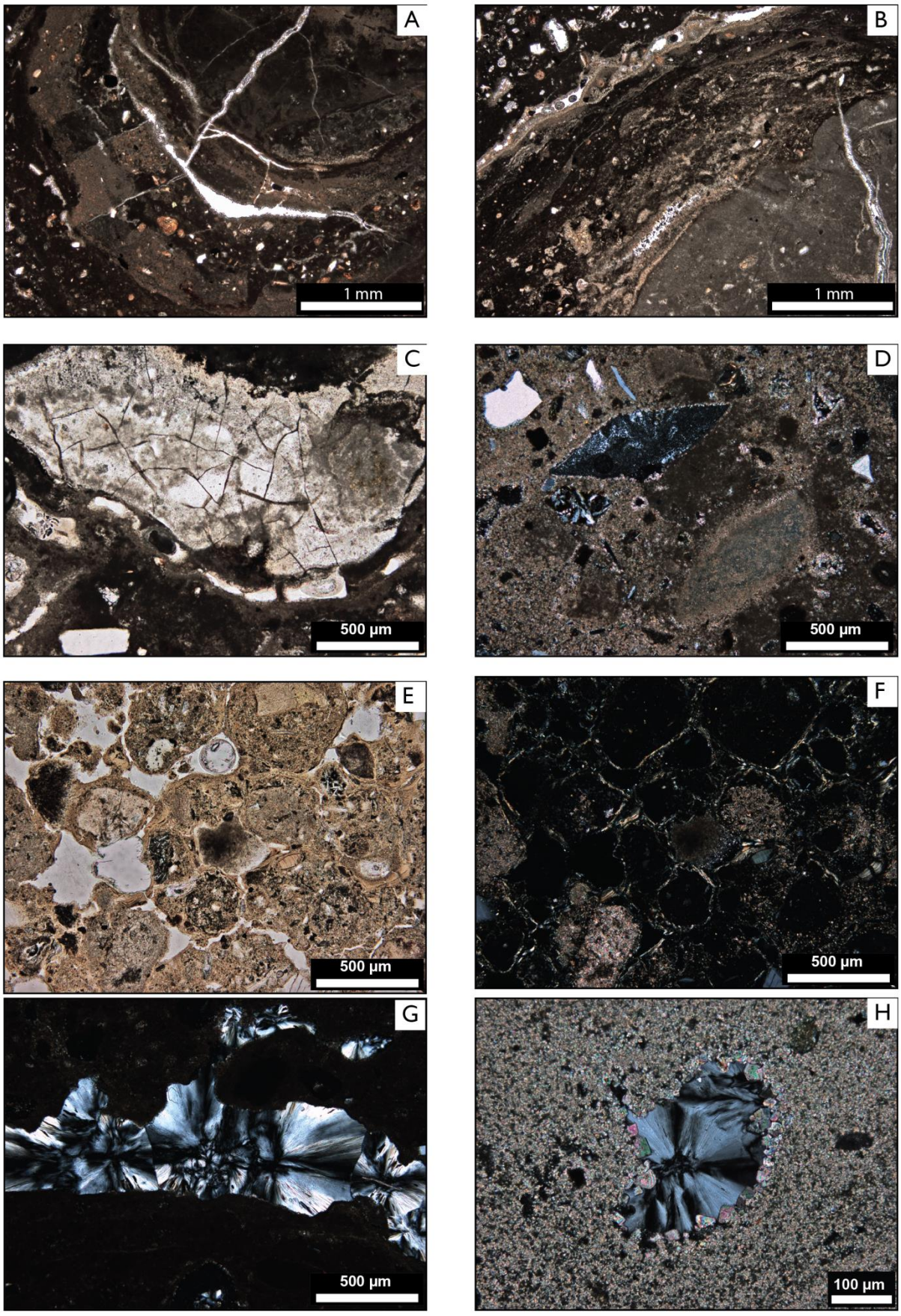
A
1 mm
B
1 mm
C
500 µm
D
500 µm
E
500 µm
F
500 µm
G
500 µm
H
100 µm

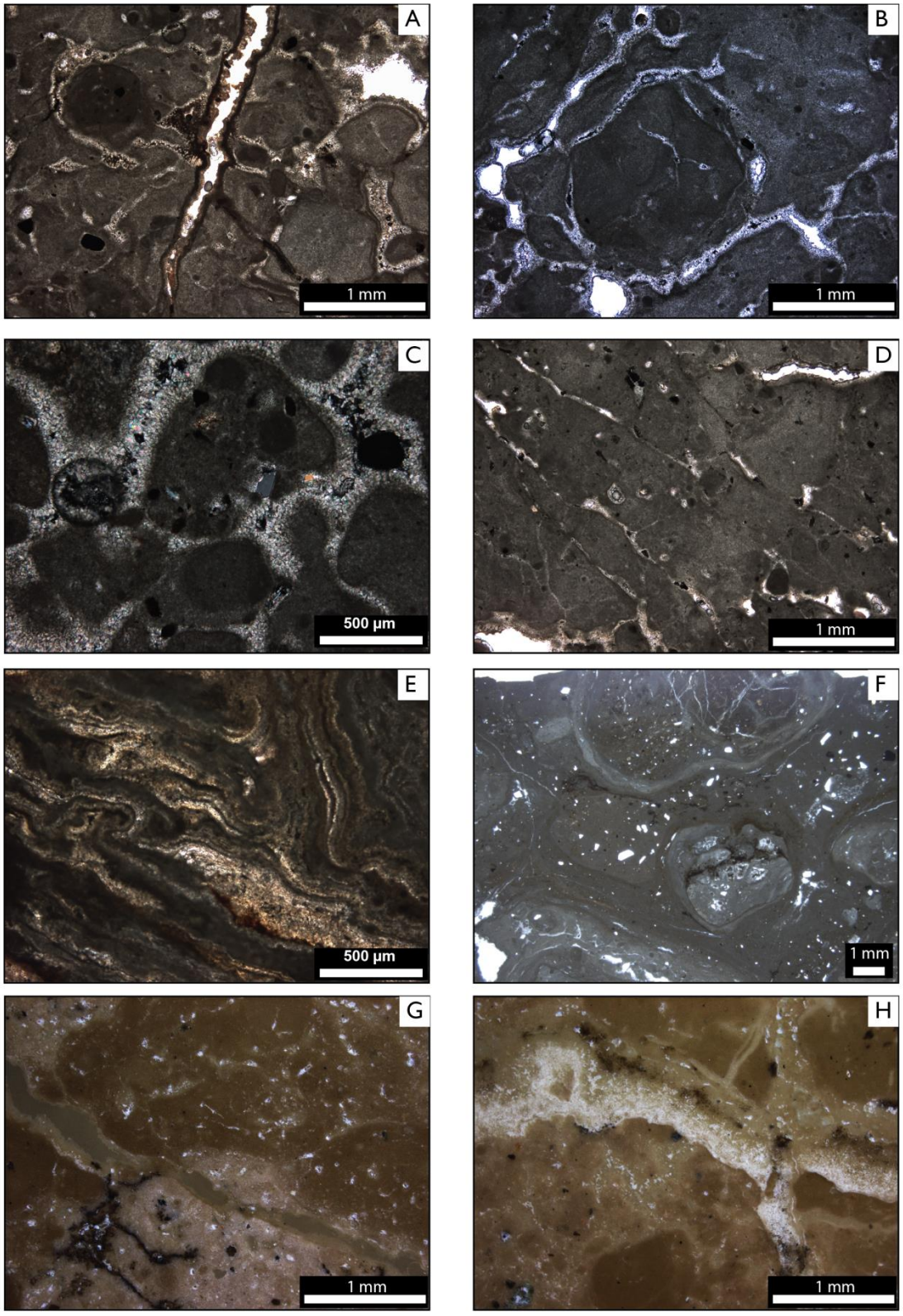

Figure 4-7. Photomicrographs of the capping calcrete at Olorgesailie. A) Dense micrite with spar-filled cracks. PPL. B) Similar to (A), though two circular pores are of interest. The fractures between (A), (B) and (D) are all similar in size

and perhaps related to root hairs. PPL. C) Small nodules surrounded by isopachous sparite. Black indicates an open pore. XPL. D) Massive dense micrite with several spar-filled or open cracks. PPL. E) Calcite cement within a large (several mm) subhorizontal structure. The cement is stained and regular. PPL. F) Pisoids in the capping calcrete. The laminae are thin and uneven. PPL. G) White-card technique (Folk, 1987) showing the spar cement (white) with two generations of micrite. Note the linear organic staining in lower left. H) Similar to (G), showing the different calcite generations and the mottled appearance from denser to less dense micrite.

4.6. Geochemistry

4.6.1. Major elements

Bulk rock geochemistry revealed a difference between the calcretes and the sediments. The Olorgesailie calcretes have SiO_2 wt.% ranging from 10.2–38.4% while the interlayered sediments have a narrower range of 44.7–52.9%. The calcretes typically have a smaller proportion of all the major oxides aside from CaO, which is roughly twice that of the sediments with ranges of 25.2–46.8 wt.% for the calcretes and 12.6–17.2 wt.% for the sediments. The other oxides are halved from the sediments to the calcretes (Table 4-1). These relationships are also apparent in Figure 3-25.

Sample	SiO_2	Al_2O_3	Fe_2O_3 (T)	MnO	MgO	CaO	Na_2O	K_2O	TiO_2	P_2O_5	LOI	Total
Pisoidal A calcrete	17.8	3.87	2.15	0.09	1.28	38.05	1.18	1.56	0.22	0.05	33.59	99.84
Pisoidal B calcrete	38.42	4.79	2.33	0.07	1.26	25.19	1.32	1.89	0.26	0.08	24.75	100.4
Capping calcrete	10.25	2.143	1.14	0.03	1.05	46.75	0.81	0.73	0.16	0.04	37.54	100.6
Sediment underlying Pisoidal A	44.69	6.61	4.02	0.12	2.54	17.19	2.14	2.4	0.36	0.09	18.61	99.06
Sediment underlying Pisoidal B	49.2	7.87	4.38	0.13	1.92	14.23	2.55	2.71	0.46	0.12	16.33	99.91
Sediment underlying capping calcrete	52.93	7.84	4.51	0.13	2.00	12.57	2.72	2.64	0.48	0.12	14.19	100.1

Table 4-1. Bulk rock geochemistry for the Olorgesailie samples.

4.6.2. REEs

The calcretes are enriched in the HREEs (Fig. 4-8) and show a more strongly negative Eu anomaly than the super- or subjacent sediments that may be indicative of oxidizing conditions. Compared to the adjacent sediments, there is a greater concentration of REEs in calcretes, HREEs in particular. The calcretes become slightly more enriched with respect to all REEs from the base of the profile to the top. Other elements showing a higher concentration in the calcretes

than sediments are: Sr, Cu, Ba, S, Br, V, Pb, Ni, Cs, Hf, Rb, Sc and U in all; and Sb in Pisoidal B.

Figure 4-9 compares rare earth data for Olorgesailie calcrete samples with possible regional source rocks. The sediments sampled (OLO-4, -5, and -6) are less enriched in HREEs than the Magadi Trachytes (KR015, KR040, and KR042) (le Roex et al., 2001), but otherwise show a similar pattern.

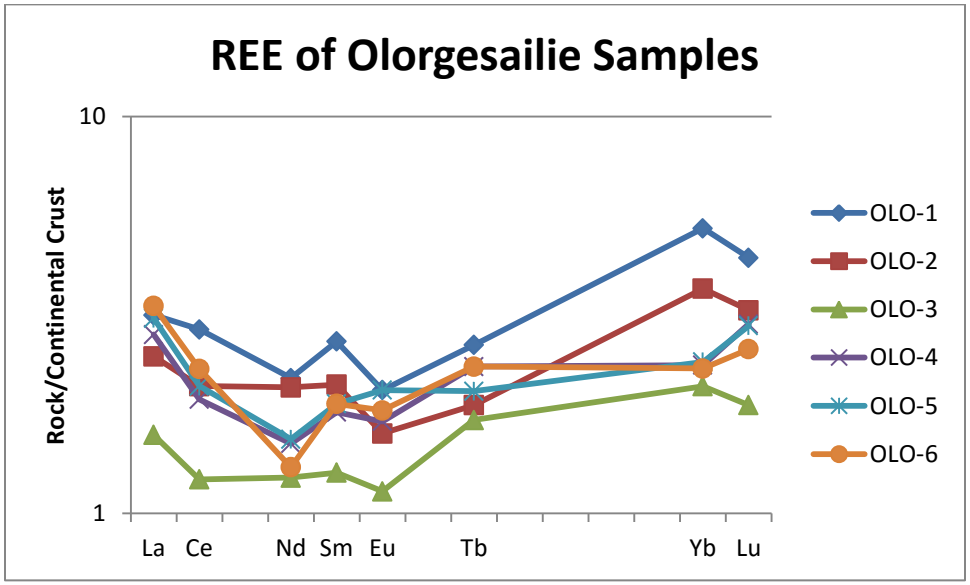

Figure 4-8. Chart of REE distribution for all Olorgesailie samples normalized to continental crust (Taylor and McLennan, 1986). Calcretes are OLO-1, 2, and 3. The sediments are OLO-4, 5 and 6. The calcretes are enriched in the HREEs, as represented by Yb, compared to the sediments.

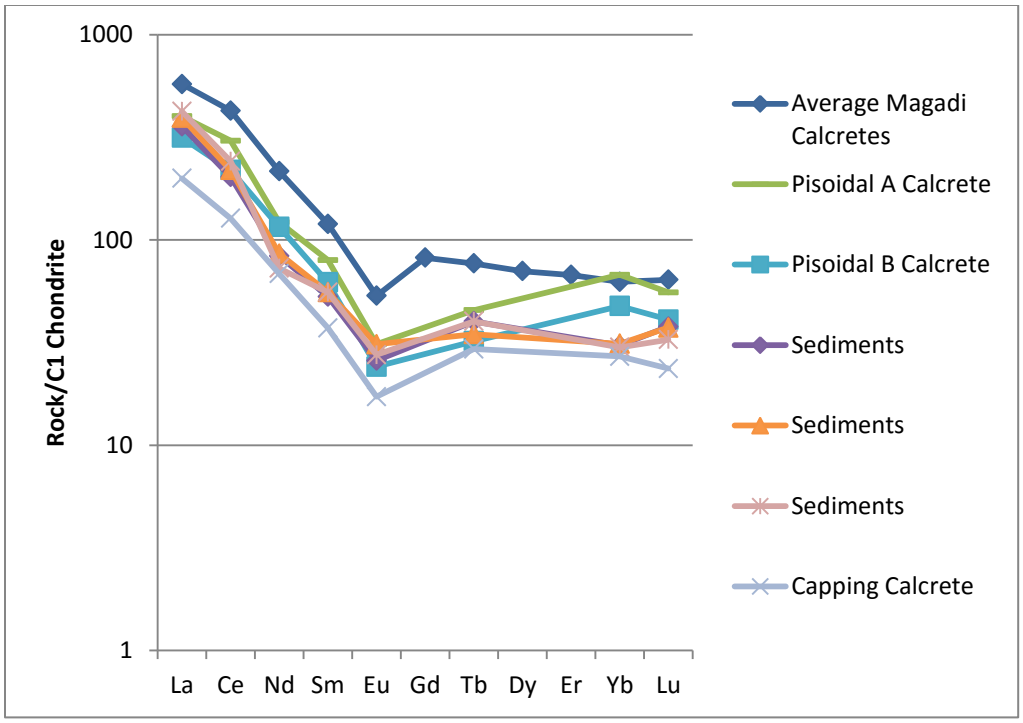

Figure 4-9. Comparison of REEs for the Olorgesailie sediments and the Magadi Trachytes. For patterns of other source rocks see Figure 3-26.

Though most of the post-Olorgesailie sediments are derived from the Magadi Trachytes, the later volcanic rocks such as the Suswa volcanics, may also be represented (Owen et al., 2014). REE patterns for the post-Olorgesailie Formation sediments are similar to those of the Olrogesailie Formation (Owen et al., 2014), but show overall depletion relative to the Magadi Trachytes, particularly in the HREEs.

4.6.3. Stable isotopes

As expected, the stratigraphic profile at Olorgesailie shows significant increase in both $\delta^{18}O$ and $\delta^{13}C$ in the calcretes compared to the adjacent sediments (Fig. 4-2). The $\delta^{13}C$ profile shows an upward increase in ^{13}C content, and the $\delta^{18}O$ profile shows an upward decrease in ^{18}O. The B calcrete is less enriched in ^{18}O than the A calcrete or the capping calcrete. Significantly, both isotope values show correlation, an indicator of evaporative enrichment (Figs. 4-2, 4-10).

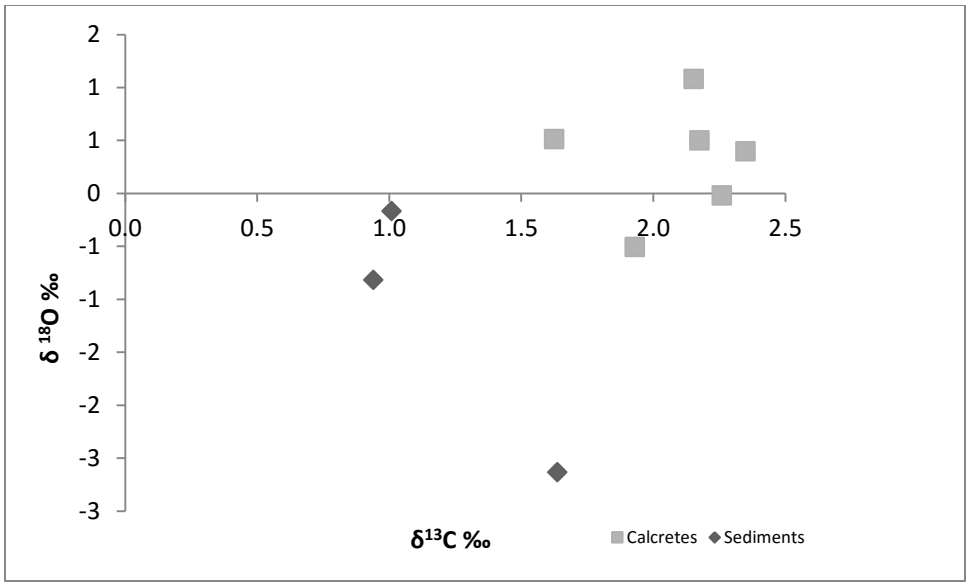

Figure 4-10. Plot of δ ^{18}O and δ ^{13}C for the Olorgesailie calcretes and their associated sediments. The calcretes plot with increasing δ ^{13}C and mostly increasing δ ^{18}O compared to the sediments and altogether have a coeval relationship.

4.7. Mineralogy

XRD analyses of each of the three calcretes at Olorgesailie revealed a mostly low-Mg calcite composition with minor amounts of feldspathoid, quartz, and anorthite. Analysis of the sediments showed a composition high in low-Mg calcite with feldspathoid, orthopyroxene and quartz.

Chert fragments are present in all these calcretes throughout and range from 0.5 mm to several millimeters. These cherts differ from those at Magadi in that they are mostly subrounded, highly fractured, non-spherulitic, and appear to show relict textures, possibly from trachyte volcaniclasts (Fig. 4-5 E and F). One silica clast found in Pisoidal Calcrete B may be a pseudomorph of titanite or gypsum (Fig. 4-6 D).

4.8. Paleoenvironment

The stratigraphy of the Olorgesailie Formation is well understood due to the presence of artifacts and anthropological fossils, and so intensive research has been done, backed up by many radiometric dates (e.g. Deino and Potts, 1990, 1992). The calcretes studied are in the post-

Olorgesailie Formation sediments which are up to ~500,000 years old but more likely formed within the range of 350,000 to 50,000 years ago (Owen et al., 2008b).

Most of the Olorgesailie Formation consists of lacustrine sediments interspersed with wetland and fluvial deposits. The sequence post-dating the Olorgesailie Formation is similar, consisting of interlayered fluvial, wetlands, shallow lake, and colluvial sediments, any of which possibly including pedogenesis (Owen et al., 2014). The calcretes mark dry periods when wetland or shallow lacustrine sediments were subaerially exposed. The calcretes studied in this thesis have been given stratigraphic context in Owen et al. (2014). The measured stratigraphic section is equivalent to their D10/B1 section.

The Pisoidal A calcrete appears to be predominantly pedogenic with possible overprinting by groundwater diagenesis. It is the most well developed calcrete in the profile and has a laminar top, indicating a relatively long depositional hiatus. Root casts/moulds are prevalent in the vertically adjacent sediments, indicating the environment at the time of deposition was accessible to plants, i.e. subaerial.

The middle calcrete, Pisoidal B calcrete, is similar though the diagenetic environment provided for the precipitation of silica cements that plug the majority of pore spaces. This is a clear indication of groundwater processes overprinting pedogenic processes. Calcite cements are predominantly vadose while the silica cements occurred during submersion. It is not clear what caused the influx of silica, but changing hydrochemistry has been indicated throughout the post-Olorgesailie Formation sediments, which include alternating and coincident carbonate, opaline, and chert rhizoliths.

The capping calcrete differs from the pisoidal calcretes in that it is massive micrite with spar-filled fractures that has little variation. Pisoids are rare and have few laminae. Microbial staining within laminae is common in both pisoids and the general micrite, but particularly where bands of cement have had a hiatus in growth. Fragments of volcaniclastics are very rare if not absent, and there is a lack of host material. Either the uppermost sediments have been completely replaced by calcite or this calcrete represents a primary depositional carbonate that has been altered by calcretisation. Chemical analyses suggest leaching of most elements of the capping calcrete. Stable isotope analyses indicate concentration of heavy isotopes as in evapoconcentration, and the values do not reflect modern meteoric values. Many of the fractures seem to be from roots; that is, they bifurcate and narrow downward. The majority of the micrite

is cemented by isopachous acicular to drusy sparite that indicates precipitation from a fluid. This thin deposit may result from carbonate sedimentation in shallow wetlands where plants flourished, and upon exposure was calcretized with the aid of microbes, and then eroded to the thickness found today.

5. BEACH CARBONATES AT NASIKIE ENGIDA, KENYA

5.1. Geologic background

Nasikie Engida, formerly called "Little Magadi", is a small saline, alkaline lake just to the north of Lake Magadi. Like Magadi, Nasikie Engida is fed mainly by hot springs. The lake is bound by a high fault scarp to the west exposing thick trachyte flows. A small narrow horst separates Nasikie Engida from the Northeast Lagoon, an extensive plain where ephemeral streams and hot spring runoff empty into Lake Magadi. The lake has a strong chemical gradient: in the north, where the springs feed the lake, the lake is more dilute (i.e. TDS < 50,000 mg/L; Renaut et al., 2013). Along the northern shoreline Na-Si-Al gels are forming where alkaline brine reacts with trachytic detritus (Eugster and Jones, 1968; Eugster, 1986). Near the springs are many cyanobacterial mats and efflorescent crusts. The lake is of low energy during summer. As the water moves towards the south it becomes progressively more saline, reaching a TDS of up to 272,000 mg/L (Renaut et al., 2013) and attaining saturation with respect to nahcolite and trona. The lake has the same general basin hydrology as Magadi, discussed in Chapter 3 of this thesis. The climate is semi-arid with evaporation potential of >3,500 mm/year and rainfall at (~ 500 mm/year.

Nasikie Engida was likely connected to Lake Magadi during former highstands, most recently at ~10,000 y BP, and small deposits of the High Magadi Beds and Oloronga Beds are preserved to the north of the lake (Baker, 1958). Behr (2002) reported a ^{14}C age of 9100 y BP for trona at Nasikie Engida, but this age is suspect because this was generally a humid period in East Africa (Butzer et al., 1972; Grove et al., 1975; Gasse, 1977; Gillespie et al., 1983; Roberts et al., 1993; Barker et al., 2002; Bergner et al., 2003).

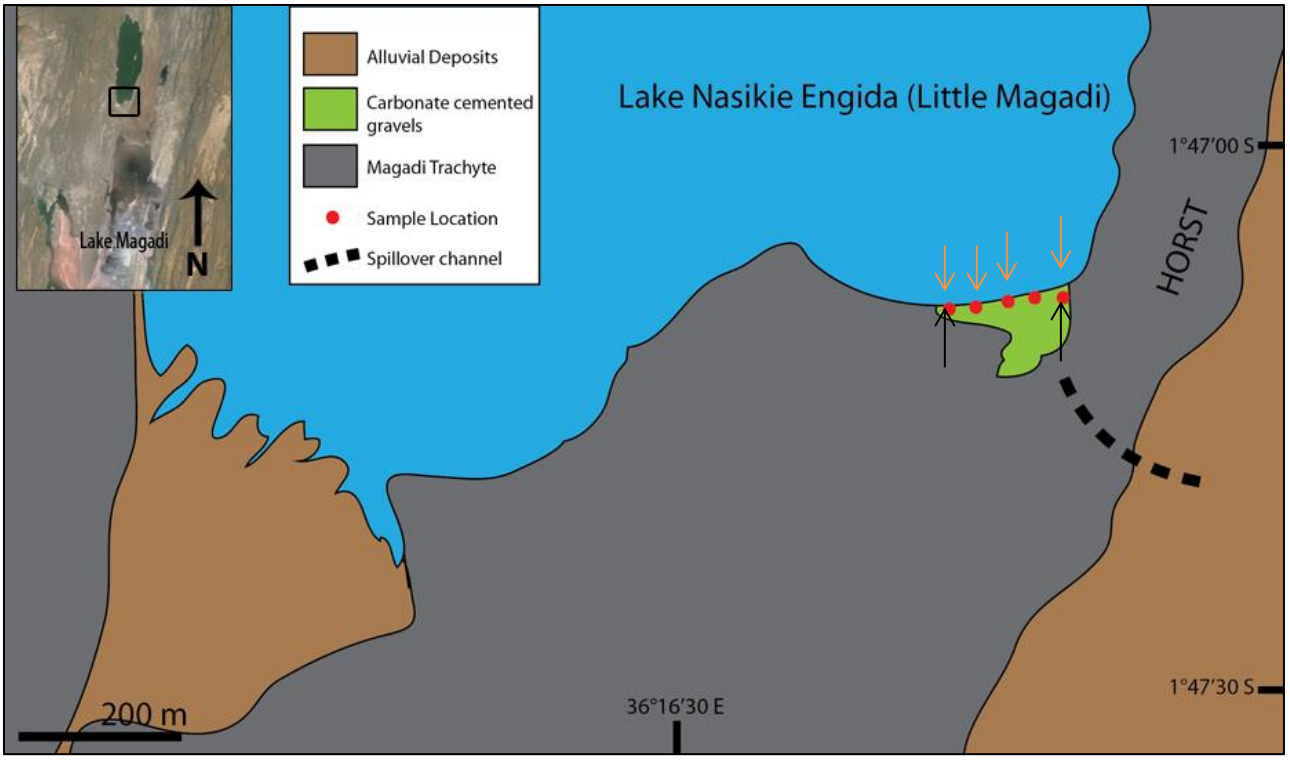

Figure 5-1. Map showing the location of the carbonate cemented gravels and sample locations. Top left image, from Google Earth©, shows regional location. Potential spillover channel is denoted by black dashed lines. Channel boundaries are derived from topography as well as traced by a small ephemeral channel. Black arrow indicates sample sites chosen for bulk-rock geochemical testing. Orange arrows indicate sample locations chosen for stable isotope testing. The site farthest to the east represents the calcrete underlying the High Magadi Beds.

5.2. Field observations

The deposits of interest are located at the southeastern shoreline of Nasikie Engida, near the horst separating Nasikie Engida from Lake Magadi (Fig. 5-1). The sediments are confined to a shallow wide valley abutting the lake and appear to be locally derived alluvial fan gravels that have been reworked along the shoreline. An ephemeral stream channel network, about 500 m long, lies directly south of the fan.

Two types of carbonate-cemented deposits occur at the southeastern end of Nasikie Engida. The first type is similar to the calcrete that overlies the Oloronga Beds elsewhere in the Magadi basin: a dark grey, pisoidal, well cemented calcrete, but containing many pebble-sized chert clasts (Fig. 5-2 B). This calcrete is a small outcrop, a few m^2 in area, continuing under an adjacent outcrop of High Magadi Beds (Fig. 5-3). The calcrete crops out < 1 m above lake level (in July 2011) and is submerged during higher lake levels (Fig. 5-4). The Oloronga Beds are

absent here, since the trachytes are at or very near the land surface. The host material for the lowermost calcrete is a thin layer of very fine sand with coarse volcaniclastic grains.

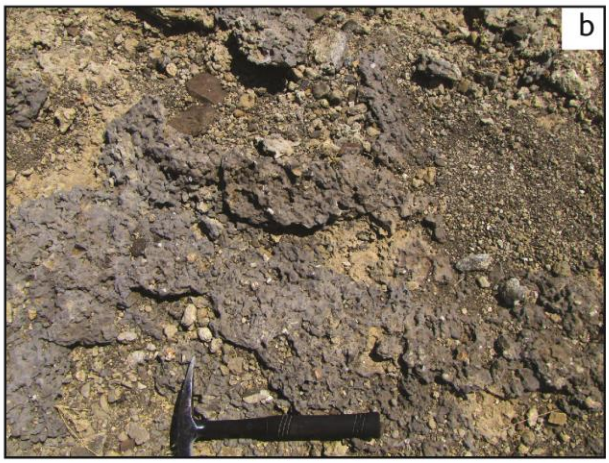

Figure 5-2. Field photographs of carbonates near Nasikie Engida. a) Overview of carbonate-cemented conglomerate at south Nasikie Engida. Vehicle in background for scale. b) Blue-grey calcrete layer underlying High Magadi Beds. c) Several fining-upwards trough cross stratified sequences in carbonate-cemented conglomerate beds d) Grey carbonate coats vertical cracks in the Nasikie Engida conglomerate. Hammer length is 32 cm.

The second carbonate-cemented horizon overlies a thin exposure of the High Magadi Beds and consists of bedded angular pebbles with layers of laminar carbonate on top and within it (Fig. 5-2 A and C). Most pebbles are opaline chert with others being volcanic detritus and thin (1–2 mm) rip-up clasts of laminar carbonate or stromatolites. Calcite stromatolites are present in places along the SE shoreline where they coat gravel and conglomerates, so their presence in the sediments is not unexpected. The carbonate and chert clasts are angular; the volcanic pebbles are angular to subangular. In the central, thickest part of the deposit the angular clasts are imbricated, showing that they were deposited in flowing water. A thin (0.5 mm) laminar carbonate coats the upper surface of the cemented gravels. A grey to white, uniform thin (0.5 mm) cement coats vertical cracks in the gravels (Fig. 5-2 D).

The conglomerate bed thickens to ~1 m in the middle of the deposit at the southeastern end of the lake, and thins completely towards the edges of the valley. At the thickest part of the conglomerate, the sediments are trough cross-bedded, with 10–20 cm thick cross-beds that appear to fine upwards (Fig. 5-2 C).

Laminated carbonate layers, where present, lie at the top of the fining-upward sequences and locally display several generations of shallow (~1 mm) vertical (polygonal) cracks producing sub-mm size clasts. These overlie similarly cracked fine sediment. Other laminar carbonate layers are less cracked, with the cracks having random orientation and appearing to postdate the laminar cementation. All laminar carbonate layers have little, if any, detritus cemented to the top (Fig. 5-5), despite being layered within the conglomerate.

Figure 5-3. Small outcrop of High Magadi Beds at the SE corner of Nasikie Engida. White clasts are Magadi-type chert. Broken block of darker brown, calcite-cemented conglomerate and breccia disconformably overlie the High Magadi beds with a minor erosional contact. Photograph taken looking SW, when standing on the older calcrete shown in Figure 5-2 B.

Figure 5-4. View westwards from the southeast corner of Nasikie Engida. Blocks of cemented gravel in foreground lie adjacent to evaporites (trona and nahcolite). The cemented gravels originate from a small drainage network south of the lake (to the left in the photograph).

Figure 5-5. Laminar carbonate coating the cemented gravels. A more solid expression of the coating lies underneath the hammer. The laminar carbonate to the lower right of the hammer is cracked and shedding small pieces. The coating is 1–2 mm thick. Hammer is 32 cm long.

5.3. Petrographic results

The low-Mg calcium-carbonate cemented conglomerates at southern Nasikie Engida consist of carbonate-coated clasts, 0.01 to 3 cm in length, within a clast-supported porous framework that is variably cemented by calcite. Many of the tabular clasts of laminated carbonate might be reworked stromatolite fragments (Fig. 5-6). These laminated carbonate clasts have mm-scale doming and some show ‘budding’ fabrics (Fig. 5-6 A, B) though there is no conclusive evidence for a microbial origin. The internal laminae do not exceed a thickness of 1

cm. Similar laminar structures can form through seasonal variations and changes in water chemistry (Grotzinger and Rothman, 1996).

Clasts of silica are present; some show replacement by calcite. Under reflected light, these silica clasts show a difference between center and rim in crystallinity and/or composition (Fig. 5-7 D). The silica is in the form of spherules 10 to 25 μm in diameter and some clasts show partial replacement by calcite (Fig. 5-8 A, B). Some silica clasts have laminar carbonate crusts on them, though many do not. Other clasts in the conglomerate are trachyte.

Two distinct cements are present: the youngest, void-filling cement is calcite, with an earlier cement composed amorphous silica that surrounds clasts. The silica cement covers clasts with an equal thickness (isopachous) and cements clasts together at point contacts (Fig. 5-8 C, E). The rocks are porous with many partially filled voids.

Some clusters of carbonate crystals, 300 to 500 μm in size (sparite), resemble *Microcodium* (Fig. 5-7 A, B, C). These predate the earlier amorphous silica cement and some show textures that imply recrystallization (e.g., pores, maybe are calcite pseudomorphs of other crystals [barite?]). A few clasts are composed of spar-sized euhedral hexagonal crystals of calcite (Fig. 5-8 D). These are possibly pseudomorphs of analcime, a common alteration product of silicate minerals in the area (Surdam and Eugster, 1976; Rabideaux et al., 2016). These pseudomorphs predate stromatolite/laminar carbonate development.

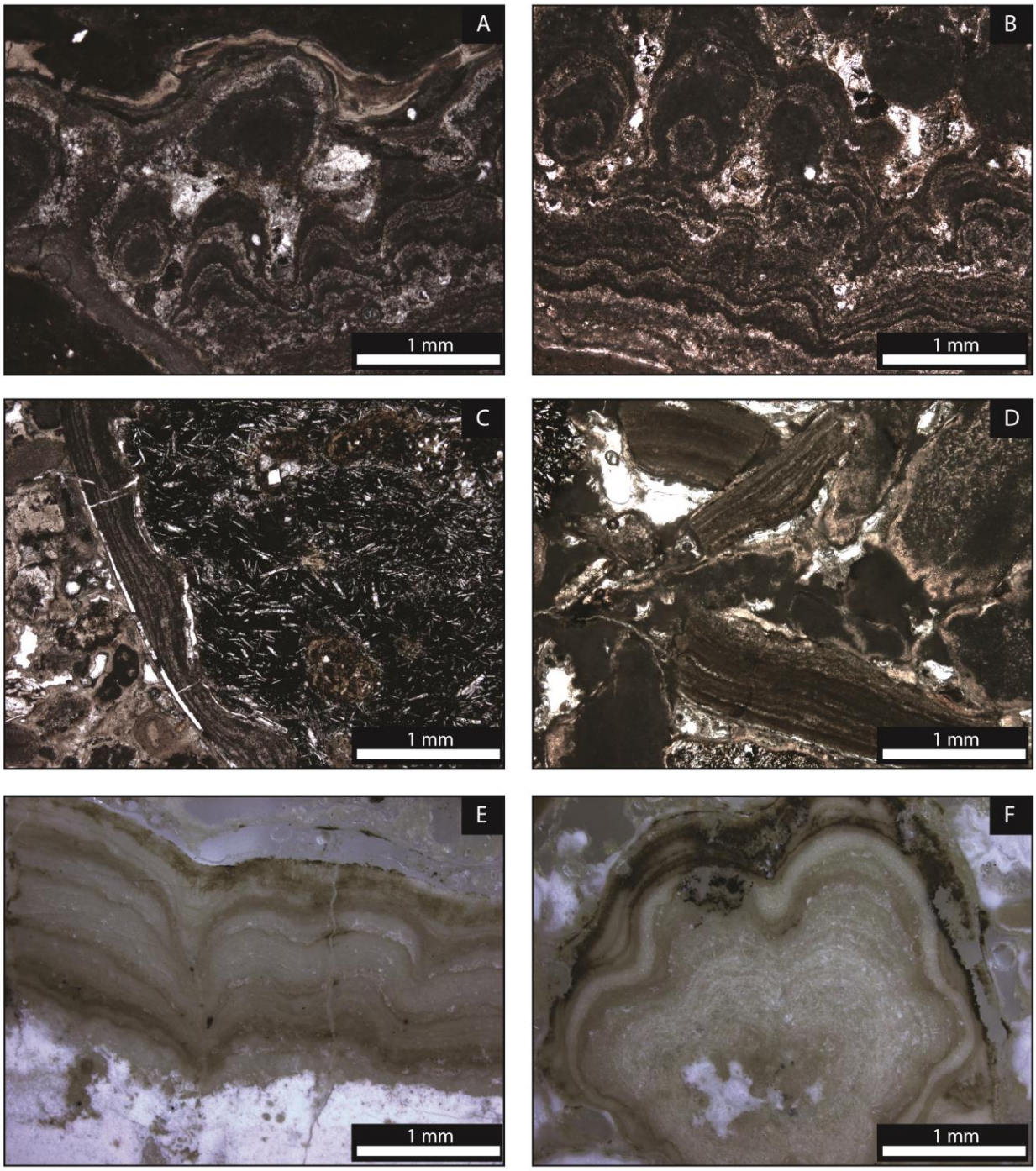

Figure 5-6. Photomicrographs of laminar features in the conglomerate. Plane polarized light. A and B) Domal fabric overlying laminar fabric. C) Laminar coating on a volcaniclast. Two horizontal cracks possibly result from shrinkage. D) Laminar carbonate clasts among clasts of silica spherules. E and F) White-card technique of (Folk, 1965) of detritus-free and continuous laminae. Note organic residue and/or oxides (Fe-Mn?) in F.

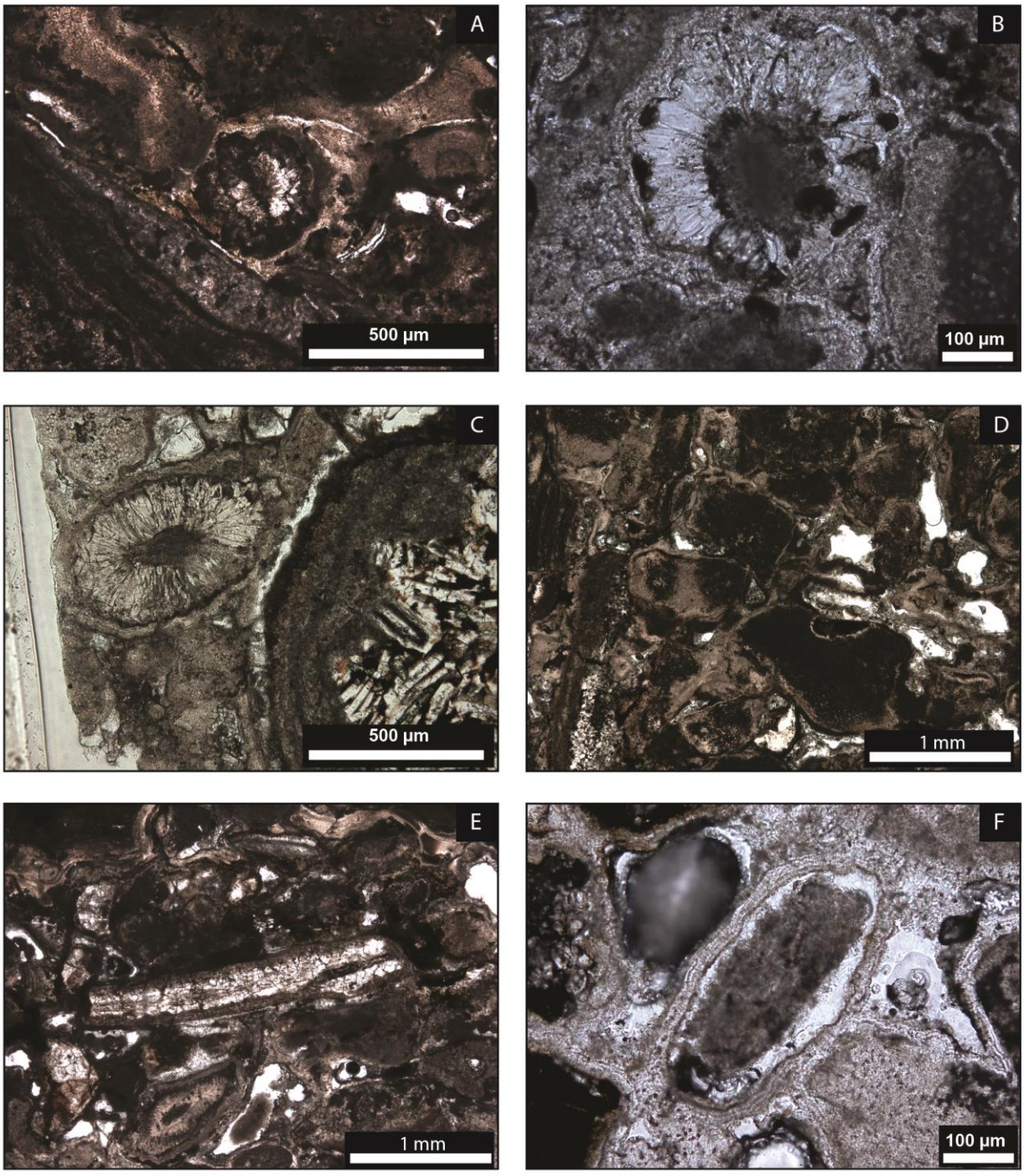

Figure 5-7. Photomicrographs of clasts in the conglomerate. All in PPL. A, B, and C) Calcite rosettes. D) Clasts of spherulitic silica. The darker parts of the clasts are composed of spherules 10-25 µm in diameter. The lighter colored material is amorphous silica. E) A calcified plant fragment. F) Dissolution fabric. A mass of calcite is outlined by a ~20 µm thick border of acicular silica cement. The calcite seems to be smaller than its original size.

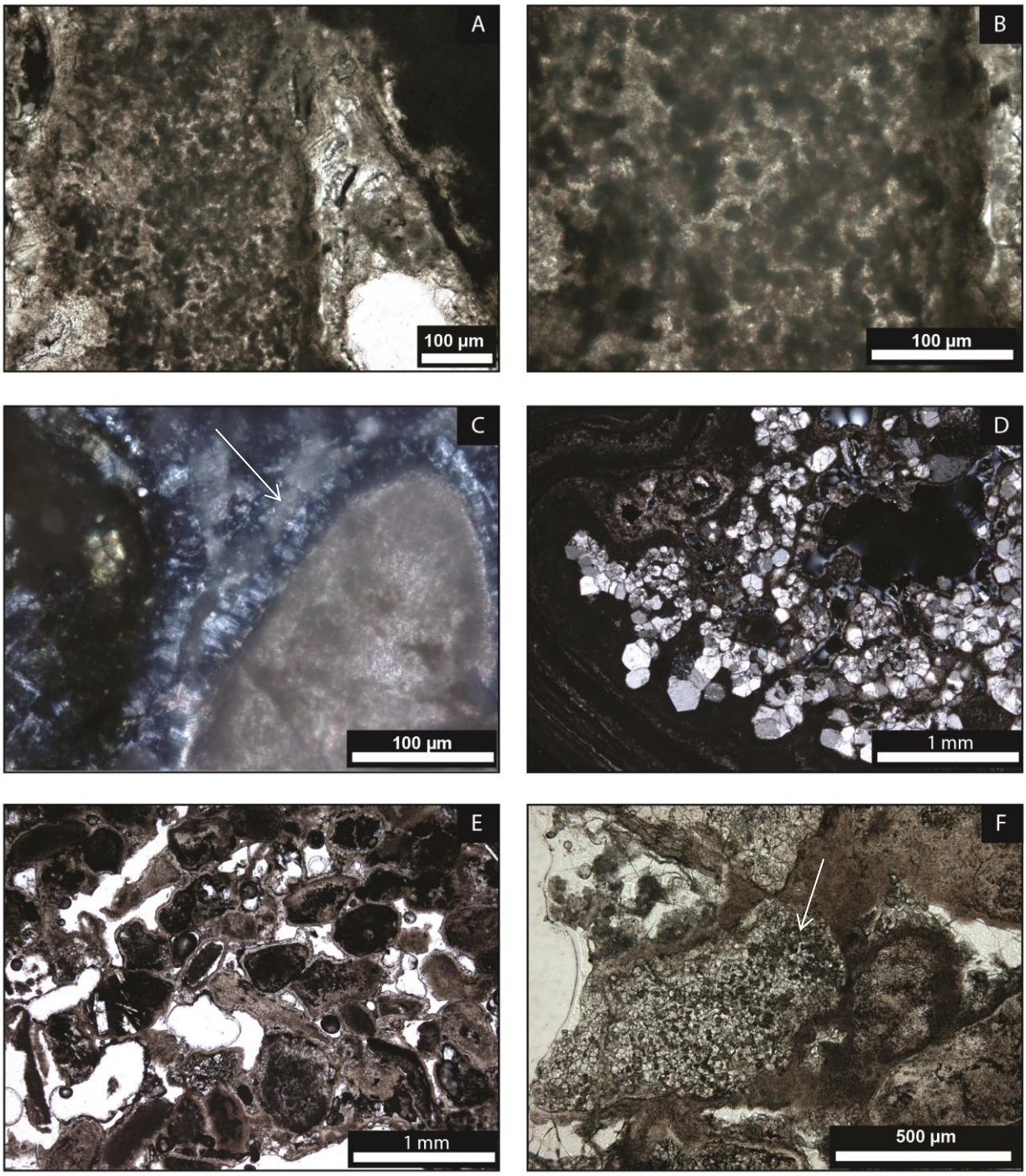

Figure 5-8. Photomicrographs of the conglomerate. A) Partially calcified silica-spherules. PPL. B) Close-up of A, PPL. C) Bladed silica cement around a micrite clast. Micritic cement (arrowed) rims the silica cement and fills voids. XPL. D) Polygonal crystals (analcime?) replaced by calcite, coated by laminar carbonate (at lower left). XPL. E) Typical appearance of silica and micrite clasts cemented together at point contacts. PPL. F) Spar crystals (arrowed) in a clast resembling the silica spherules indicating possible replacement. PPL.

5.4. Geochemical data

Only one sample of the carbonate-cemented conglomerate was analysed for bulk rock geochemistry (Table 5-1; see Fig. 5-1 for location). Although a single sample is not necessarily representative, it can be compared with the Oloronga-capping calcretes (Chapter 3), the nearby calcrete underlying the High Magadi Beds, and a calcrete sample from north of Nasikie Engida that disconformably overlies Oloronga Beds (sample location 4 in Fig. 3-6).

Sample	SiO_2	Al_2O_3	Fe_2O_3(T)	MnO	MgO	CaO	Na_2O	K_2O	TiO_2	P_2O_5	LOI	Total
SE Nasikie Engida Conglomerate	49.0	1.71	0.96	0.14	0.53	22.39	2.26	0.64	0.094	0.1	22.55	100.4

Table 5-1. Bulk rock geochemistry for the carbonate-cemented conglomerate at southern Nasikie Engida.

As shown in Figure 3-25, the Nasikie Engida conglomerate contains more silica than most other carbonates sampled from Lake Magadi (see Chapter 3), and the silica concentration is higher than would be expected from the detrital grain content alone. Petrographic analyses confirm the presence of authigenic silica. The conglomerate sample also has much higher P content than was measured in other samples, and has more Na, which is not explained by higher amounts of silicate detritus, as implied by deviations from the general Na/Ti ratios for the Magadi sediments. The higher Na content likely comes from evaporative concentration of the lake water. The phosphorus might come from the organic matter in the stromatolitic clasts.

The calcrete at SE Nasikie Engida underlying the conglomerate is similar chemically to the calcrete capping the Oloronga Beds and the laminar calcrete discussed in Chapter 3. The only difference between the calcrete below the conglomerate and the carbonate-cemented conglomerate is a slight increase in silica compared to other Oloronga-capping calcretes, and the high Ba content of both the calcrete and conglomerate.

5.4.1. Stable isotopes

Sample Location	$\delta^{13}C$ (‰, V-PDB)	$\delta^{18}O$ (‰, V-PDB)
West margin	3.89	3.89
Intermediate	3.55	3.76
Center of deposit	1.10	2.27
Older calcrete	1.79	2.98
Average value of conglomerate (n=3)	2.85	3.31

Table 5-2 - Isotope data for the Nasikie Engida carbonates. V-PDB is the Vienna Pee Dee Belemnite standard.

The stable isotopes of the conglomerate show enriched values relative to the spring water values of +0.4‰$_{PDB}$ $\delta^{13}C$ and -1.3‰$_{SMOW}$ $\delta^{18}O$ (Hillaire-Marcel and Casanova, 1987). The most enriched sample comes from the western margin of the conglomerate, while the least enriched sample is from the thickest part of the deposit, near the middle of the conglomerate outcrop. This may indicate lower evaporative concentration in the middle of the small drainage basin. The C and O isotopes are coeval, implying evaporation in a closed basin (Talbot, 1990). The carbonates within the conglomerate have higher stable isotope values than the underlying calcrete and the other Oloronga-capping calcretes of the Magadi area.

It is difficult to differentiate different carbonates in only one sample. In a bulk-rock sample, it is hard to differentiate which components the isotope values represent, but all values are reasonable for the area and types of deposit. The abundant stromatolitic carbonate clasts are probably the main source of calcite recorded by these isotopic measurements. Those values fall within the reported range of Magadi-Natron Basin stromatolites (the most recent generation formed at ~ 12,000–10,000 y BP), which have values ranging from +1-4‰ $\delta^{18}O$ and +2–5‰ $\delta^{13}C$ (Hillaire-Marcel and Casanova, 1987). The values of the laminar carbonates at SE Lake Magadi near Graham's Lagoon have average values of -0.75‰ $\delta^{18}O$ and +1.57‰ $\delta^{13}C$.

5.5. Discussion

5.5.1.Origins of the conglomerates at southeastern Nasikie Engida

The cross bedding, grain size and sorting show deposition in a high energy environment, with fluctuation in energy levels seen in the fine/coarse sequences. At present the lake does not seem to have high enough energy to produce such a deposit from wave action though this was a possibility in the past. Nonetheless coarse gravel is moderately sorted along the present eastern shoreline, so high energy conditions may develop occasionally during storms. The trough cross beds are oriented perpendicular to the shoreline indicating a N-S or S-N current. Since the conglomerate is restricted to the shallow ephemeral stream valley at the SE of the lake and is absent from other shorelines, processes in the immediate area must have caused sedimentation and the local cementation by calcite and silica.

The cross bedded gravels are locally capped by a laminar carbonate layer. This carbonate layer is largely free of siliciclastic grains and can be smooth or cracked, suggesting a lack of clastic sedimentation during its formation. These carbonate layers imply calm hiatuses between periods of higher energy sedimentation.

Initially this deposit was viewed as a possible calcrete but more detailed analysis has shown that it lacks calcrete features such as pervasive replacement of original minerals or displacive cement. Additionally, the deposit is largely cemented by amorphous silica as well as a late calcite cement. The deposit consists of trough and planar cross-bedded gravels that dip lakewards (north) at a shallow angle (<10°) which interfinger with bedded gravels that dip more gently landwards (south). These contrasting dips, and the cementation of the conglomerate by carbonate and silica, is characteristic of beach rock (Vousdoukas et al., 2007). Lacustrine beachrock, though uncommon, has been described from many locations, and is composed of calcite (Binkley et al., 1980; Cohen and Thouin, 1987; Erginal et al., 2012), aragonite (Burke and Gerhard, 2000; Erginal et al., 2012), dolomite (Last and De Deckker, 1990) and less commonly, silica (Jones et al., 1997).

The imbricated conglomerate could represent lakeward-dipping beach gravels and landward-dipping beach-berm sediments (Renaut and Owen, 1991), deposited when the lake had higher littoral energy. The conglomerate was later cemented into a Si-Ca beachrock.

5.5.2. Clast and cement origins

The conglomerate is composed of clasts of laminar carbonate, volcanic rock fragments, and pebble-sized grains of authigenic calcite and silica. The trachyte clasts derive from the underlying Magadi Trachyte. The clasts composed of calcite or silica, however, could have several origins.

5.5.2.1. Laminar carbonate clasts

Laminar and stromatolitic carbonates can form abiotically (e.g. Read, 1976; Grotzinger and Rothman, 1996), including from evaporation of thin water films and precipitation from high-temperature fluids. Given the regularity and conformity of the laminae, the alternation of light and dark laminae, and the 'budding' microfabric on several clasts, calcite precipitation in some of the laminae in carbonate clasts might have been related to biomediation in microbial mats or biofilms.

Stromatolite-forming microbial mats are common in saline lakes (e.g. Casanova, 1986; McCall, 2010; Last et al., 2010; Awramik and Buchheim, 2015), and have formed at Nasikie Engida and Magadi in the past (Hillaire-Marcel and Casanova, 1987; Behr, 2002; Brenna et al., 2014). Modern microbial mats are forming along the northern shoreline of Nasikie Engida at the local hot springs, but stromatolites are not forming there today because the spring and lake waters are calcium poor, and the hot spring waters are undersaturated with respect to amorphous silica at the points of discharge (R. Renaut, pers. comm.).

Given the possible stromatolitic laminated calcite clasts present in the conglomerates, it would be tempting to compare their isotope values with those of the stromatolites in the Magadi basin studied by Hillaire-Marcel and Casanova (1987). However, the new isotope values obtained were from whole-rock samples; microsampling would have to be undertaken to determine the values of the stromatolitic clasts in the conglomerate. Their inclusion as detrital clasts in post-High Magadi Beds sediments implies that the youngest calcite stromatolites might have formed about 10,000 years ago during the African Humid Period, which is the age of the "third generation" of those reported by Hillaire-Marcel and Casanova (1987). The Nasikie Engida stromatolitic clasts, however, might be unrelated to the stromatolites discussed by

Hillaire-Marcel and Casanova (1987). The clasts could be related to the *in situ* stromatolite coatings on trachyte along the SE shore, ~150 m north of the study site, whose age is unknown.

An alternative possibility is that the stromatolitic clasts formed as encrustations on older carbonate-cemented gravel that were broken and re-deposited in almost the same location. Because little gravel became cemented into these laminated carbonates, it is unlikely that they formed diagenetically after burial, and more likely formed during depositional hiatuses when microbial mats could form in relatively quiet water. These mats would form the thin layers of stromatolites, which would then be covered by successive layers of gravels during wetter times (Alonso-Zarza, 1999). Some of the stromatolites would be fractured and be incorporated into the gravel deposit.

5.5.1.2. Silica

Opaline chert clasts are common in the conglomerate. Currently, Na-Si-Al gels are forming in low-energy settings at the north end of Nasikie Engida upon older muds (Eugster and Jones, 1968). The eponymous magadiite has formed in the past in the lake; the silica spherules in the cherts might be evidence of magadiite formation—the spherules in the opaline silica are the same size as the 10–20 µm spherules in magadiite-type chert (Figure 5-8 A, B). The character of the silica clasts, however, differs from typical occurrences of Magadi-type chert in that they are small discrete clasts without the typical reticulated shrinkage cracks that form by alteration of a proven magadiite precursor.

While not the focus of this thesis, the origin of the silica is not readily apparent and has multiple possibilities. The authigenic silica may have precipitated from an alkaline Si-rich lake, as Nasikie Engida is today, as a result of many factors including: the lowering of pH from microbial activity or by injection of geothermal CO_2 into the lake water, pH alteration by silicate hydrolysis, or evapoconcentration of pore fluids.

5.5.1.3. Cements

The amorphous silica cement predates calcite cements in the beach deposits, indicating a change in lake water chemistry. The calcite is then followed by localized chalcedony cement. Based on petrography, calcite is a minor cement in the conglomerates, but the overall calcite content of the rock is inflated because of stromatolitic clasts.

The amorphous silica cement formed first after the conglomerate had been deposited, which included authigenic silica clasts. A supply of calcium from either dissolved stromatolite or laminar carbonate clasts, as is implied in thin section, or from external meteoric water, provided Ca^{2+} for calcite to form. Calcite dissolution could have resulted from a decrease in pH, either by organic processes or mixing of saline and fresh waters, which also may have contributed to formation of the silica cement. The botryoidal texture of the second phase of silica cement indicates another change in water chemistry and slower rates of precipitation.

5.5.3. Hydrochemistry of Nasikie Engida

Nasikie Engida receives most of its annual recharge from hot springs at the northern end. A north-south salinity gradient is present in summer months, from ~ 35 g/l Total Dissolved Solids (TDS) at the northern end of the lake to almost 300 g/l at the southern shoreline (Renaut et al., 2013), where nahcolite and trona often precipitate in calm water. Mixing likely occurs at other times of the year when energy levels are higher.

The Si-Ca cemented gravels are found only along the southeastern shoreline of Nasikie Engida, implying that the waters involved in their formation were limited to, or only effective along that part of the shoreline, and are probably related to dilute influx from the southeast along the gravel fan axis. The stable isotope analyses of the carbonate-cemented gravels support this interpretation; the high oxygen values likely reflect enrichment related to evaporative concentration in a closed lake. However, the presence of older stromatolite clasts could have masked the carbonate cement signal in that analysis. More analyses will be needed to resolve this.

The stable isotope analysis shows that the deposit is enriched in heavy C and O isotopes.. The influence of calcification related to microenvironmental changes induced by microbes could have played a role if the laminar carbonates are microbialites; however, the ^{13}C values for the deposits are within the same range (~2–5‰ PDB) as those of the Magadi and Natron stromatolites studied by Hillaire-Marcel and Casanova (1987), which is only slightly higher than other local carbonates (see Chapter 3). Stable isotope values increase towards the margin of the deposit; the central, thickest portion has lower values. This may indicate fresher water towards the center of the deposit. More samples are needed to test this, but this relationship might

indicate that a main feeder channel on the alluvial fan or fan-delta that received more dilute inflow than the lateral margins.

5.5.4. Paleoenvironmental interpretation

The cemented gravels along the southern shoreline of Nasikie Engida are linked geographically with two valleys that played important roles in its formation. One, a wide shallow drainage basin, provided the alluvial gravels. The other, a small dry valley, cuts the horst between Lake Magadi and the southeastern corner of Nasikie Engida and is the lowest point between the two sub-basins (Fig. 5-9). This valley is the topographic sill between the two lakes, and the most likely site where the two lakes were last united. The chronology of former connections between Nasikie Engida and Lake Magadi remains unknown. It seems clear, however, that they were probably connected during the late Quaternary, and probably during earlier humid phases in the mid-to-late Pleistocene when they formed a single lake. With present data, however, it is not possible to determine the chronology of the links, and to assess if and when Lake Magadi flowed into Nasikie Engida or *vice versa*. It seems probable, however, that the formation of the beachrock at SE Nasikie Engida is in some way linked to the proximity of the inferred overflow and linkage.

Figure 5-9. Photo showing narrow valley between lakes. Blue shaded area denotes the extent of the conglomerate. Note erosion of horst towards Lake Magadi. Photo from R. Renaut.

The conglomerates, derived partly from local alluvial-fan drainage, are located in the drainage basin that is next to an overwash channel, perhaps active when a paleolake Magadi was high and overflowing into Nasikie Engida. Though Nasikie Engida is at a slightly higher elevation today (about 3–4 m higher than Magadi based on GPS estimates), it has a small catchment. During deposition of the gravels, Nasikie Engida might have been only ~ 2 m above its present level. Lake Magadi, in contrast, would have been 10–16 m higher than today for spillover to occur. These relative elevations assume that tectonics has not modified them, which is likely the case since there have been no major tectonic episodes during the last 10,000 years when these deposits were forming.

No sediments record former flow from Nasikie Engida into Lake Magadi. The possibility for spillover is based on topographic data that assumes that, during rains, Nasikie Engida filled more quickly than Lake Magadi, which has a larger catchment. While Nasikie Engida may have periodically spilled into Magadi through the same area, the relationship of spillover to the sediments is unclear. It is difficult to speculate without further data, but it seems more logical that the deposits formed during a period when Lake Magadi flowed into Nasikie Engida, and not

the other way around. This overflow phase may have contributed to the reworking of the gravels along the beach.

Based on the amount of authigenic silica present, with both stromatolitic (laminar or truly microbial) and micrite clasts, and alternating siliceous and carbonate cements, conditions clearly changed often during deposition and cementation. Carbonate cement is minor and the most recent phase of development and probably represents modern conditions of semi-aridity and precipitates as efflorescent crust.

The trough cross-bedded gravels indicate a flow perpendicular to the shoreline. Fluctuations in lake level can be seen by the laminar carbonate layers capping the discrete cross-beds indicating times of stability and, possibly, microbial mat growth during which little sedimentation occurred. These laminae were in turn broken during flooding or weakened by periodic desiccation and/or shrinkage, accounting for some of the laminar clasts in the deposit. Carbonate cement was produced by the mixing and subsequent evaporation of relatively fresh Ca-bearing meteoric or shallow groundwater and the saline water of Nasikie Engida and cemented the gravels to form an unusual beachrock (Schmalz, 1971).

Stratigraphic relationships show that the conglomerate and the laminar carbonate layers formed after the deposition of the High Magadi Beds, about 10,000 to 5000 years b.p. Climate studies from various places in East Africa show fluctuation conditions during this time with increasing aridity since 5000 y BP (Roberts et al., 1993; Berke et al., 2012; Garcin et al., 2012). While the drier conditions since the Late Pleistocene led to a Ca deficit in the lake and groundwater, calcium carbonates formed in Lake Magadi as recently as 5000 y BP (Casanova and Tiercelin, 1982). Some of the laminar carbonate, particularly that filling and encrusting the most recent beachrock surfaces, may be 5000 years old or younger though the previous laminar carbonate and gravel portions are older.

5.6. Summary

These deposits are difficult to fully explain without more data. The sorted gravels that make up the conglomerate were deposited under high energy conditions. The sediment is composed primarily of trachyte debris and clasts of authigenic silica, both of which may be

coated by laminar carbonate, which also forms individual clasts. This laminar carbonate has stromatolitic features and indicates the presence of dilute, Ca-bearing waters during their formation. During dry phases with periodic influx of dilute water, laminar carbonate also encrusted the gravels. The gravels and the laminar carbonate are interlayered suggesting a marked fluctuation in conditions from high to low energy. This may reflect seasonality or a small-scale climate cycle during which forceful spillover from Lake Magadi would deposit and rework the gravels, after which the conditions would be calm and dry for laminar carbonate to form. After sediment deposition the gravels were cemented alternately by silica and minor amounts of calcite. Calcite also variably replaced trachyte and silica clasts.

6. CONCLUSIONS

6.1. Lake Magadi

There are several calcretes at Lake Magadi, the major one of which is the Oloronga-capping calcrete. This calcrete is polygenic, having been produced by both pedogenic and groundwater precipitation processes. There may have been multiple phases of overlap, but it appears that some pedogenesis took place before the groundwater cementation, with some later pedogenesis occurring after the bulk of the calcrete had been formed. It is likely the calcrete was lake-marginal during a time when the lake level was low, and formed after the majority of the Oloronga Beds had been deposited and subsequently exposed. The Oloronga-capping calcrete is >100,000 years old, predating the Green Beds, and probably formed within the range 300–200 ka, though it likely took much less than 100,000 years to form.

The laminar calcrete at the SE of Lake Magadi was formed chiefly by physicochemical processes, particularly high evaporation. Its age is unclear; it could be up to 300,000 years old but is likely much younger.

Because they are quite common in the area, a basin-wide survey of calcretes with a many more samples would be ideal to determine the chemical signatures of the different calcretes, which may also help in stratigraphic correlation of the basin.

6.2. Olorgesailie

Three calcretes in succession in the Post-Olorgesailie Formation Sediments are part of a sequence of shallow wetlands and terrestrial deposits. Analysis of the microfabrics indicates a predominance of pedogenic calcrete with groundwater diagenetic alteration and intervening lacustrine silts. This corroborates other evidence in the basin of shallow lacustrine, wetlands, and dry land paleoenvironments during the deposition of the Post-Olorgesailie Formation Sediments. There are many other calcretes within the Post-Olorgesailie Sediments as well as in the Olorgesailie Formation that have not been studied in detail. These may provide further resolution of local climate data.

6.3. Nasikie Engida

The beachrock at Nasikie Engida represents a time of about 5000 years during which the climate fluctuated facilitating the deposition of both gravels and calm water deposits in a typically calm lake. Spillover from and to Lake Magadi was likely and the location of the beachrock in abrupt juxtaposition with the spillover channel is an unlikely coincidence, leading to the idea that the spillover contributed to the formation of the beachrock. It is difficult to reconcile the high energy needed to form gravel beds with the low energy required for laminar carbonate formation but these two types of deposits are interlayered. More work is needed to ascertain whether the laminar carbonate is truly microbial, and if so, is it derived from the stromatolites from the shoreline crusts to the NE or were they formed at the site of the deposit. Additionally, study of the spherulitic silica clasts may provide some clues to the history of the lake in terms of water chemistry.

REFERENCES

Albaric, J., Déverchère, J., Petit, C., Perrot, J., Le Gall, B., 2009. Crustal rheology and depth distribution of earthquakes: Insights from the central and southern East African Rift System. Tectonophysics 468, 28-41.

Allen, D.J., Darling, W.G., Burgess, W.G., 1989. Geothermics and hydrogeology of the southern part of the Kenya Rift Valley with emphasis on the Magadi-Nakuru area. British Geological Survey, Research Report (Hydrogeology Series) SD/89/1.

Alonso-Zarza, A.M., 1999. Initial stages of laminar calcrete formation by roots: examples from the Neogene of central Spain. Sedimentary Geology 126, 177-191.

Alonso-Zarza, A.M., 2003. Palaeoenvironmental significance of palustrine carbonates and calcretes in the geological record. Earth-Science Reviews 60, 261-298

Alonso-Zarza, A.M., Genise, J.F., Verde, M., 2011. Sedimentology, diagenesis and ichnology of Cretaceous and Palaeogene calcretes and palustrine carbonates from Uruguay. Sedimentary Geology 236, 45-61.

Alonso-Zarza, A.M., Jones, B., 2007. Root calcrete formation on Quaternary karstic surfaces of Grand Cayman. Geologica Acta 5, 77-88.

Alonso-Zarza, A.M., Silva, P.G., 2002. Quaternary laminar calcretes with bee nests: evidences of small-scale climatic fluctuations, Eastern Canary Islands, Spain. Palaeogeography, Palaeoclimatology, Palaeoecology 178, 119-135.

Alonso-Zarza, A. Wright, V.P., 2010. Calcretes, pp. 225-267. In A.M. Alonso-Zarza and L. Tanner (Eds.), Carbonates in Continental Settings: Facies, Environments and Processes. Developments in Sedimentology 61, Elsevier. Oxford. 226-257.

Anderson, G.D. Talbot, L.M., 1965. Soil factors affecting the distribution of the grassland types and their utilization by wild animals on the Serengeti plains, Tanganyika. J. Ecol. 53:33-56.

Awramik, S.M., Buchheim, H.P., 2015. Giant stromatolites of the Eocene Green River Formation (Colorado, USA). Geology 43, 691-694.

Bachman, G.O., Machette, M.N., 1977. Calcic soils and calcretes in the southwestern United States. U.S. Geological Survey Open-file Report 77-794, 163 pp.

Baker, B.H., 1958. Government of Kenya; Ministry of Commerce and Industry, Geological Survey of Kenya; Geology of the Magadi Area, Degree Sheet 51, SW Quarter. Report No. 42, 1958.

Baker, B.H., 1963. Government of Kenya; Ministry of Commerce and Industry, Geological Survey of Kenya; Geology of the Baragoi Area, Degree Sheet 27, NE. Quarter. Report No. 53, 1963.

Baker, B.H., 1975. Geology and geochemistry of the Ol Doinyo Nyokie trachyte ignimbrite vent complex, south Kenya Rift Valley. Bulletin of Volcanology 39, 420-440.

Baker, B.H., Mitchell, J.G., Williams, L.A.J., 1988. Stratigraphy, geochronology and volcano-tectonic evolution of the Kedong-Naivasha-Kinangop region, Gregory Rift Valley, Kenya. Journal of the Geological Society 145, 107-116.

Baker, B.H., Mitchell, J.G., 1976. Volcanic stratigraphy and geochronology of the Kedong-Olorgesailie area and the evolution of the South Kenya rift valley. Journal of the Geological Society, London 132, 467-484.

Baker, B.H., Wohlenberg, J., 1971. Structure and evolution of the Kenya Rift Valley. Nature 299, 538-542.

Barker, P., Telford, R., Gasse, F., Thevenon, F., 2002. Late Pleistocene and Holocene palaeohydrology of Lake Rukwa, Tanzania, inferred from diatom analysis. Palaeogeography, Palaeoclimatology, Palaeoecology 187, 295-305.

Becht, R., Mwango, F., Muno, F.A., 2006. Groundwater links between Kenyan Rift Valley lakes. In: Proceedings of the 11th world lakes conference, 31 October - 4 November 2005. International Lake Environment Committee (ILEC), 2006. Vol. II. pp. 7-14.

Behr, H.-J., Röhricht, C., 2000. Record of seismotectonic events in siliceous cyanobacterial sediments (Magadi cherts), Lake Magadi, Kenya. International Journal of Earth Science 89, 268-283.

Behr, H.-J., 2002. Magadiite and Magadi chert: a critical analysis of the silica sediments in the Lake Magadi basin, Kenya. *In* Renaut, R.W., and Ashley, G.M., (Eds.), Sedimentation in Continental Rifts, SEPM Special Publication No. 73, p 257-273.

Behrensmeyer, A.K., 2008. Paleoenvironmental context of the Pliocene A.L. 333 “First Family” hominin locality, Hadar Formation, Ethiopia. Geological Society of America Special Paper 446, 203-214.

Behrensmeyer, A.K., Quade, J., Cerling, T.E., Kappelman, J., Khan, I.A., Copeland, P., Roe, L., Hicks, J., Stubblefield, P., Willis, B.J., Latorre, C., 2007. The structure and rate of late Miocene expansion of C_4 plants: Evidence from lateral variation in stable isotopes in paleosols of the Siwalik Group, northern Pakistan. GSA Bulletin 119, 1486-1505.

Berke, M.A., Johnson, T.C., Werne, J.P., Schouten, S., Sinninghe Damsté, J.P., 2012. A mid-Holocene thermal maximum at the end of the African Humid Period. Earth and Planetary Science Letters 351-352, 95-104

Bergner, A.G.N., Trauth, M.H., Bookhagen, B., 2003. Paleoprecipitation estimates for the Lake Naivasha basin (Kenya) during the last 175 k.y. using a lake-balance model. Global and Planetary Change 36, 117-136.

Bestland, E.A., Retallack, G.J., 1993. Volcanically influenced calcareous palaeosols, from the Miocene Kiahera Formation, Rusinga Island, Kenya. Journal of the Geological Society, London 150: 293-310.

Binkley, K.L., Wilkinson, B.H., Owen, R.M., 1980. Vadose beachrock cementation along a Southeastern Michigan marl lake. Journal of Sedimentary Petrology 50, 953-962.

Bishop, W.W., 1966. Stratigraphical geomorphology. A review of some East African landforms. In: G.H. Dury (Ed.), Essays in Geomorphology, American Elsevier Pub. Co., London, pp. 139–176.

Bobe, R., 2006. The evolution of arid ecosystems in eastern Africa. Journal of Arid Environments 66, 564-584.

Bonny, S.M., Jones, B.,2008a. Controls on the precipitation of barite ($BaSO_4$) crystals in calcite travertine at Twitya Spring, a warm sulphur spring in Canada's Northwest Territories. Sedimentary Geology 203, 36-53.

Bonny, S.M., Jones, B., 2008b. Experimental precipitation of barite ($BaSO_4$) among streamers of sulfur-oxidizing bacteria. Journal of Sedimentary Research 78, 357-365.

Brasier, A.T., 2011. Searching for travertines, calcretes and speleothems in deep time: Processes, appearances, predictions and the impact of plants. Earth-Science Reviews 104, 213-239.

Brock-Hon, A.L., Robins, C.R., Buck, B.J., 2012. Micromorphological investigation of pedogenic barite in Mormon Mesa petrocalcic horizons, Nevada USA: Implications for genesis. Geoderma 179-180, 1-8.

Brooks, A.S., Helgren, D.M., Cramer, J.S., Franklin, A., Hornyak, W., Keating, J.M., Klein, R.G., Rink, W.J,. Schwarcz, H., Leith Smith, J.N., Stewart, K., Todd, B.E., Verniers, J., and Yellen, J.E., 1995. Dating and context of three Middle Stone Age Sites with bone points in the Upper Semliki Valley, Zaire. Science 268, 548-553.

Budd, D.A., Pack, S.M., Fogel, M.L., 2002. The destruction of paleoclimatic isotopic signals in Pleistocene carbonate soil nodules of Western Australia. Palaeogeography, Palaeoclimatology, Palaeoecology 188, 249-273.

Bustillo, M.A., Alonso-Zarza, A.M., 2007. Overlapping of pedogenesis and meteoric diagenesis in distal alluvial and shallow lacustrine deposits in the Madrid Miocene Basin, Spain. Sedimentary Geology 198, 255-271.

Brenna, B.L, Renaut, R.W., Owen, R.B., 2014. The chemical, physical and microbial origins of Pleistocene cherts at Lake Magadi, Kenya Rift Valley. Abstracts with Programs, Geological Society of America, 46, 747

Burke, R.B., Gerhard, L.C., 2000. Aragonite cementation and related sedimentary structures in Quaternary lacustrine deposits, Great Salt Lake, Utah. *In* King, J.K., Willis, G.C. (Eds.) The Geology of Antelope Island, Davis County, Utah. Utah Geological Survey Miscellaneous Publication 00-1. pp 99-115.

Butzer, K.W., Isaac, G.L., Richardson, J.L., Washbourn-Kamau, C., 1972. Radiocarbon dating of East African Lake Levels. Science 175 (4026), 1069-1076.

Candy, I., Black, S., Sellwood, B.W., Rowan, J.S., 2003. Calcrete profile development in Quaternary alluvial sequences, southeast Spain: Implications for using calcretes as a basis for landform chronologies. Earth Surface Processes and Landforms 28, 169-185.

Capo, R.C., Chadwick, O.A., 1999. Sources of strontium and calcium in desert soil and calcrete. Earth and Planetary Science Letters 170, 61-72.

Carlisle, D., 1983. Concentration of uranium and vanadium in calcretes and gypcretes. Geological Society, London, Special Publications 11, 185-195.

Carozzi, A.V., 1993. Sedimentary petrology. Prentice Hall, New Jersey. 263 p.

Casanova, J., Tiercelin, J-J., 1982. Constructions stromatolitiques en milieu carbonate sodique: les oncolites des plaines inondables du lac Magadi (Kenya). C.R. Acad. Sc. Paris 295, 1139-1144.

Cerling, T.H., 1984. The stable isotopic composition of modern soil carbonate and its relationship to climate. Earth and Planetary Science Letters 71, 229-240.

Cerling, T.E., 1992. Development of grasslands and savannas in East Africa during the Neogene. Palaeogeography, Palaeoclimatology, Palaeoecology 97, 241-247.

Cerling, T.E., 1994. Lake Turkana and its precursors in the Turkana Basin, East Africa (Kenya and Ethiopia). . In Gierlowski-Kordesch, E., Kelts, K., (Eds.), Global Geological Record of Lake Basins; Volume 1. Cambridge University Press, Cambridge, UK. pp. 341-344.

Cerling, T.E. Hay, R.L., 1986. An isotopic study of paleosol carbonates from Olduvai Gorge. Quaternary Research 25, 63-78.

Cerling, T.E., Hay, R.L., O'Neil, J.R., 1977. Isotopic evidence for dramatic climatic changes in East Africa during the Pleistocene. Nature 267, 137-138.

Cerling, T.E., Bowman, J.R., and O`Neil, J.R., 1988. An isotopic study of a fluvial-lacustrine sequence: The Plio-Pleistocene Koobi Fora Sequence, East Africa. Palaeogeography, Palaeoclimatology, Palaeoecology 63, 335-356.

Chiquet, A., Michard, A., Nahon, D., Hamelin, B., 1990. Atmospheric input vs in situ weathering in the genesis of calcretes: an Sr isotope study at Galvez (Central Spain). Geochimica et Cosmochimica Acta 63, 311-323.

Chorowicz, J., 2005. The East African rift system. Journal of African Earth Sciences 43, 379-410.

Climate Data. <http://www.climatedata.eu > accessed 14 Jun 2011.

Cohen, A.S., 1982. Palaeoenvironments of root casts from the Koobi Fora Formation, Kenya. Journal of Sedimentary Petrology 52, 401-414.

Cohen, A.S., Thouin, C., 1987. Nearshore carbonate deposits in Lake Tanganyika. Geology 15, 414-418.

Colson, J., Cojan, I., 1996. Groundwater dolocretes in a lake-marginal environment: an alternative model for dolocrete formation in continental settings (Danian of the Provence Basin, France). Sedimentology 43, 175-188.

Compton, J.S., White, R.A., Smith, M., 2003. Rare earth element behavior in soils and salt pan sediments of a semi-arid granitic terrain in the Western Cape, South Africa. Chemical Geology 201, 239-255.

Coplen, T.B., 2007. Calibration of the calcite – water oxygen-isotope geothermometer at Devils Hole, Nevada, a natural laboratory. Geochimica et Cosmochimica Acta 71, 3948-3957.

Craig, H., 1957. Isotopic standards for carbon and oxygen and correction factors for mass-spectrometric analysis of carbon dioxide. Geochimica et Cosmochimica Acta 12, 133-149.

Damnati, B., Taieb, M., Williamson, D., 1992. Laminated deposits from Lake Magadi (Kenya). Climatic contrast effect during the maximum wet period between 12,000-10,000 yrs B.P. Bull. Soc. géol. France 163, 407-414.

Darling, W.G., 2001. Magadi and Suguta: the contrasting hydrogeochemistry of two soda lake areas in the Kenya Rift Valley. Water-Rock interaction : proceedings of the tenth international symposium on water-rock interaction : WRI-10, Villasimius, Italy, 10.-15. July 2001, pp. 95-98.

Darlington, J.P.E.C., 2011. Trace fossils interpreted in relation to the extant termite fauna at Laetoli, Tanzania *in* T. Harrison (Ed.), Palaeontology and Geology of Laetoli: Human

Evolution in Context. Volume 2: Fossil Hominins and the Associated Fauna, Vertebrate Paleobiology and Palaeoanthropology, Springer, pp 555-565.

Davis, L.E., 2012. An astrobiological study of an alkaline-saline hydrothermal environment, relevant to understanding the habitability of Mars. PhD Thesis, University College London.

Dawson, J.B., 1964. Carbonatitic volcanic ashes in Northern Tanganyika. Bulletin Volcanologique 27, 81-91.

Dawson, J.B., 1992. Neogene tectonics and volcanicity in the North Tanzania sector of the Gregory Rift Valley: contrasts with the Kenya sector. Tectonophysics 204, 81-92.

Dawson, J.B., 2008. The Gregory Rift Valley and Neogene–Recent Volcanoes of Northern Tanzania. Geological Society, London, Memoirs 33, 91 p.

de Cort, G., Bessems, I., Keppens, E., Mees, F., Cumming, B., Verschuren, D., 2013. Late-Holocene and recent hydroclimatic variability in the central Kenya Rift Valley: The sediment record of hypersaline lakes Bogoria, Nakuru and Elementeita. Palaeogeography, Palaeoclimatology, Palaeoecology 388, 69-80.

Deino, A., Potts, R., 1992. Age-Probability spectra for examination of single-crystal $^{40}Ar/^{39}Ar$ dating results: examples from Olorgesailie, southern Kenya rift. Quaternary International 13/14, 47-53.

de la Torre, I., Mora, R., Martinez-Moreno, J., 2008, The early Acheulean in Peninj (Lake Natron, Tanzania). Journal of Anthropological Archaeology 27, 244-264.

de Menocal, P., Ortiz, J., Guilderson, T., Sarnthein, M., 2000. Coherent high- and low-latitude climate variability during the Holocene warm period. Science 288, 2198-2202.

Deocampo, D.M., 2004. Authigenic clays in East Africa: Regional trends and paleolimnology at the Plio-Pleistocene boundary, Olduvai Gorge, Tanzania. Journal of Paleolimnology 31, 1-9.

Deocampo, D.M., Behrensmeyer, A.K., Potts, R., 2010. Ultrafine clay minerals of the Pleistocene Olorgesailie Formation, Southern Kenya Rift: Diagenesis and paleoenvironments of early hominins. Clays and Clay Minerals 58, 294-310.

Deutz, P., Montañez, Monger, H.C., Morrison, J., 2001. Morphology and isotope heterogeneity of Late Quaternary pedogenic carbonates: Implications for paleosol carbonates as paleoenvironmental proxies. Palaeogeography, Palaeoclimatology, Palaeoecology 166, 293-317.

Dietzel, M., Tang, J., Leis, A., Köhler, S.J., 2009. Oxygen isotope fractionation during inorganic calcite precipitation—Effects of temperature, precipitation rate and pH. Chemical Geology 268, 107-115.

Diez Martín, F., Luque, L., Domínguez-Rodrigo, M., 2009. ST-69: an Acheulean assemblage in the Moinik Formation of Type Section of Peninj (Lake Natron, Tanzania). In: Domínguez-Rodrigo, M., Alcalá, L., Luque, L. (Eds.), Peninj. A research project on the archaeology of human origins (1995-2005). Oxbow, Cambridge, pp. 193–206.

Ditchfield, P., Harrison, T., 2011. Sedimentology, lithostratigraphy and depositional history of the Laetoli Area, *in* Harrison, T., (Ed.), Paleontology and Geology of Laetoli: Human Evolution in Context, Volume 1: Geology, Geochronology, Paleoecology and Paleoenvironment, Vertebrate Paleobiology and Paleoanthropology, pp 47-76.

Dodson, R. G., 1963. Geology of the South Horr area: degree sheet 19, south-east quarter (with two coloured geological maps) (No. 60). Geological Survey of Kenya.

Dominiguez-Rodrigo, M., de la Torre, I., de Luque, L., Alcala, L., Mora, R., Serrallonga, J., & Medina, V., 2002. The ST site complex at Peninj, West Lake Natron, Tanzania: Implications for early hominid behavioural models, Journal of Archaeological Science 29, 639-665.

Dunningham, J.P., 2005. Long-term Evolution of Normal Fault Systems: Controls on the Development and Evolution of Extensional Structures in the Neotectonic Kenyan Rift, East Africa. PhD thesis, University of Edinburgh.

Dworkin, S.I., Nordt, L., Atchley, S., 2005. Determining terrestrial paleotemperatures using the oxygen isotopic composition of pedogenic carbonate. Earth and Planetary Science Letters 237, 56-68.

Dypvik, H., Hankel, O., Nilsen, O., Kaaya, C., Kilembe, E., 2001. The lithostratigraphy of the Karoo Supergroup in the Kilombero Rift Valley, Tanzania. Journal of African Earth Sciences 32, 451-470.

Dypvik, H., Nilsen, O., 2002. Rift valley sedimentation and diagenesis, Tanzanian Examples – A review. South African Journal of Geology 105, 93-106.

Ebinger, C., Poudjom Djomani, Y., Mbede, E., Foster, A., Dawson, J.B., 1997. Rifting Archaean lithosphere: the Eyasi-Manyara-Natron rifts, East Africa. Journal of the Geological Society, London 154, 947-960.

Erginal, A.E., Kiyak, N.G., Öztürk, M.Z., Avcioğlu, M., Bozcu, M., Yiğitbaş, E., 2012. Cementation characteristics and age of beachrocks in a fresh-water environment, Lake İznik, NW Turkey. Sedimentary Geology 243-244, 148-154.

Esteban, M. Klappa, C.F., 1983. Subaerial exposure environments. In Scholle, P.A., Bebout, D.G., Moore, C.H. (Eds.), Carbonate depositional environments. AAPG Memoir 33, 1-54.

Eugster, H.P., 1967. Hydrous sodium silicates from Lake Magadi, Kenya: Precursors of bedded chert. Science 157(3793), 1177-1180.

Eugster, H.P., Jones, B.F., 1968. Gels composed of sodium-aluminum silicate, Lake Magadi, Kenya. Science 161(3837), 160-163.

Eugster, H.P., 1970. Chemistry and origin of the brines of Lake Magadi, Kenya. Special Paper – Mineralogical Society of America, 3, 213-235.

Eugster, H.P., 1980. Lake Magadi, Kenya, and its precursors. *in* Nissenbaum, A (Ed.), Hypersaline Brines and Evaporitic Environments, Proceedings of the Bat Sheva Seminar on Saline Lakes and Natural Brines. Elsevier, Developments in Sedimentology 28, 195-232.

Eugster, H.P., 1986. Lake Magadi, Kenya: a model for rift valley hydrochemistry and sedimentation? *In* Frostick, L.E. et al. (Eds) Sedimentation in the African Rifts, Geological Society Special Publication No. 25, 177-189.

Fairhead, J.D., Mitchell, J.G., Williams, L.A.J., 1972. New K/Ar determinations on rift volcanics of S. Kenya and their bearing on age of rift faulting. Nature 238, 66-69.

Fordham, A.M., North, C.P., Hartley, A.J., Archer, S.G., Warwick, G.L., 2010. Dominance of lateral over axial sedimentary fill in dryland rift basins. Petroleum Geoscience 16, 299-304.

Fralick, P., 2003. Geochemistry of clastic sedimentary rocks: ratio techniques. In Lentz, D.R., (Ed.), Inorganic Geochemistry of Sediments and Sedimentary Rocks: Evolutionary Considerations to Mineral Deposit-Forming Environments. Geological Association of Canada, Geotext 4, p. 85-103.

Friedman, I. O'Neil, J,R., 1977. Compilation of stable isotope fractionation factors of geochemical interest. U.S. Geological Survey Professional Paper. 12pp.

Gabitov, R.I., Watson, E.B., Sadekov, A., 2012. Oxygen isotope fractionation between calcite and fluid as a function of growth rate and temperature: An in situ study. Chemical Geology 306-307, 92-102.

Garcin, Y., Melnick, D., Strecker, M.R., Olago, D., Tiercelin, J-J., 2012. East African mid-Holocene wet-dry transition recorded in paleo-shorelines of Lake Turkana, northern Kenya Rift. Earth and Planetary Science Letters 331-332, 322-334.

Gasse, F., 2000. Hydrological changes in the African tropics since the Last Glacial Maximum. Quaternary Science Reviews 19, 189-211.

Gasse, F. 1977., Evolution of Lake Abhé (Ethiopia and TFAI), from 70,000 b.p. Nature 265, 42-45.

Gathogo, P.N., Brown, F.H., 2006. Stratigraphy of the Koobi Fora Formation (Pliocene and Pleistocene) in the Ileret region of northern Kenya. Journal of African Earth Sciences 45, 369-390

Genise, J.F., Alonso-Zarza, A.M., Verde, M, Meléndez, A., 2013. Insect trace fossils in aeolian deposits and calcretes from the Canary Islands: Their ichnotaxonomy, producers, and palaeoenvironmental significance. Palaeogeography, Palaeoclimatology, Palaeoecology 377, 110-124.

Gikunju, J.K., Maitho, T.E., Birkeland, J.M., and Lokken, P., 1992. Fluoride levels in water and fish from Lake Magadi (Kenya). Hydrobiologia 234, 123-127.

Gile, L.H., Peterson, F.F., Grossman, R.B., 1966. Morphological and genetic sequences of carbonate accumulation in desert soils. Soil Science 101, 347-360.

Gillespie, R., Street-Perrott, F.A., Switsur, R., 1983. Post-glacial arid episodes in Ethiopia have implications for climate prediction. Nature 306, 680-683.

Goetz, C., Hillaire-Marcel, C., 1992. U-series disequilibria in early diagenetic minerals from Lake Magadi sediments, Kenya: Dating potential. Geochimica et Cosmochimica Acta 56, 1331-1341.

Goudie, A., 1973. Duricrusts in Tropical and Subtropical Landscapes. Clarendon Press; Oxford Research Studies in Geography. 174 p.

Goudie, A. 1983. Calcrete. In: Goudie, A.S., Pye, K., (Eds.), Chemical Sediments and Geomorphology. London, Academic Press. pp93-131.

Grove, A.T., Alayne, Street, F., Goudie, A.S., 1975. Former lake levels and climatic change in the rift valley of southern Ethiopia. The Geographical Journal 141(2), 177-194.

Grotzinger, J.P., Rothman, D.H., 1996. An abiotic model for stromatolite morphogenesis, Nature 383, 423-425.

Guth, A., Wood, J., 2013. Geological Map of the Southern Kenya Rift. The Geological Society of America, Map DMCH016.

Hailemichael , M., Aronson, J.L., Savin, S., Tevesz, M.J.S., Carter, J.G., 2002. $D^{18}O$ in mollusk shells from Pliocene Lake Hadar and modern Ethiopian lakes: implications for history of the Ethiopian monsoon. Palaeogeography, Palaeoclimatology, Palaeoecology 186, 81-99.

Halldórsson, S.A., Hilton, D.R., Scarsi, P., Abebe, T., Hopp, J., 2014. A common mantle plume source beneath the entire East African Rift System revealed by coupled helium-neon systematic. Geophysical Research Letters, 41, 2304-2311.

Harrison, T., 2011. Laetoli Revisited: Renewed paleontological and geological investigations at localities on the Eyasi Plateau in Northern Tanzania, *in* Harrison, T., (Ed.), Paleontology and Geology of Laetoli: Human Evolution in Context, Volume 1: Geology, Geochronology, Paleoecology and Paleoenvironment, Vertebrate Paleobiology and Paleoanthropology, pp 1-15.

Harrison, T., Kweka, A., 2011, Paleontological Localities on the Eyasi Plateau, Including Laetoli, *in* Harrison, T., (Ed.), Paleontology and Geology of Laetoli: Human Evolution in Context, Volume 1: Geology, Geochronology, Paleoecology and Paleoenvironment, Vertebrate Paleobiology and Paleoanthropology, pp 17-45.

Hay, R.L., 1968. Chert and its sodium-silicate precursors in sodium-carbonate lakes of East Africa. Contributions to Mineralogy and Petrology 17, 255-274.

Hay, R.L., Kyser, T.K., 2001, Chemical sedimentology and paleoenvironmental history of Lake Olduvai, a Pliocene lake in northern Tanzania. GSA Bulletin 112, 1505-1521.

Hay, R.L., Reeder, R.J., 1978, Calcretes of Olduvai Gorge and the Ndolanya Beds of northern Tanzania. Sedimentology 25, 649-673.

Hillaire-Marcel, C., Casanova, J., 1987. Isotopic hydrology and paleohydrology of the Magadi (Kenya)-Natron (Tanzania) Basin during the Late Quaternary, Palaeogeography, Palaeoclimatology, Palaeoecology 58, 155-181.

Ibs-von Seht, M., Blumenstein, S., Wagner, R., Hollnack, D., Wohlenberg, J., 2001. Seismicity, seismotectonics and crustal structure of the southern Kenya Rift—new data from the Lake Magadi area. Geophysical Journal International 146, 439-453.

Isaac, G.Ll.,1965. An annotated list of the most important palaeontological (mammalian) and archaeological assemblages associated with the rift valleys of Kenya. Report on the Geology and Geophysics of the East African Rift System, pp. 44-49.

Isaac, G.Ll., 1967. The stratigraphy of the Peninj group; early middle Pleistocene formations west of Lake Natron, Tanzania. In: Bishop, W.W. and Clarke, J.D., (Eds.), Background to Evolution in Africa, University of Chicago Press, pp. 229-257.

Isaac, G.Ll., 1977. Olorgesailie: Archeological Studies of a Middle Pleistocene Lake Basin in Kenya. Chicago: University of Chicago Press. 272 p.

Isaac, G.Ll., 1978. The Olorgesailie Formation: Stratigraphy, tectonics and the palaeogeographic context of the Middle Pleistocene archaeological sites. In Bishop, W.W. (Ed.),

Geological Background to Fossil Man: Recent Research in the Gregory Rift Valley, East Africa, Geological Society, London, Special Publications v.6, 173-206.

IUSS Working Group WRB, 2015, World Reference Base for Soil Resources 2014, update 2015 International soil classification system for naming soils and creating legends for soil maps. World Soil Resources Reports No. 106. FAO, Rome.

Johannesson, K.H., Lyons, W.B., 1994. The rare earth element geochemistry of Mono Lake Water and the importance of carbonate complexing. Limnology and Oceanography 39, 1141-1154.

Johnson, C.R., Ashley, G.M., De Wet, C.B., Dvoretsky, R., Park, L., Hover, V.C., Owen, R.B., McBrearty, S., 2009. Tufa as a record of perennial fresh water in a semi-arid rift basin, Kapthurin Formation, Kenya. Sedimentology 56, 1115-1137.

Jolly, D., Harrison, S.P., Damnati, B., Bonnefille, R., 1998. Simulated climate and biomes of Africa during the Late Quaternary: Comparison with pollen and lake status data. Quaternary Science Reviews 17, 629-657.

Jones, B.F., Rettig, S.L., Eugster, H.P., 1967. Silica in alkaline brines. Science 158, 1310-1314.

Jones, B.F., Eugster, H.P., Rettig, S.L., 1977. Hydrochemistry of the Lake Magadi Basin, Kenya. Geochimica et Cosmochimica Acta 41, 53-72.

Jones, B., Rosen, M.R., Renaut, R.W., 1997. Silica-cemented beachrock from Lake Taupo, North Island, New Zealand. Journal of Sedimentary Research 67, 805-814.

Jones, B.E., Grant, W.D., Duckworth, A.W., Owenson, G.G., 1998. Microbial diversity of soda lakes. Extremophiles 2, 191-200.

Jutras, P, Utting, J., McLeod, J., 2007. Link between long-lasting evaporitic basins and the development of thick and massive phreatic calcrete hardpans in the Mississippian Windsor and Percé groups of eastern Canada. Sedimentary Geology 201, 75-92.

Kabanov, P. Anadón, P., Krumbein, W.E., 2008. *Microcodium*: An extensive review and a proposed non-rhizogenic biologically induced origin for its formation. Sedimentary Geology 205, 79-99.

Kaemmerer, M., Revel, J.C., 1999. New data on the laminar horizon genesis of calcrete developed on Morocco coarse quaternary alluvium: Consequences on the desertification process. Arid Soil Research and Rehabilitation 10, 107-123.

Keller, J. Zaitsev, A.N., 2006. Calciocarbonatite dykes at Oldoinyo Lengai, Tanzania: the fate of natrocarbonatite. Canadian Mineralogist 44, 857-876.

Kerrich, R., Renaut, R.W., Bonli, T., 2002. Trace-element composition of cherts from alkaline lakes in the East African Rift: A probe for ancient counterparts. *In* Renaut, R.W., and Ashley, G.M., (Eds.), Sedimentation in Continental Rifts, SEPM Special Publication No. 73, 275-294.

Klappa, C.F., 1979. Calcified filaments in Quaternary calcretes: Organo-mineral interactions in the subaerial vadose environment. Journal of Sedimentary Petrology 49, 955-968.

Khalaf, F.I., 2007. Occurrences and genesis of calcrete and dolocrete in the Mio-Pleistocene fluviatile sequence in Kuwait, northeast Arabian Peninsula. Sedimentary Geology 199, 129-139.

Kidney, C.L., 2012. Pliocene Stratigraphy and Geology of the Northeastern Ileret Region, Kenya. MSc Thesis. University of Utah.

Košir, A., 2004. *Microcodium* revisited: root calcification products of terrestrial plants on carbonate-rich subsrates. Journal of Sedimentary Research 74, 845-857.

Kraus, M.J., 1999. Paleosols in clastic sedimentary rocks: their geologic applications. Earth-Science Reviews 47, 41-70.

Krumbein, W.E., Giele, C., 1979. Calcification in a coccoid cyanobacterium associated with the formation of desert stromatolites. Sedimentology 26, 593-604.

Last, F.M., Last, W.M., Halden, N.M., 2010. Carbonate microbialites and hardgrounds from Manito Lake, an alkaline, hypersaline lake in the northern Great Plains of Canada. Sedimentary Geology 225, 34-49.

Last, W.M., De Deckker, P., 1990. Modern and Holocene carbonate sedimentology of two saline volcanic maar lakes, southern Australia. Sedimentology 37, 967-981.

Leakey, L.S.B., Leakey, M.D., 1964. Recent discoveries of fossil hominids in Tanganyika: At Olduvai and near Lake Natron. Nature 202, 5-7.

Lee, R.K.L., Owen, R.B., Renaut, R.W., Behrensmeyer, A.K., Potts, R., Sharp, W.D., 2013. Facies, geochemistry and diatoms of late Pleistocene Olorgesailie tufas, southern Kenya Rift. Palaeogeography, Palaeoclimatology, Palaeoecology 374, 197-217.

Le Gall, B., Nonnotte, P., Rolet, J., Benoit, M., Guillou, H., Mousseau-Nonnotte, Albaric, J., Deverchère, J., 2008. Rift propagation at craton margin. Distributions of faulting and volcanism in the North Tanzanian Divergence (East Africa) during Neogene times. Tectonophysics 448, 1-19.

Lentz, D.R., 2003. Geochemistry of sediments and sedimentary rocks: historical to research perspectives, *in* Lentz, D.R., (Ed.), Inorganic Geochemistry of Sediments and

Sedimentary Rocks: Evolutionary Considerations to Mineral Deposit-Forming Environments: Geological Association of Canada, Geotext 4, p. 1-6

Le Roex, A.P., Späth, A., Zartman, R.E., 2001. Lithospheric thickness beneath the southern Kenya Rift: implications from basalt geochemistry. Contributions to Mineralogy and Petrology 142, 89-106.

Le Turdu, C., Tiercelin, J.J., Coussement, C., Rolet, J., Renaut, R.W., Richert, J.P., Xavier, J.P., Coquelet, D. 1995. Basin structure and depositional pattern interpreted using a 3D remote sensing approach: the Baringo-Bogoria basins, central Kenya Rift, East Africa. Bulletin des Centre de Recherche Exploration-Production Elf-Aquitaine, 19, 1-37.

Levin, N.E., Quade, J., Simpson, S.W., Semaw, S., Rogers, M., 2004. Isotopic evidence for Plio-Pleistocene environmental change at Gona, Ethiopia. Earth and Planetary Science Letters 219, 93-110.

Levin, N.E., Zipser, E.J., Cerling, T.E., 2009. Isotopic composition of waters from Ethiopia and Kenya: Insights into moisture sources for eastern Africa. Journal of Geophysical Research 114, D23306, 13 p.

Levin, N.E., Brown, F.H., Behrensmeyer, A.K., Bobe, R., Cerling, T.E., 2011. Paleosol carbonates from the Omo Group: Isotopic records of local and regional environmental change in East Africa. Palaeogeography, Palaeoclimatology, Palaeoecology 307, 75-89.

Mace, W.D., 2012. Environmental differences in tropical soil temperatures in Kenya. Unpublished MSc thesis. University of Utah. 116 pp.

Machette, M.N., 1985. Calcic soils of the southwestern United States. *In* Weide, D.L. (Ed.), Soils and Quaternary geology of the southwestern United States: Geological Society of American Special Paper 203, 1-2.1

Melson, W.G. Potts, R., 2002, Origin of reddened and melted zones in Pleistocene sediments of the Olorgesailie Basin, Southern Kenya Rift. Journal of Archaeological Science 29, 307-316.

McCall, J., 2010. Lake Bogoria, Kenya: Hot and warm springs, geysers and Holocene stromatolites. Earth-Science Reviews 103, 71-79.

McCall, G.J.H., Baker, B.H., and Walsh, J., 1967. Late Tertiary and Quaternary sediments of the Kenya Rift Valley. *In* Bishop, W.W., Clark, J.D., (Eds.), Background to evolution in Africa. University of Chicago Press, Chicago. pp. 191-220.

McConnell, R.B., 1972. Geological Development of the Rift System of Eastern Africa. Geological Society of America Bulletin 83, 2549-2572.

McLaren, S., 2004. Characteristics, evolution and distribution of Quaternary channel calcretes, southern Jordan. Earth Surface Processes and Landforms 29, 1487-1507.

McLennan, S.M., Bock, B., Hemming, S.R., Hurowitz, J.A., Lev, S.M., McDaniel, D.K., 2003, The roles of provenance and sedimentary processes in the geochemistry of sedimentary rocks, in Lentz, D.R., (Ed.), Inorganic Geochemistry of Sediments and Sedimentary Rocks: Evolutionary Considerations to Mineral Deposit-Forming Environments: Geological Association of Canada, Geotext 4, 7-38.

McPherson, J.G., 1979. Calcrete (caliche) palaeosols in fluvial redbeds of the Aztec Siltstone (Upper Devonian), southern Victoria Land, Antarctica. Sedimentary Geology 22, 267-285.

Monger, H.C., Daugherty, L.A., Lindemann, W.C., Liddell, C.M., 1991. Microbial precipitation of pedogenic calcite. Geology 19, 997-1000.

Mount, J.F. Cohen, A.S., 1984. Petrology and geochemistry of rhizoliths from Plio-Pleistocene fluvial and marginal lacustrine deposits, east Lake Turkana, Kenya. Journal of Sedimentary Petrology 54, 263-275.

Mpawenayo, B. Mathooko, J.M., 2005. The structure of diatom assembleges associated with *Cladophora* and sediments in a highland stream in Kenya. Hydrobiologia 544, 55-67.

Mulwa, J.K., Kimata, F., Suzuki, S., Kuria, Z.N., 2014. The seismicity in Kenya (East Africa) for the period 1906-2010; a review. Journal of African Earth Sciences 89, 72-78.

Mwatha, W.E., Grant, W.D., 1993. *Natronobacterium vacuolata* sp. nov., a Haloalkaliphilic Archaeon Isolated from Lake Magadi, Kenya. International Journal of Systematic Bacteriology 43, 401-404.

Naiman, Z., Quade, J., Patchett, P.J., 2000. Isotopic evidence for eolian recycling of pedogenic carbonate and variations in carbonate dust sources throughout the Southwest United States. Geochimica et Cosmochimica Acta 64, 3099-3109.

Nash, D.J., Smith, R.F., 1998. Multiple calcrete profiles in the Tabernas Basin, southeast Spain: their origins and geomorphic implications. Earth Surface Processes and Landforms 23, 1009-1029.

Nash, D.J., McLaren, S.J., 2003. Kalahari valley calcretes: their nature, origins, and environmental significance. Quaternary International 111, 3-22.

Nash, D.J., Smith, R.F., 2003. Properties and development of channel calcretes in a mountain catchment, Tabernas Basin, southeast Spain. Geomorphology 50, 227-250.

Naujoks, M., Jahr, T., Jentzsch, Kurz, J.H., Hofman, Y., 2007. Investigations about earthquake swarm areas and processes, *in* Tregoning, P., Rizos, C. (Eds.), Dynamic Planet:

Monitoring and Understanding a Dynamic Planet with Geodetic and Oceanographic Tools, IAG Symposium, Cairns, Australia, Springer, p 528-535.

Nehza, O., Woo, K.S., Lee, K.C., 2009. Combined textural and stable isotopic data as proxies for the mid-Cretaceous paleoclimate: A case study of lacustrine stromatolites in the Gyeongsang Basin, SE Korea. Sedimentary Geology 214, 85-99.

Nielsen, J.M., 1999. East African magadi (trona): fluoride concentration and mineralogical composition. Journal of African Earth Sciences 29, 423-428.

Neumeier, U., 1999. Experimental modelling of beachrock cementation under microbial influence. Sedimentary Geology 126, 35-46.

Nordt, L.C., Hallmark, C.T., Wilding, L.P., Boutton, T.W., 1998. Quantifying pedogenic carbonate accumulations using stable carbon isotopes. Geoderma 82, 115-136.

Nordt, L., Orosz, M., Driese, S., Tubbs, J., 2006. Vertisol carbonate properties in relation to mean annual precipitation: implications for paleoprecipitation estimates. Journal of Geology 114, 501-510.

Nyamweru, C.K., 1986. Quaternary environments of the Chalbi basin, Kenya: sedimentary and geomorphological evidence. In Frostick, L.E. et al. (Eds.) 1986, Sedimentation in the African Rifts, Geological Society Special Publication No. 25, 297-310.

Nyblade, A.A., 2011. The upper-mantle low-velocity anomaly beneath Ethiopia, Kenya, and Tanzania: Constraints on the origin of the African superswell in eastern Africa and plate versus plume models of mantle dynamics. Geological Society of America Special Papers 478, 37-50.

Ogola, J.S., Behr, H.J., 2000. Mineralogy and trona formation in Lake Magadi, Kenya. In Rammlmair, D. et al. (Eds.), Applied Mineralogy in Research, Economy, Technology, Ecology and Culture: Proceedings of the Sixth International Congress on Applied Mineralogy : Göttingen, Germany, 17-19 July 2000, A.A. Balkema, Rotterdam, 383-386.

Olaka, L.A., Odada, E.O., Trauth, M.H., Olago, D.O., 2010. The sensitivity of East African rift lakes to climate fluctuations. Journal of Paleolimnology 44, 629-644.

Owen, R.B., Renaut, R.W., 1981. Palaeoenvironments and sedimentology of the middle Pleistocene Olorgesailie Formation, southern Kenya Rift valley. Palaeoecology of Africa and of the Surrounding Islands and Antarctica 13, 147-174.

Owen, R.A. Owen, R.B., Renaut, R.W., Scott, J.J., Jones, B., Ashley, G.M., 2008a. Mineralogy and origin of rhizoliths on the margins of saline, alkaline Lake Bogoria, Kenya Rift Valley. Sedimentary Geology 203, 143-163.

Owen, R.B., Potts, R., Behrensmeyer, A.K., Ditchfield, P., 2008b. Diatomaceous sediments and environmental change in the Pleistocene Olorgesailie Formation, southern Kenya Rift Valley. Palaeogeography, Palaeoclimatology, Palaeoecology 269, 17-37.

Owen, R.B., Renaut, R.W., Scott, J.J., Potts, R., Behrensmeyer, A.K., 2009. Wetland sedimentation and associated diatoms in the Pleistocene Olorgesailie Basin, southern Kenya Rift Valley. Sedimentary Geology 222, 124-137.

Owen R.B., Renaut, R.W., Potts, R., Behrensmeyer, A.K., 2011. Geochemical trends through time and lateral variability of diatom floras in the Pleistocene Olorgesailie Formation, southern Kenya Rift Valley. Quaternary Research 76, 167-179.

Owen, R.B., Renaut, R.W., Behrensmeyer, A.K., Potts, R., 2014. Quaternary geochemical stratigraphy of the Kedong-Olorgesailie section of the southern Kenya Rift valley. Palaeogeography, Palaeoclimatology, Palaeoecology 396, 194-212.

Passey, B.H., Levin, N.E., Cerling, T.E., Brown, F.H. Eiler, J.M., 2010. High-temperature environments of human evolution in East Africa based on bond ordering in paleosol carbonates. PNAS 107 11245-11249.

Peterson, T.D., 1989. Peralkaline nephelinites. I. Comparative petrology of Shombole and Oldoinyo L'Engai, East Africa. Contributions to Mineralogy and Petrology 101, 458-478.

Pickford, M., 1986. Sedimentation and fossil preservation in the Nyanza Rift System, Kenya. In Frostick, L.E. et al. (Eds.) 1986, Sedimentation in the African Rifts, Geological Society Special Publication No. 25, 345-362.

Pickford, M., 1985. A New Look at *Kenyapithecus* based on recent discoveries in Western Kenya. Journal of Human Evolution 14, 113-143.

Pimentel, N.L., Wright, V.P., Azevedo, T.M., 1996. Distinguishing early groundwater alteration effects from pedogenesis in ancient alluvial basins: examples from the Palaeogene of southern Portugal. Sedimentary Geology 105, 1-10.

Potts, R., Shipman, P., Ingall, E., 1988. Taphonomy, paleoecology, and hominids of Lainyamok, Kenya. Journal of Human Evolution 17, 597-614.

Potts, R., Behrensmeyer, A.K., Ditchfield, P., 1999. Paleolandscape variation and Early Pleistocene hominid activities: Members 1 and 7, Olorgesailie Formation, Kenya. Journal of Human Evolution 37, 747-788.

Potts, R., Behrensmeyer, A.K., Deino, A., Ditchfield, P., Clark, J., 2004. Small Mid-Pleistocene Hominin Associated with East African Acheulean Technology. Science 305 (5680), 75-78.

Prodehl, C., Ritter, J.R.R., Mechie, J., Keller, G.R., Khan, M.A., Jacob, B., Fuchs, K., Nyambok, I.O., Obel, J.D., Riaroh, D., 1997. The KRISP 94 lithospheric investigation of southern Kenya – the experiments and their main results. Tectonophysics 278, 121-147.

Prudêncio, M.I., Dias, M.I., Waerenborgh, J.C., Ruiz, F., Trindade, M.J., Abad, M., Marques, R., Gouveia, M.A., 2011. Rare earth and other trace and major elemental distribution in a pedogenic calcrete profile (Slimene, NE Tunisia). Catena 87, 147-156.

Quade, J., Cerling, T.E., Bowman, J.R., 1989. Systematic variations in the carbon and oxygen isotopic composition of pedogenic carbonate along elevation transects in the southern Great Basin, United States. Geological Society of America Bulletin 101, 464-475.

Quade, J., Cerling, T.E., 1995. Expansion of C_4 grasses in the Late Miocene of Northern Pakistan: evidence from stable isotopes in paleosols. Palaeogeography, Palaeoclimatolgoy, Palaeoecology 112, 91-116.

Quinn, R.L., Lepre, C.J., Feibel, C.S., Wright, J.D., Mortlock, R.A., Harmand, S., Brugal, J-P., Roche, H., 2013. Pedogenic carbonate stable isotopic evidence for wooded habitat preference of early Pleistocene tool makers in the Turkana Basin. Journal of Human Evolution 65, 65-78.

Rabideaux, N.M., Deocampo, D.M., Potts, R., Behrensmeyer, A., Lowenstein, T.K., Renaut, R.W., Owen, R.B., Cohen, A.S., 2015. Zeolitic Alteration in saline, alkaline paleolake basins in the Southern Kenya Rift based on analysis of minerals from Koora Plain (ODP) and Lake Magadi (HSPDP) Core Samples. *In* Rosen, M.R., et al., (Eds.), Sixth International Limnogeology Congress—Abstract Volume, Reno, Nevada, June 15-19, 2015: U.S. Geological Survey Open-File Report 2015-1092, pp. 173-174.

Raidla, V., Kirismäe, K., Vaikmäe, R., Kaup, E., Martma, T., 2012. Carbon isotope systematics of the Cambrian-Vendian aquifer system in the northern Baltic Basin: Implications to the age and evolution of groundwater. Applied Geochemistry 27, 2042-2052.

Ramakrishnan, D., Tiwari, K.C., 1998. REE Chemistry of Arid zone calcrete profiles—A case study from the Thar desert, India. Tubitak: T. Jour. of Earth Sciences 7(2), 97-103.

Read, J.F., 1976. Calcretes and their distinction from stromatolites. In: Walter, M.R. (ed.) Stromatolites (Developments in Sedimentology 20). Elsevier, Amsterdam, pp. 55-72.

Reeves, C.C.Jr., 1975. Calcrete (caliche); its origin, morphology, and developmental history. AAPG Bulletin 59, 920-921.

Renaut, R.W., 1982. Late Quaternary geology of the Lake Bogoria fault-trough, Kenya Rift Valley. Unpublished PhD thesis, University of London, 498pp.

Renaut, R.W. Tiercelin, J-J., 1994. Lake Bogoria, Kenya Rift valley; a sedimentological overview. Special Publication – Society for Sedimentary Geology 50, 101-123.

Renaut, R.W., 1993. Zeolitic diagenesis of late Quaternary fluviolacustrine sediments and associated calcrete formation in the Lake Bogoria Basin, Kenya Rift Valley. Sedimentology 40, 271-301.

Renaut, R.W., Owen, R.B., Lowenstein, T.K., 2013. The recent sediments and hydrochemistry of Nasikie Engida; a perennial lake fed by hot springs in the semi-arid Magadi Basin, southern Kenya Rift valley. Abstracts – Colloquium of African Geology [CAG] 24, 111.

Renaut, R.W., Ego, J., Tiercelin, J.-J., Le Turdu, C., Owen, R.B. 1999. Saline, alkaline palaeolakes of the Tugen Hills-Kerio Valley region, Kenya Rift Valley. In: Banham, P. and Andrews, P. (Eds.) Late Cenozoic Environments and Hominid Evolution: A Tribute to Bill Bishop. Geological Society, London, p. 41-58.

Renaut, R.W., Tiercelin, J.J. Owen, R.B., 1986. Mineral precipitation and diagenesis in the sediments of the Lake Bogoria basin, Kenya Rift Valley. In Frostick, L.E. et al. (Eds.) 1986, Sedimentation in the African Rifts, Geological Society, London, Special Publications 25, 159-175

Retallack, G.J., Greaver, T., Jahren, A.H., 2007. Return to Coalsack Bluff and the Permian-Triassic boundary in Antarctica. Global and Planetary Change 55, 90-108.

Retallack, G.J., 2004. Pedogenic carbonate proxies for amount and seasonality of precipitation in paleosols. Geology 33, 333-336.

Retallack, G.J.,Wynn, J.G., Benefit, B.R., McCrossin, M.L., 2002. Palaeosols and palaeoenvironments of the middle Miocene, Maboko Formation, Kenya. Journal of Human Evolution 42, 659-703.

Retallack, G.J., 1994. The environmental factor approach to the interpretation of paleosols. In R. Amundson, J. Harden and M. Singer (Eds.), Factors in soil formation – a fiftieth anniversary perspective. Special Publication of the Soil Science Society of America, Madison, 33, 31-64.

Roberts, N., Taieb, M., Barker, P., Damnati, B., Icole, M., Williamson, D., 1993. Timing of the Younger Dryas event in East Africa from lake-level changes. Nature 366, 146-148.

Roberts, E.M., O'Connor, P.M., Stevens, N.J., Gottfried, M.D., Jinnah, Z.A., Choh, A.M., Armstrong, R.A., 2010. Sedimentology and depositional environments of the Red Sandstone Group, Rukwa Rift Basin, southwestern Tanzania: New insight into Cretaceous and Paleogene terrestrial ecosystems and tectonics in sub-equatorial Africa. Journal of African Earth Sciences 57, 179-212.

Roberts, E.M., O'Connor, P.M., Gottfried, M.D., Stevens, N., Kapalima, S., Ngasala, S., 2004. Revised stratigraphy and age of the Red Sandstone Group in the Rukwa Rift Basin, Tanzania. Cretaceous Research 25, 749-759.

Robinson, S.A., Andrews, J.E., Hesselbo, S.P., Radley, J.D., Dennis, P.F., Hardin, I.C., Allen, P., 2002. Atmospheric pCO_2 and depositional environment from stable-isotope geochemistry of calcrete nodules (Barremian, Lower Cretaceous, Wealden Beds, England). Journal of the Geological Society, London 159, 215-224.

Röhricht, C., 1999. Lithologie und Genese der Chertserien des Magadibeckens, Kenya. Dissertation, Univ Göttingen.

Rowe, P.J., Maher, B.A., 2000. 'Cold' stage formation of calcrete nodules in the Chinese Loess Plateau: evidence from U-series dating and stable isotope analysis. Palaeogeography, Palaeoclimatology, Palaeoecology 157, 109-125.

Saggerson, E.P., 1952. Government of Kenya; Ministry of Commerce and Industry, Geological Survey of Kenya; Geology of the Kisumu District, Degree Sheet 41, NE Quarter. Report No. 21, 1952.

Sakai, T., Saneyoshi, M., Tanaka, S., Sawada, Y., Nakatsukasa, M., Mbua, E., and Ishida, M., 2010. Climate shift recorded at around 10 Ma in Miocene succession of Samburu Hills, northern Kenya Rift, and its significance. Geological Society, London, Special Publications, 342, 109-127.

Schmalz, R.F., 1971. Formations of beachrock at Eniwetok Atoll. In, Bricker, O.P., (Ed.), Carbonate Cements. Johns Hopkins Press, Baltimore, pp. 17-24.

Scott, J.J., 2010. Saline lake ichnology: Composition and distribution of Cenozoic traces in the saline, alkaline lakes of the Kenya Rift Valley and Eocene Green River Formation, U.S.A. Unpublished PhD Thesis. University of Saskatchewan, Saskatoon, Saskatchewan. 526 pp.

Seegers, L. Tichy, H., 1999. The *Oreochromis alcalicus* flock (Teleostei: Cichlidae) from lakes Natron and Magadi, Tanzania and Kenya, with descriptions of two new species. Ichthyological Exploration of Freshwaters 10, 97–146.

Shipman, P., Potts, R., Pickford, M., 1983. Lainyamok, a new middle Pleistocene hominid site. Nature 306, 365-368.

Singh, B.P., Lee, Y.I., Pawar, J.S., Charak, R.S., 2007. Biogenic features in calcretes developed on mudstone: Examples from Paleogene sequences of the Himalaya, India. Sedimentary Geology 201, 149-156.

Smith, J.J., Platt, B.F., Ludvigson, G.A., Thomasson, J.R., 2011. Ant-nest ichnofossils in honeycomb calcretes, Neogene Ogallala Formation, High Plains region of western Kansas, U.S.A. Palaeogeography, Palaeoclimatoloy, Palaeoecology 308, 383-394..

Soil Classification Working Group, 1998. The Canadian System of Soil Classification, 3rd ed. Agriculture and Agri-Food Canada Publication 1646, 187 pp.

Soil Survey Staff, 1999. Soil taxonomy: A basic system of soil classification for making and interpreting soil surveys. 2nd edition. Natural Resources Conservation Service. U.S. Department of Agriculture Handbook 436.

Spoor, F., Leakey, M.G., Gathogo, P.N., Brown, F.H., Anton, S.C., McDougall, I., Kiarie, C., Manthi, F.K., Leakey, L.N., 2007. Implications of new early *Homo* fossils from Ileret, east of Lake Turkana, Kenya. Nature 448, 688-691.

Stokes, M., Nash, D.J., Harvey, A.M., 2007. Calcrete 'fossilisation' of alluvial fans in SE Spain: The roles of groundwater, pedogenic processes and fan dynamics in calcrete development. Geomorphology 85, 63-84.

Strong, G.E., Giles, J.R.A., Wright ,V.P., 1992. A Holocene calcrete from North Yorkshire, England: implications for interpreting palaeoclimates using calcretes. Sedimentology 39, 333-347.

Sun, S.-s., McDonough, W.F., 1989. Chemical and isotopic systematics of oceanic basalts: implications for mantle composition and processes. Geological Society, London, Special Publications 42, 313-345.

Surdam, R.C., Eugster, H.P., 1976. Mineral reactions in the sedimentary deposits of the Lake Magadi region, Kenya. Geological Society of America Bulletin 87, 1739-1752.

Talbot, M.R., 1990. A review of the palaeohydrological interpretation of carbon and oxygen isotopic ratios in primary lacustrine carbonates. Chemical Geology (Isotope Geoscience Section) 80, 261-279.

Tallon, P.W., 1978. Geological setting of the hominid fossils and Acheulian artifacts from the Kapthurin Formation, Baringo District, Kenya. In Bishop, W.W. (Ed.), Geological background to fossil man; recent research in the Gregory Rift valley, East Africa. Scott. Acad. Press: Edinburgh, United Kingdom. pp 361-373.

Talma, A.S., Netterberg, F., 1983. Stable isotope abundances in calcretes. Geological Society, London, Special Publications 11, 221-233.

Tandon, S.K., Andrews, J.E., 2001. Lithofacies associations and stable isotopes of palustrine and calcrete carbonates: examples from an Indian Maastrichtian regolith. Sedimentology 48, 339-355.

Tanner, L.H., 2010. Continental carbonates as indicators of paleoclimate. In A.M. Alonso-Zarza and L. Tanner (Eds.), Carbonates in Continental Settings: Facies, Environments and Processes. Developments in Sedimentology 61, Elsevier. Oxford. 180-206.

Tarits, C., Renaut, R.W., Tiercelin, J-J. Hérissé, Cotton, J., Cabon, J-Y., 2006. Geochemical evidence of hydrothermal recharge in Lake Baringo, central Kenya Rift Valley. Hydrological Processes 20, 2027-2055.

Taylor, S.R. McLennan, S.M., 1986. The chemical composition of the Archaean crust. *In* Dawson et al. (Eds.) The Nature of the Lower Continental Crust, Geological Society Special Publication No. 24, pp. 173-178.

Tichy H., Seegers L., 1999, The *Oreochromis alcalicus* flock (Teleostei: Cichlidae) from Lakes Natron and Magadi, Tanzania and Kenya, a model for the evolution pf "new" species flocks in historical times? Ichthyological Exploration of Freshwaters 10: 147-174

Tiercelin, J-J., 1986. The Pliocene Hadar Formation, Afar depression of Ethiopia. In Frostick, L.E. et al. (Eds.) 1986, Sedimentation in the African Rifts, Geological Society, London, Special Publications, 25. p. 221-240.

Tiercelin, J.-J., Lezzar, K.E., 2002. A 300 million years history of rift lakes in Central and East Africa: an updated broad review. In: Odada, E.O., Olago, D.O., (Eds.), The East African Great Lakes: Limnology, Paleolimnology and Biodiversity 12. Advances in Global Change Research, pp. 3-60.

Tiercelin, J.-J., Schuster, M., Roche, H., Brugal, J.-P., Thuo, P., Prat, S., Harmand, S., Davtian, G., Barrat, J.-A., Bohn, M., 2010. New considerations on the stratigraphy and environmental context of the oldest (2.34 Ma) Lokalalei archaeological site complex of the Nachukui Formation, West Turkana, northern Kenya Rift. Journal of African Earth Sciences 58, 157-184.

Trauth, M.H., Maslin, M.A., Deino, A.L., Junginger, A., Lesoloyia, M., Odada, E.O., Olago, D.O., Olaka, L.A., Strecker, M.R., Tiedemann, R., 2010. Human evolution in a variable environment: The amplifier lakes of Eastern Africa. Quaternary Science Reviews, 29, 2981-2988.

Trump, E.C., 1967. Vegetation. In Morgan, W.T.W., Ed., Nairobi: City and Region. Oxford University Press, pp. 39-47.

Tuite, C.H., 1981. Standing crop densities and distribution of *Spirulina* and benthic diatoms in East African alkaline saline lakes. Freshwater Biology 11, 345-360.

Verrecchia, E.P., 1996. Morphometry of microstromatolites in calcrete laminar crusts and a fractal model of their growth. Mathematical Geology 28, 87-109

Verrecchia, E.P., Freytet, P., Verrecchia, K.E., Dumont, J-L., 1995. Spherulites in calcrete laminar crusts: biogenic $CaCO_3$ precipitation as a major contributor to crust formation. Journal of Sedimentary Research, A65: 690-700.

Verrecchia, E.P., Dumont, J-L., 1996. A Biogeochemical Model for Chalk Alteration by Fungi in Semiarid Environments. Biogeochemistry 35, 447-470.

Vincens, A., Casanova, J., 1987. Modern background of Natron-Magadi basin (Tanzania-Kenya): physiography, climate, hydrology and vegetation. Sciences Géologiques Bulletin 40, 9-21.

Vincens, A., Bonnefille, R., Buchet, G., 1990. Étude palynologique du sondage Magadi NF1 (Kenya). Implications paléoclimatiques. Geobios 24, 549-558.

Vousdoukas, M.I., Velegrakis, A.F., Plomaritis, T.A., 2007. Beachrock occurrence, characteristics, formation mechanisms and impacts. Earth-Science Reviews 85, 23-46.

Wang, Y., Nahon, D., Merino, E., 1994. Dynamic model of the genesis of calcretes replacing silicate rocks in semi-arid regions. Geochimica et Cosmochimica Acta 58, 5131-5145.

Watson, A. Nash, D., 1997. Desert crusts and varnishes, In: Thomas, D.S.G. (Ed.) Arid Zone Geomorphology: Process, Form and Change in Drylands. Chichester: John Wiley & Sons, pp. 69–107.

Walsh, J., Dodson, R. G., 1969. Geology of Northern Turkana, degree sheets 1, 2, 9, and 10 (No. 82). Geological Survey of Kenya.

White, J.C., Espejel-García, V.V., Anthony, E.Y., Omenda, P., 2012. Open system evolution of peralkaline trachyte and phonolite from the Suswa volcano, Kenya rift. Lithos 152, 84-104..

Williamson, P.G., Savage, R.J.G., 1986. Early rift sedimentation in the Turkana basin, northern Kenya. *In* Frostick, L.E. et al. (Eds.) 1986, Sedimentation in the African Rifts, Geological Society Special Publication No. 25, pp. 267-283.

Williamson, D., Taieb, M., Damnati, B., Icole, M., Thouveny, N., 1993. Equatorial extension of the younger Dryas event: rock magnetic evidence from Lake Magadi (Kenya). Global and Planetary Change 7, 235-242.

Wilson, P.J., Wood, C.M., Walsh, P.J., Bergman, A.N., Bergman, H.I., Laurent, P., White, B.N., 2004. Discordance between genetic structure and morphological, ecological, and physiological adaptation in Lake Magadi Tilapia. Physiological and Biochemical Zoology 77, 537-555.

Wright, V.P., 1986. The role of fungal biomineralization in the formation of Early Carboniferous soil fabrics. Sedimentology 33, 831-838.

Wright, V.P., Platt, N.H., Wimbledon, W.A., 1988. Biogenic laminar calcretes: evidence of calcified root-mat horizons in paleosols. Sedimentology 35, 603-620.

Wright, V.P., 1989. Terrestrial stromatolites and laminar calcretes: a review. Sedimentary Geology 65, 1-13.

Wright, V.P., 2007. Calcrete. In: Nash, D.J., McLaren, S.J., (Eds.), Geochemical Sediments and Landscapes. Blackwell, Oxford, p. 10-45.

Wright, V.P., 1990. A micromorphological classification of fossil and Recent calcic and petrocalcic microstructures. Developments in Soil Science 19, 401-407.

Wright, V.P., and Tucker, M.E., 1991. Calcretes: An introduction. In: Wright, V.P., and Tucker, M.E., (Eds.) Calcretes. Reprint Series Volume 2 of the International Association of Sedimentologists. Blackwell, Oxford, p. 1-22.

Wright, V.P., Platt, N.H., Marriott, S.B., Beck, V.H., 1995. A classification of rhizogenic (root-formed) calcretes, with examples from the Upper Jurassic-Lower Cretaceous of Spain and Upper Cretaceous of southern France. Sedimentary Geology 100, 143-158.

Wynn, J.G., 2007. Carbon isotope fractionation during decomposition of organic matter in soils and paleosols; impliucations for paleoecological interpretations of paleosols. Palaeogeography, Palaeoclimatology, Palaeoecology 251, 437-448.

Wynn, J.G., Roman, D.C., Alemseged, Z., Reed, D., Geraads, D., Munro, S., 2008. Stratigraphy, depositional environments, and basin structure of the Hadar and Busidima Formations at Dikika, Ethiopia. Geological Society of America Special Papers, 446, 87-118.

Wynn, J.G., Retallack, G.J., 2001. Paleoenvironmental reconstruction of middle Miocene paleosols bearing *Kenyapithecus* and *Victoriapithecus*, Nyakach Formation, southwestern Kenya. Journal of Human Evolution 40, 263-288.

Yaalon, D.H., 1988. Saharan dust and desert loess; effect on surrounding soils. In Petit-Maire, N. (Ed.), Deserts; past and future evolution; First annual meeting of the International Geological Correlation Program. CNRS, Lab. Geol. Quaternaire, Marseilles, France, p. 199-201.

Yan, J.P., Hinderer, M., Einsele, G., 2002, Geochemical evolution of closed-basin lakes: general model and application to Lakes Qinghai and Turkana. Sedimentary Geology 148, 105-122.

Yuretich, R.F., 1982. Possible Influences upon Lake Development in the East African Rift Valleys, Journal of Geology 90, 329-337.

Yuretich, R.F., Cerling, T.E., 1983. Hydrogeochemistry of Lake Turkana, Kenya: Mass balance and mineral reactions in an alkaline lake. Geochimica et Cosmochimica Acta 47, 1099-1109.

Zhou, J., Chafetz, H.S., 2009. Biogenic caliches in Texas: The role of organisms and effect of climate. Sedimentary Geology 222, 207-225.